IMPACT OF IMPULSIVE NOISE ON OFDM OSTBC MIMO WIRELESS COMMUNICATION SYSTEM WITH HYBRID DIVERSITY

MD ABDUL HALIM

Ph.D. THESIS

DEPARTMENT OF ELECTRICAL, ELECTRONIC AND COMMUNICATION ENGINEERING

MILITARY INSTITUTE OF SCIENCE AND TECHNOLOGY

DHAKA, BANGLADESH

MARCH 2025

IMPACT OF IMPULSIVE NOISE ON OFDM OSTBC MIMO WIRELESS COMMUNICATION SYSTEM WITH HYBRID DIVERSITY

MD ABDUL HALIM (SN. 1014160021)

A thesis submitted in Partial Fulfilment of the Requirements for the Degree of Doctor of Philosophy in Electrical Electronic and Communication Engineering

DEPARTMENT OF ELECTRICAL, ELECTRONIC AND COMMUNICATION ENGINEERING
MILITARY INSTITUTE OF SCIENCE AND TECHNOLOGY
DHAKA, BANGLADESH

MARCH 2025

IMPACT OF IMPULSIVE NOISE ON OFDM OSTBC MIMO WIRELESS COMMUNICATION SYSTEM WITH HYBRID DIVERSITY

Ph. D. Thesis

By

MD ABDUL HALIM (SN. 1014160021)

Approved as to style and content by the Board of Examination on 27 March 2025:

Dr. Satya Prasad Majumder Professor of Electrical and Electronic Engineering BUET, Dhaka	Chairman (Supervisor) Board of Examination
Dr. A K M Nazrul Islam Registrar, University of Asia Pacific	Member (Co Supervisor) Board of Examination
Captain A N M Didarul Alam, (L), NUP, psc, BN Senior Instructor of Electrical Electronic and Communication Engineering MIST, Dhaka	Head of the Department Member (Ex-officio)

Department of Electrical, Electronic and Communication Engineering MIST, Dhaka

_____ Member (Internal)

Dr. Md. Hossam-E-Haider Board of Examination

Professor of Electrical Electronic and Communication Engineering

MIST, Dhaka

_____ Member (Internal)

Lt Col Md. Tawfiq Amin, Ph.d. Board of Examination

Instructor Class 'A', Electrical Electronic and Communication Engineering

MIST, Dhaka

_____ Member (Exterernal)

Prof. Dr. Md Saiful Islam Board of Examination

IICT, BUET

_____

Dr. Md Forkan Uddin Member (Internal)

Professor of Electrical and Electronic Engineering Board of Examination

BUET, Dhaka

_____

Dr. Subrata Kumar Aditya Member (External)

Professor of Electrical and Electronic Engineering Board of Examination

Dhaka University

_____

Dr. Ramjee Prasad Member (External)

Professor Emeritus of BDT Dept. Board of Examination

Aarhus University, Denmark

Department of Electrical, Electronic and Communication Engineering MIST, Dhaka

IMPACT OF IMPULSIVE NOISE ON OFDM OSTBC MIMO WIRELESS COMMUNICATION SYSTEM WITH HYBRID DIVERSITY

DECLARATION

I hereby declare that the study reported in this thesis entitled as above is my own original work and has not been submitted before anywhere for any degree or other purposes. Further I certify that the intellectual content of this thesis is the product of my own work and that all the assistance received in preparing this thesis and sources have been acknowledged or cited in the reference section.

_____

Md Abdul Halim

Department of Electrical, Electronic and Communication Engineering MIST, Dhaka

IMPACT OF IMPULSIVE NOISE ON OFDM OSTBC MIMO WIRELESS COMMUNICATION SYSTEM WITH HYBRID DIVERSITY

A Thesis

By

Md Abdul Halim

DEDICATION

Dedicated to my family members for supporting and encouraging me to believe in myself.

ACKNOWLEDGEMENTS

I wish to express my sincere gratitude to my supervisor Prof. Dr. Satya Prasad Majumder and co-supervisor Prof. Dr. A K M Nazrul Islam for providing me the opportunity to work with them in the field of Broadband Wireless Communication System. I would like to thank them for their constant guidance, encouragement and kind cooperation related to my research over the past ten years.

I would like to express my gratitude to the doctoral committee members, Prof. Dr. Hossam-E-Haider, Lt Col Md. Tawfiq Amin, Ph.D. of EECE Dept., MIST, Prof. Dr. Md Saiful Islam and Prof. Dr. Md Forkan Uddin, IICT and Dept. of EEE, BUET respectively, for their generous support and numerous advice during every stage of the program.

I express my sincere gratitude to the Chief of Air Staff of Bangladesh Air Force, Asst. Chief of Air Staff (Maintenance), Air Secretary, Director Air Training, Director Education, and related officers and personnel for supporting me with the opportunity to complete the research work.

I also express my sincere gratitude to Head of EECE Dept., MIST, Lt Col Nyeem, PhD, EECE, MIST and Lt Col Amin, PhD, EECE, MIST for all their support and cooperation during the research work. The support I received from them was a sort of constant push-forward to complete the work. May Almighty Allah grant them appropriate returns.

My deepest thanks from the bottom of my heart, of course, must go to my wife for her love, mental support, constant encouragement and utmost patience without which nothing would have been possible. I would also like to express my endless love to my son Talha Halim and daughter Ajra Sabiha, who are my wish and who always make me lively, confident and happy.

Finally, I would like to express my heartiest gratitude to Almighty ALLAH Sub-ha-nahu-wa-ta'la for giving me the ability to explore the unknown world of Broadband Wireless Communication and making me able to complete the dissertation for the Ph. D degree in the department of EECE, MIST.

ABSTRACT

Impact of Impulsive Noise on OFDM OSTBC MIMO Wireless Communication System with Hybrid Diversity

Multipath-induced fading is the major performance limiting factor in broadband wireless communication systems. Link performance is severely degraded by fading and to maintain an acceptable performance, powerful countermeasures such as diversity techniques should be employed. In literature, different diversity combining schemes have been proposed which are Selection Combining (SC), Equal Gain Combining (EGC) and Maximal Ratio Combining (MRC). In this research work, Hybrid Diversity Combining techniques are well discussed with utmost importance. SC-MRC, MRC-SC and SC-EGC hybrid diversity techniques are studied, and comparative analysis is made, and it has been observed that considering implementation complexity and performance gain, SC-EGC hybrid diversity scheme shows better result.

Impulsive, non-Gaussian noise is present in many wireless communication systems due to man-made electro-magnetic interference, atmospheric noise, or ignition noise etc. As above mentioned, hybrid diversity combining schemes are designed for Gaussian noise, but when impulsive noise is present, its performance may degrade. As such, the necessity of designing hybrid diversity techniques considering impulsive noise is felt. Middleton Class-A and Symmetric Alpha Stable (SαS) are the two most common widely accepted models for analysing wireless communication system under impulsive noise.

In this research, an analytical approach utilizing hybrid diversity reception has been carried out to evaluate the performance improvement of a broadband wireless communication channel in Rayleigh fading and impulsive noise environment. This impulsive noise is considered time variant which has random occurrences with high power spectral density and short duration. The effect of impulsive noise and fading in terms of BER can be improved greatly by using Orthogonal Frequency Division

Multiplexing (OFDM). The system BER is compared numerically for Binary Phase Shift Keying (BPSK) and OFDM system. It has been observed that there is a significant improvement in performance in terms of BER. Moreover, performance is tremendously amplified using hybrid diversity and BER performance is calculated analytically and also investigated using multiple antennas.

Considering OFDM with BPSK modulation and using Orthogonal Space-Time Block Codes (OSTBC) expressing SNR and BER is found out through analytical process. Middleton Class-A and Symmetric Alpha Stable (SαS) model is considered to evaluate the effect of impulsive noise under Rayleigh Fading environment. The results are assessed analytically considering the multipath transfer function model. The numerical results exhibit that the system suffers significant power penalty due to impulsive noise which is higher for higher channel bandwidth and can be minimized by increasing number of OFDM subcarriers.

This work investigates the effect of impulsive noise-modeled via the Middleton Class-A distribution on FDM-based MIMO systems that employ OSTBC with hybrid diversity schemes. OFDM provides resilience against frequency-selective fading, and OSTBC ensures spatial diversity; however, impulsive noise presents non-Gaussian, burst-like disturbances that degrade system performance significantly. Under such conditions, impulsive noise spreads energy across OFDM subcarriers, lowering BER performance more than conventional Gaussian noise.

Mitigation strategies- such as blanking/ clipping, analog nonlinear limiting, and Maximum Likelihood (ML) detection assuming impulsive noise show significant BER improvement. In particular, ML detectors designed with Middleton based likelihood metrices provide up to 7 dB SNR gain over conventional Gaussian based ML detectors.

Thus, by integrating robust detection techniques and adaptive hybrid diversity mechanisms, OFDM-OSTBC MIMO systems can tolerate impulsive impairments in harsh wireless environments such as power substations, in-vehicle networks, or PLL systems. The trade-off between complexity (e.g. ML-IN detectors, Parameter estimation)

and performance gains (reduced BER, regained diversity order) thoroughly discussed, offering insights for designing resilient next-generation wireless links.

সারসংক্ষেপ

Impact of Impulsive Noise on OFDM OSTBC MIMO Wireless Communication System with Hybrid Diversity

ব্রডব্যান্ড ওয়্যারলেস যোগাযোগ ব্যবস্থায় মাল্টিপাথ-প্ররোচিত ফেইডিং হল প্রধান কর্মক্ষমতা সীমিতকারী ফ্যাক্টর। ফেইডিংয়ের ফলে লিঙ্ক কর্মক্ষমতা মারাত্মকভাবে হ্রাস পায় এবং একটি গ্রহণযোগ্য কর্মক্ষমতা বজায় রাখার জন্য, বৈচিত্র্য কৌশলের মতো শক্তিশালী প্রতিকার ব্যবহার করা উচিত। সাহিত্যে, বিভিন্ন বৈচিত্র্য সমন্বয় প্রকল্প প্রস্তাব করা হয়েছে যেমন নির্বাচন সমন্বয় (SC), সমান লাভ সমন্বয় (EGC) এবং সর্বাধিক অনুপাত সমন্বয় (MRC)। এই গবেষণা কাজে, হাইব্রিড বৈচিত্র্য সমন্বয় কৌশলগুলি অত্যন্ত গুরুত্ব সহকারে আলোচনা করা হয়েছে। SC-MRC, MRC-SC এবং SC-EGC হাইব্রিড বৈচিত্র্য কৌশলগুলি অধ্যয়ন করা হয়েছে, এবং তুলনামূলক বিশ্লেষণ করা হয়েছে, এবং দেখা গেছে যে বাস্তবায়ন জটিলতা এবং কর্মক্ষমতা বৃদ্ধি বিবেচনা করে, SC-EGC হাইব্রিড বৈচিত্র্য প্রকল্পটি আরও ভাল ফলাফল দেখায়।

মানুষের তৈরি তড়িৎ-চৌম্বকীয় হস্তক্ষেপ, বায়ুমণ্ডলীয় শব্দ, বা ইগনিশন শব্দ ইত্যাদির কারণে অনেক বেতার যোগাযোগ ব্যবস্থায় আবেগপ্রবণ, অ-গাউসীয় শব্দ উপস্থিত থাকে। উপরে উল্লিখিত হিসাবে, হাইব্রিড বৈচিত্র্য সমন্বয় প্রকল্পগুলি গাউসীয় শব্দের জন্য ডিজাইন করা হয়েছে, কিন্তু যখন আবেগপ্রবণ শব্দ উপস্থিত থাকে, তখন এর কর্মক্ষমতা হ্রাস পেতে পারে। এইভাবে, আবেগপ্রবণ শব্দ বিবেচনা করে হাইব্রিড বৈচিত্র্য কৌশল ডিজাইন করার প্রয়োজনীয়তা অনুভূত হয়। আবেগপ্রবণ শব্দের অধীনে বেতার যোগাযোগ ব্যবস্থা বিশ্লেষণের জন্য মিডলটন ক্লাস-এ এবং সিমেট্রিক আলফা স্টেবল ($S\alpha S$) হল দুটি সর্বাধিক গৃহীত মডেল যা ব্যাপকভাবে গৃহীত হয়।

এই গবেষণায়, Rayleigh ফেইডিং এবং ইম্পালসিভ নয়েজ পরিবেশে ব্রডব্যান্ড ওয়্যারলেস কমিউনিকেশন চ্যানেলের কর্মক্ষমতা উন্নতি মূল্যায়ন করার জন্য হাইব্রিড ডাইভারসিটি রিসেপশন ব্যবহার করে একটি বিশ্লেষণাত্মক পদ্ধতি ব্যবহার করা হয়েছে। এই ইম্পালসিভ নয়েজকে টাইম ভেরিয়েন্ট হিসেবে বিবেচনা করা হয় যার উচ্চ ক্ষমতার বর্ণালী ঘনত্ব এবং স্বল্প সময়কাল সহ এলোমেলো ঘটনা ঘটে। অর্থোগোনাল ফ্রিকোয়েন্সি ডিভিশন মাল্টিপ্লেক্সিং (OFDM) ব্যবহার করে BER-এর ক্ষেত্রে ইম্পালসিভ নয়েজ এবং ফেইডিংয়ের প্রভাব ব্যাপকভাবে উন্নত করা যেতে পারে। বাইনারি ফেজ শিফট কীয়ং (BPSK) এবং OFDM সিস্টেমের জন্য BER সিস্টেমের সংখ্যাগত তুলনা করা হয়েছে। দেখা গেছে যে BER-এর ক্ষেত্রে কর্মক্ষমতার উল্লেখযোগ্য উন্নতি হয়েছে। তাছাড়া, হাইব্রিড ডাইভারসিটি ব্যবহার করে কর্মক্ষমতা ব্যাপকভাবে বৃদ্ধি করা হয় এবং BER কর্মক্ষমতা বিশ্লেষণাত্মকভাবে গণনা করা হয় এবং একাধিক অ্যান্টেনা ব্যবহার করেও তদন্ত করা হয়।

বিশ্লেষণাত্মক প্রক্রিয়ার মাধ্যমে BPSK মড্যুলেশনের মাধ্যমে OFDM বিবেচনা করা এবং SNR এবং BER প্রকাশকারী অর্থোগোনাল স্পেস-টাইম ব্লক কোড (OSTBC) ব্যবহার করে এটি নির্ণয় করা হয়। Rayleigh Fading পরিবেশের অধীনে আবেগপ্রবণ শব্দের প্রভাব মূল্যায়ন করার জন্য Middleton Class-A এবং Symmetric Alpha Stable (SαS) মডেল বিবেচনা করা হয়। মাল্টিপাথ ট্রান্সফার ফাংশন মডেল বিবেচনা করে বিশ্লেষণাত্মকভাবে ফলাফল মূল্যায়ন করা হয়। সংখ্যাসূচক ফলাফলগুলি দেখায় যে আবেগপ্রবণ শব্দের কারণে সিস্টেমটি উল্লেখযোগ্য পাওয়ার পেনাল্টি ভোগ করে যা উচ্চ চ্যানেল ব্যান্ডউইথের জন্য বেশি এবং OFDM সাবক্যারিয়ার সংখ্যা বৃদ্ধি করে এটি হ্রাস করা যেতে পারে।

এই কাজটি মিডলটন ক্লাস-এ ডিস্ট্রিবিউশনের মাধ্যমে ইম্পুলসিয়াল নয়েজ-মডেল করা FDM-ভিত্তিক MIMO সিস্টেমগুলিতে প্রভাব তদন্ত করে যা হাইব্রিড ডাইভারসিটি স্কিম সহ OSTBC ব্যবহার করে। OFDM ফ্রিকোয়েন্সি-সিলেকটিভ ফেইডিংয়ের বিরুদ্ধে স্থিতিস্থাপকতা প্রদান করে এবং OSTBC স্থানিক বৈচিত্র্য নিশ্চিত করে ; তবে, ইম্পুলসিয়াল নয়েজ অ-গাউসিয়ান, বার্স্ট-সদৃশ ব্যাঘাত উপস্থাপন করে যা সিস্টেমের কর্মক্ষমতা উল্লেখযোগ্যভাবে হ্রাস করে। এই ধরনের পরিস্থিতিতে, ইম্পুলসিয়াল নয়েজ OFDM

সাবক্যারিয়ারগুলিতে শক্তি ছড়িয়ে দেয়, যা প্রচলিত গাউসিয়ান শব্দের তুলনায় BER কর্মক্ষমতা বেশি হ্রাস করে।

প্রশমন কৌশল - যেমন ব্ল্যাঙ্কিং/ক্লিপিং, অ্যানালগ নন-লিনিয়ার লিমিটিং, এবং ম্যাক্সিমাম লিইকলিহুড (ML) সনাক্তকরণ, যদি ধরে নেওয়া হয় যে ইম্পালসিয়াল নয়েজ উল্লেখযোগ্য BER উন্নতি দেখায়। বিশেষ করে, মিডলটন ভিত্তিক সম্ভাবনা মেট্রিক্স দিয়ে ডিজাইন করা ML ডিটেক্টরগুলি প্রচলিত গাউসিয়ান ভিত্তিক ML ডিটেক্টরের তুলনায় 7 dB পর্যন্ত SNR লাভ প্রদান করে।

সুতরাং, শক্তিশালী সনাক্তকরণ কৌশল এবং অভিযোজিত হাইব্রিড বৈচিত্র্য প্রক্রিয়াগুলিকে একীভূত করে, OFDM-OSTBC MIMO সিস্টেমগুলি পাওয়ার সাবস্টেশন, যানবাহনের নেটওয়ার্ক বা PLL সিস্টেমের মতো কঠোর ওয়্যারলেস পরিবেশে আবেগপ্রবণ প্রতিবন্ধকতা সহ্য করতে পারে। জটিলতা (যেমন ML-IN ডিটেক্টর, প্যারামিটার অনুমান) এবং কর্মক্ষমতা লাভ (হ্রাসকৃত BER, বৈচিত্র্য ক্রম পুনরুদ্ধার) এর মধ্যে লেনদেন পুঙ্খানুপুঙ্খভাবে আলোচনা করা হয়েছে, যা স্থিতিস্থাপক পরবর্তী প্রজন্মের ওয়্যারলেস লিঙ্কগুলি ডিজাইন করার জন্য অন্তর্দৃষ্টি প্রদান করে।

TABLE OF CONTENTS

LIST OF TABLES

LIST OF FIGURES

LIST OF SYMBOLS

x(t)	Transmitted signal
h(t, •)	Impulse response of signal with delay t.
r(t)	Received signal
Ps	Signal power at the transmitting end
Pd	Signal power at the receiving end
n(t)	Noise component of received signal
SαS	Symmetrical Alpha Stable
Rb	Bit rate
α	Instantaneous noise variance
fc	Carrier frequency
δ	Signal period
A1, B1	Fourier coefficients of cyclostationary noise
a0, a1	Attenuation parameters
di	Length of the 1-th path
λ	Arrival rate of Impulsive noise in Poisson's process, units per second
Pbi	BER under impulsive noise
Pbw	BER under A WGN
Pk	Probability distribution in Poisson's process
Pi	The total average occurrence of the impulsive noise duration in time T
P0	The average duration without impulsive noise in time T
αk,n	The information to be sent over the k-th symbol interval
vn(t)	Complex envelope of transmitted signal in the n-th sub-band
Znl	PDF of the output voltage
Tc	SNR in OFDM
K	Ratio between the power in the direct path and scattered path

Ω	Total power from both paths, acts as a scaling factor to the distribution
fn	OFDM subchannel carrier frequency
g	Fading gain
I0	Modified Bessel function of zero order
$\hat{g}$ (n)	Rician distributed fading normalized gain
A	Impulsive noise index
T	Ratio of Gaussian noise power to Impulsive noise power
A0n	Average output voltage
p(1/0)	Probability of bit error for n-th sub-carrier channel for a '1' transmitted with "0" received
p(0/1)	Probability of bit error for n-th sub-carrier channel for '0' transmitted with '1' received
γ	Propagation constant
σ'	Attenuation
β	Phase constant
ɥc	Permeability of conducting material
αC	Conductivity of conducting material
αg2	Fading variance
αimp	Variance of impulsive noise
N0	AWGN noise power
Ni	Impulsive noise power

LIST OF ABBREVIATIONS AND ACRONYMS

ACI	Adjacent channel interference
ASK	Amplitude shift keying
ATM	Asynchronous Transfer Mode
AWGN	Additive White Gaussian Noise
BER	Bit Error Rate
BPSK	Binary phase shift keying
BS	Base Station
CCI	Co-channel interference
CDF	Cumulative Distribution Function
CMI	Common-mode interference
DFT	Discrete Fourier Transform
DPSK	Differential Phase Shift Keying
DSP	Digital Signal Processing
DSL	Digital subscriber line
EGC	Equal Gain Combining
EMI	Electromagnetic Interference
FSK	Frequency shift keying
GDD	Generalized Delay Diversity
GI	Guard Interval
GMD	Geometric Mean Distance
GMR	Geometric Mean Radian
IED	Intelligent Electronics Device
IAT	Inter Arrival Time
INI	Impulsive Noise Index
ISI	Inter-symbol interference
ICI	Inter-carrier interference
ITU	International Telecommunication Union

IMF	Interface Management Function
LOS	Line of Sight
MCM	Multicarrier Modulation
MIMO	Multiple Input Multiple Output
MRC	Maximal Ratio Combining
MSC	Mobile Switching Center
M-QAM	M- ary Quadrature Amplitude Modulation
NLOS	Non Line of Sight
OFDM	Orthogonal frequency division multiplexing
PDC	Personal Digital Cellular
PDF	Probability Distribution Function
PSD	Power spectral density
PαS	Positive Alpha-table
QPSK	Quadrature Phase Shift Keying
QAM	Quadrature Amplitude Modulation
RFID	Radio Frequency Identification
SC	Selection Combining
SFBC	Frequency block codes
SISO	Single Input Single Output
SIMO	Sngle Input Multiple Output
SNR	Signal to noise ratio
STBC	Space time block coding
STC	Space time coding
SSRLS	State-Space Recursive Least Squares
SαS	Symmetric Alpha Stable
UWB	Ultra-Wide Band
VLSI	Very Large Scale Integrated Circuits
WPAN	Wireless Private Area Network

CHAPTER 1

INTRODUCTION

1.1 Introduction to Wireless Communication

Wireless communication is a communication method in which information and data are sent between two or more nodes without the need of electric wire as a medium. This network provides a flexible information transfer platform that allows users to travel without experiencing unacceptable performance degradation. A wireless communication network is made up of a base station (BS) that serves as the wireless information distribution center for all mobile stations (MS) within its signal coverage region. The radio channel from an MS to its serving BS is called the uplink or reverse channel, and the radio channel from the BS to the MSs is called the downlink or forward channel [1].

To extend the geographical coverage of a single BS, mobile switching centers (MSC) are connected to the BS via wireless. Wirelines connect MSCs to other MSCs, ensuring a wired backbone network or Asynchronous Transfer Mode (ATM). To provide a hybrid connection, this technology integrates a front-end wireless network with a backbone landline network.

A wireless channel, on the other hand, has channel impairments that limit the usable spectral breadth and result in residual error profiles that are relatively high and nonconstant. The geographical coverage is limited, and propagation is considerable. Multipath delay spread, doppler spread, intracell interference, fading ambient noise, and other types of channel impairments exist in the radio propagation channel. To resist interference and distortion in the signal, effective and efficient transmitters, receivers, and communication protocols are required.

Wireless communication is a global technology with worldwide interest in its development. It enables data transfer at narrow or broadband speeds through wireless

network by using advanced modulation technology [2]. Wireless communication technology is emerging with a great promise to meet up future demand for ultra-high speed data communications and networking [3-5]. Orthogonal Frequency Division Multiplexing (OFDM) is a multicarrier technique that suits well for high-speed wired and wireless applications [6]. OFDM offers added spectral efficiency as well as robustness against selective fading, narrowband interference and impulsive noise which makes it a contender for high-speed communication system. Further to capture sufficient multipath energy the information in each sub band is modulated by utilizing OFDM technique. Thus, multiband OFDM is one of the leading proposal for wireless personal area network (WPAN) standards. [7-10].

Diversity techniques have been employed to combat the effect of multi-path fading on wireless communication systems [11-14]. Recent interest in emerging high-data-rate wireless systems has led to renewal of the subject. Classical diversity techniques include maximum ratio combining (MRC), equal gain combining (EGC) and selection combining (SC). An L-branch MRC performs the best with the highest complexity. On the other hand, SC performs the worst comparatively with the least complexity. This motivates the development of hybrid diversity whose complexity and performance lie between these two extreme cases. Therefore, several suboptimum diversity combining schemes that achieve a tradeoff between performance and implementation complexity have recently been proposed and studied in the literature.

OFDM is a form of multi-carrier transmission technique widely used in the modern wireless network to achieve high-speed data transmission with good spectral efficiency. However, in the impulsive noise environment BER performances of these systems, originally designed for a Gaussian noise model, are much degraded.

1.2 Brief History of Wireless Communication

The history of Wireless Communications started with the understanding or magnetic and electric properties observed during the early days by the Chinese, Greek and

Roman cultures and experiments carried out in the 17th and 18th centuries. French mathematician Jean Baptiste Joseph Fourier discovered Fourier's theorem in 1807. Danish physicist Hans Christian Orsted discovered the electromagnetic field caused by electric current. The French physicist Dominique Francois Jean Arago showed that a wire became a magnet when current flowed through it. French mathematician and physicist Andre-Marie Ampere discovered electrodynamics and proposed an Electromagnetic Telegraph in 1820 [15].

American dentist Dr. Mahlon Loomis described and demonstrated a wireless transmission system which he patented in 1866. Loomis demonstrated the transmission of signals between two mountains, a distance of 22 km. American physicist, Amos Emerson Dolbear, was granted a patent for a wireless transmission system using an induction coil, microphone and telephone receiver and battery. Nathan Stubblefield transmitted audio signals without wires 1882. Heaviside introduced impedance as the ratio of voltage over current. Hertz started his work to demonstrate the existence of radio waves and published his results in 1888.

Marconi transmitted and received a coded message at a distance of 1.75 miles near his home in Bologna, Italy. Indian physicist, Sir Jagadis Chunder Bose generated and detected wireless signals and produced many devices such as waveguides, horn antennas, microwave reflectors and more in 1895. In the year of 1897, Marconi demonstrated a radio transmission to a tugboat over an 18 mile path over the English Channel. The first wireless company, Wireless Telegraph and Signal Company was founded – they bought most of Marconi's patents. Lord Rayleigh suggests EM wave propagation in waveguides and analysis of propagation through dielectrically filled waveguides. Lodge patented various types of antennas.

In the year of 1904, Frank J. Sprague developed the idea of the printed circuit. W. Pickard filed a patent application for a crystal detector where a thin wire was in contact with silicon. It was the central component in early radio receivers called crystal radios. J. C. Bose was granted a patent on point contact diodes that were used for

many years as detectors in the industry. Fleming suggested the rectifying action of the vacuum-tube diode for detecting high frequency oscillation – the first practical radio tube.

The German physicist Walter Schottky discovered the effect of electric field on the rate of electron emission from thermionic emitters named after him. Fleming discovered atmospheric refraction and its importance in the transmission of EM waves around the Earth in 1914. Carl R. Englund was the first to develop the equation of a modulated wave (AM) and also discovered the frequencies related to sidebands. Frequency modulation of a carrier was proposed to accommodate more channels within the available bandwidths.

In 1918, Armstrong invented the Superheterodyne Radio Receiver using 8 valves – most receivers still use this design today. Langmuir patented the feedback amplifier. E. H. O Shaughnessy development of direction finding was one of the key weapons in England during WWI – Bellini-Tosi aerials were installed around the coast to locate transmission from ships and aircrafts. Louis Alan Hazeltime invented the neutrodyne circuit with tuned RF amplifier with neutralization.

Baird conducted the first transatlantic TV broadcast and built the first color TV in 1928. Nyquist published a classic paper on the theory of signal transmission in telegraphy. He developed the criteria for the correct reception of telegraph signals transmitted over dispersive channels in the absence of noise. C.S. Franklin patented the coaxial cable in England to be used as an antenna feeder.

The word Telecommunication was coined, and the International Telecommunications Union (ITU) was formed in 1932. George C. Southworth and J. F. Hargreaves developed the circular waveguide. Karl Jansky accidentally discovered radio noise coming from outer space giving birth to radio astronomy. R. Darbord developed the UHF Antenna with parabolic reflector. In 1934, the Federal Communications Commission (FTC) was created in the US. W.L. Everitt obtained the optimum

operating conditions for Class C amplifiers. F. E. Terman demonstrated a transmission line as a resonant circuit. German physicist Oskar Ernst Heil applied for a patent on technology relating electrical amplifiers and other control arrangements that was the theoretical invention of capacitive current control in FETs.

During 1948, W. H. Branttain, J. Bardeen and W. Shockley of Bell Labs built the junction transistor. E. L. Ginzton and others developed distributed wideband amplifier using pentodes in parallel. Shannon laid out the theoretical foundations of digital communications in a paper entitled "A Mathematical Theory of Communication." Paine described the BALUN. In 1963, W. S. Mortley and J. H. Rowen developed surface acoustic wave (SAW) devices. John B. Gunn of IBM demonstrated microwave oscillations in GaAs and InP diodes. The Institute of Electrical and Electronic Engineers (IEEE) was formed by merging IRE and AIEE.

The first digital radio-relay system went into operation in Japan using 2 GHz operating frequency in the year of 1969. ARPANET was launched (precursor to Internet) in the same year. AT&T Bell Labs started testing a mobile telephone system based on cells in 1978 [15].

1.3 Limitations of Wireless Communication

Wireless transmission media have limitations such as interference, security issues, limited range, and lower speed. Wireless transmission media, such as Wi-Fi, Bluetooth, and cellular networks, have become increasingly popular due to their convenience and flexibility. However, they also come with several limitations. One of the most significant is interference. Wireless signals can be disrupted by other electronic devices, physical obstacles like walls and buildings, and even atmospheric conditions. This can lead to a loss of signal strength, reduced line of sight connection, reduced data transfer rates, reduced signal strength or complete loss of connection [16].

Another major limitation is security. Wireless signals can be intercepted by unauthorized users, making them less secure than wired connections. Although encryption and other security measures can help to mitigate this risk, it is still a significant concern, particularly for sensitive data. The range of wireless transmission is also limited. While this can be extended with the use of repeaters or boosters, it still falls short of the distances achievable with wired connections. This can be a problem in large buildings or across wide areas, where a wired connection may not be feasible.

Finally, wireless transmission media typically have lower speeds than wired connections. This is due to the fact that wireless signals are subject to interference and signal degradation, which can slow down data transfer rates. Additionally, the speed of a wireless connection can be affected by the number of devices connected to the network, with each additional device potentially reducing the available bandwidth.

In summary, while wireless transmission media offer many advantages, they also have several limitations. These include interference from other devices and physical obstacles, security risks, limited range, and lower speeds compared to wired connections. Understanding these limitations is crucial when designing and implementing wireless networks, to ensure that they can meet the needs of users and provide a reliable and secure connection.

1.3.1 Noise and Distortion in Wireless Communication Systems

Noise is acknowledged as unwanted signals that interfere with the measurement of another core signal. With the help of noise examination, the condition of the source can be estimated. distortion can be regarded as any change in core signal that modifies the basic waveform or the relationship between various frequency components [17-19].

The main constraints limiting the capacity of data transmission in telecommunications and the accuracy of signal monitoring devices are noise and distortion. As a result, the modeling and removal of noise and distortion effects have been at the heart of communications and signal processing theory and practice. In applications such as cellular mobile communications, noise reduction and distortion removal are critical.

There are a number of noise categories that affect the mobile communication system such as:

On the basis of source:

a. Acoustic noise: One of the common types of noise that is present in the environment in various degrees it emerges from vibration, movement and collision.

b. Electromagnetic noise: Present at all frequencies, but especially in the radio frequency range (kHz to GHz), where telecommunications occur. Electromagnetic noise is produced by all electric devices, including radio and television transmitters and receivers.

c. Channel distortions, echo and fading because of the non-ideal communication channel characteristics. The propagation characteristics of the channel environment and signal fading are particularly sensitive to radio channels, such as those utilized by cellular mobile phone operators at GHz frequencies.

On the basis of frequency spectrum:

a. White noise: It contains all types of noise with equal intensity, as a result, it has a flat frequency spectrum giving rise to constant power.

b. Impulsive noise: They are sudden sharp and small duration of noises, detrimental to signal components severely. Here are different branches of impulsive noise models, which can be categorized as follows:

(1) Memory-less impulse noise model a) Middleton Class-A noise model b) Symmetric Alpha-Stable distribution (SαS) c) Bernoulli-Gaussian distribution

(2) Memory-based impulse noise model a) Markov-Middleton noise model b) Markov-Gaussian noise model

c. Transient noise pulses: Similar to impulsive noise just having a longer duration of pulses

1.3.1.1 Multipath Propagation of Electromagnetic Signals

In electromagnetic waves, the signals cannot reach the receiver directly due to the absence of a line of sight. As a result, the signals reflect at random objects and scatter as multiple components having superposition of scattered signal due to reflection, refraction and diffraction. The receiver receives these signals in various amplitude, phases and times. These phenomena is called multipath propagation. The presence of scatterers resulting from different phases and amplitude creates a different environment, signal smearing and delays the time to reach the signal to the receivers. If there is no multipath the source point signal will appear as another point signal at the receiver. multipath propagation can be described with the help of two parameters: Time dispersion and Fading [20-24]

Time dispersion: If the sender and receiver are at the foci and the scatterers are at the perimeter of an ellipse then, propagation due to the same ellipse will result in the same propagation delay. There are two conditions-

Maximum differential delay spread < symbol duration of transmitted signal = flat fading

Maximum differential delay spread > symbol duration of transmitted signal = frequency selective fading

Fading: Fading is the fluctuation in the strength of a signal on the receiver side in wireless communication. Time, location, and radio frequency are some variables considered in the variation of the attenuation of the received signal. Fading is termed as a random process. A communication channel that fades is referred to as a fading channel which depends on the carrier frequency and delay difference of the received signal. When two signal components are added destructively, they result in deep fading where the instantaneous signal power is low yielding poor signal strength.

1.3.1.2 Large-Scale Fading

Large scale fading denoted as statistical signal power attenuation and path loss due to movement over large area. The topographical structure between the transmitter and receiver affects it over a long distance. On the observation of the power, it shows that it fluctuates around a mean value and these fluctuation have a long period. The statistics of large-scale fading can be used to calculate path loss as a function of distance using a mean-path loss (nth -power law) and a log-normally distributed variance around the mean. [25-26]

1.3.1.3 Small-Scale Fast Signal Fading

If a radio signal amplitude fluctuates at a very short duration of time it is called small signal fading. Small fading occurs at the receiver end when two or more multipath signal component reaches at a very short difference of time [27].

Small-scale fading effects are created by multipath in the radio channel:

a. Rapid fluctuations in signal strength over a short travel distance or time interval

b. Random frequency modulation due to variable Doppler shifts on separate multipath signals.

c. Multipath propagation delays generate time dispersion (echoes).

1.3.1.4 Doppler Shift

In general, linear time invariant system, there is no new frequency component to the output of the signal than that of input. But in nonlinear time varying system, there prevails new frequency components other than input signals. In wireless mobile communication, the mobile and scatterers are not stationary. As a result, it is a mixture of linear but time variant system. The introduction to the frequency shift in sent signal is regarded as Doppler shifts [28].

The Doppler effect, often known as the Doppler Shift (or just Doppler), is the change in frequency of a wave as the observer moves away from the wave source. The wavelength of an emission is shortened or lengthened when a body emitting radiation has a non-zero radial velocity relative to an observer, depending on whether the body is moving towards or away from the observer. The Doppler shift refers to the change in wavelength or frequency noticed.

1.3.1.5 Small Scale Multipath Fading

The fast fluctuations in the amplitude and phase of a radio signal over a short period of time (in the order of seconds) or a short distance (a few wavelengths) are referred to as small-scale fading. When the receiver is shifted by a fraction of a wavelength in small-scale fading, the instantaneously received signal power can change by as much as 30 to 40 dB. Each path has its own Doppler shift, time delay, and path attenuation in a mobile-radio environment, and multipath propagation results in a time-varying signal as the location of the mobile moves [29].

The nature of the broadcast signal in relation to the channel characteristics determines small-scale fading. Different transmitted signals will experience different types of fading depending on the relationship between signal parameters such as bandwidth and symbol period on one hand, and channel parameters such as coherence time,

Doppler spread, coherence bandwidth and delay spread on the other hand. Time dispersion and frequency-selective fading are caused by delay spread. Frequency dispersion and time-selective fading are caused by Doppler spread. Dispersion in time and frequency is caused by separate propagation mechanisms. It occurs when two or more signal components experience interference. These are multipath waves which are combined at the receiver antenna. By observing the characteristics of PDFs of the envelope $\alpha(t)$ and phase $\theta(t)$ at any time t, the type of fading can be determined.

1.3.1.6 Rayleigh Fading (NLOS Propagation)

When there is no line-of-sight component, small-scale fading is also known as Rayleigh fading because the envelope of the received signal is statistically represented by a Rayleigh distribution when the number of versions of the transmitted signal arriving at slightly different time is significant. A Rician distribution is used to characterize the line-of-sight component if one exists. Non-line-of-sight (NLOS) signals are more likely to have attenuation between $\frac{1}{d^3}$ and $\frac{1}{d^6}$. When some of the reflected signals are lost, this extra loss of power occurs in propagation channels. When there is no direct ray component, Rayleigh fading is utilized to approximate rapid amplitude variations. Rayleigh fading is generally referred to as the worst-case fading type since it lacks a direct ray component. This small-scale distribution models the consequences of rapid amplitude fluctuation when the receiver traverses a few wavelengths using a one ray model. A great number of rays arrive at the receiver from different directions. The signals combine in and out of phase, causing amplitude fluctuations that vary at a rate determined by the receiver's speed. The Rayleigh probability distribution model is the statistical model that is used to characterize the amplitude variations. Because of the Doppler effect, the signal spreads in the frequency domain as the receiver moves [30-31].

1.3.1.7 Rician Fading (LOS Propagation)

Before reaching the receiver in a wireless environment, the sent signal may be subjected to several scatterings. This causes random oscillations in the received signal, which is referred to as fading. The signal's scattered version is referred to as the non-line of sight (NLOS) component. The fading process can be modeled as the sum of a large number of complex Gaussian process whose probability-density-function matches the Rayleigh distribution if the number of LOS components is large enough. In the absence of a dominant line of sight (LOS) path between the transmitter and the receiver, the Rayleigh distribution is well suited. If a line of sight path exists the envelope distribution becomes Rician rather than Rayleigh. The fading process can be written as the sum of a complex exponential and a narrowband complex Gaussian process if there is a dominating LOS component [32].

1.4 Power Spectral Density (PSD)

The power spectral density (PSD) of a signal is a measurement of how the signal's power is spread over frequency. It is a frequency-domain measure of a signal's power intensity. The PSD of a signal can be calculated as the square of the DFT magnitude. In the perspective of wide-sense stationary process, it can be proved that power spectrum is the fourier transform of auto correlation function written as [33]:

$$P_{xx}(f) = E[X(f)X^*(f)]$$
$$= \sum_{m=-\infty}^{\infty} r_{xx}(k)e^{-j2\pi fm}$$

where r_{xx} (m) and P_{xx} (m) are denoted as autocorrelation and power spectrum of x(m). the power spectrum may be written as For a real-valued stationary process as:

$$P_{xx}(f) = r_{xx}(0) + \sum_{m=1}^{\infty} 2r_{xx}(m)cos(2\pi fm)$$

The inverse Fourier transform of the power spectrum can be used to obtain the autocorrelation sequence of a random process. Which is:

$$r_{xx}(m) = \int_{-1/2}^{1/2} P_{xx}(f)e^{j2\pi fm}\, df$$

The Wiener-Khinchin theorem can be used to compute the power spectral density of a stochastic signal if a suitable and reliable statistical model is available. The PSD can be calculated as the Fourier transform of the signal's autocorrelation function for a wide-sense stationary random process, according to this formula.

$$S_{xx}(f) = F[R_{xx}(\tau)] = \int_{-\infty}^{\infty} R_{xx}(\tau)e^{-j2\pi f\tau}d\tau$$

where, Rxx(τ) is the auto-correlation function of the random process x(t) given by,

$$R_{xx}(\tau) = E\big(X(t)X(t-\tau)\big) = \int_{-\infty}^{\infty} x(t)x(t+\tau)dt$$

The fact that computing PSD is equal to fourier transformation of the auto correlation function can be proved as follows:

$$F[R_{xx}(\tau)] = \int_{-\infty}^{\infty} R_{xx}(\tau)e^{-j2\pi f\tau}d\tau$$

$$= \int_{-\infty}^{\infty}\int_{-\infty}^{\infty} x(t)x(t+\tau)e^{-j2\pi f\tau}d\tau dt$$

$$= \int_{-\infty}^{\infty} x(t) \underbrace{\int_{-\infty}^{\infty} x(t+\tau)e^{-j2\pi f\tau}d\tau dt}_{F[x(t+\tau)] = X(f)e^{j2\pi ft}}$$

$$= X(f) \int_{-\infty}^{\infty} x(t) e^{j2\pi f t} dt$$

$$= X(f) X^*(f) = |X(f)|^2$$

1.5 Diversity Mechanisms

Diversity methods deal with the transmission and reception of multiple copies of a signal, or a mixture of signals, along multiple independent paths, such as time slots, frequency channels, multipath reflections, spatial directions, or polarizations.

All signal paths in a diversity scheme transmit the identical set of messages, but channel characteristics, noise, and fading are uncorrelated. As a result, replicas of messages from several routes can be analyzed and concatenated to improve SNR. The degree to which noise and fading on distinct diversity branches are uncorrelated, as well as how information from different routes and channels is processed and merged, determines the success of diversity schemes [34].

1.5.1 Frequency Diversity

Signals are sent to the receiver over a number of frequency slots. These frequency slots should be separated enough so that each slot has individual fading and uncorrelation. The signal fading would be essentially uncorrelated for frequency separations greater than many times the coherence bandwidth.

1.5.2 Time Diversity

The signals are transmitted repeatedly over several time periods. The separation between the time periods must be such that the fading of one period of signal is independent of all other periods of signals. If the time interval between consecutive periods is large enough there will be a significant time delay, frequency exploitation, forward error correction and retransmission request.

1.5.3 Space Diversity

The sender and receiver often have more than one antennas. The spacing between consecutive antennas should be such that each antenna has independent fading. It is estimated that if two antenna have half of the carrier wavelength separation, the corresponding signal experience independent fading. The separation of at least 10 carrier wavelength can diminish the shadowing effect. Though this diversity adds more cost with more antenna, however, it does not require any extra system capacity.

1.5.4 Angle Diversity

Sometimes the antennas sends the signal components in various directions and the receiver receive the scattered signal from all direction. This is called angle diversity. It is considered as another form of space diversity as it also requires a number of antennas

1.5.5 Path Diversity

The use of direct sequence spread spectrum modulation allows the intended signal to be sent over a significantly broader frequency bandwidth than the channel coherence bandwidth. As long as path delays are separated by at least one chip period, the spread spectrum signal can resolve multipath components. By employing code correlation, a Rake receiver may separate the receive signal components from various propagation paths.

1.5.6 Polarization diversity

A horizontally polarized wave or a vertically polarized wave can be transmitted via antennas. When both waves are transmitted at the same time, the fading statistics of the received signals will be uncorrelated. Because distinct antennas are employed, this technique might be regarded as a specific case of space diversity. However, because there are only two orthogonal polarizations, there are only two diversity branches available.

1.6 Literature Review

A lot of research works have been done on wireless communication with transmit diversity and receive diversity to improve receiver sensitivity and range of operation [35]. Radio Frequency Identification (RFID) [36] communication systems are also getting more and more importance in wireless networking using UWB technology. More recently, research is done on application of diversity in UWB RFID wireless communication systems to increase in the range of RFID network. The research works expressed that various methods have been developed for combining independently faded signal components, and the tradeoff among these methods is the receiver complexity versus transmission performance improvement. Research works also shows that, diversity is used to overcome flat fading and equalization to overcome inter symbol interference due to channel time dispersion. Some of the research works are given below:

Diversity combining techniques have been of great importance as far as improving performance is concerned in wireless communications. In this reference work, a new hybrid diversity scheme has been proposed for Rayleigh fading channel in which L number of Maximal Ratio Combiner (MRC) receiver, each Selection Combiner (SC) having branches at its input, are selection combined to obtain the final output at the receiver [37].

Dual Carrier Modulation (DCM) is widely used as the higher data rate modulation technique for Multiband Orthogonal Frequency Division Multiplexing (MB-OFDM) Ultra Wideband (UWB) in European Computer Manufacture Association (ECMA-368) standard. DCM is one of the high data rate modulation technique that provides a significant frequency diversity improvement by modulating the information symbols across non-adjacent subcarriers of OFDM modulator [38].

Diversity combining is the effective way to mitigate the effects of multipath fading. The independent signal paths have low probability of experiencing deep fades

simultaneously is the fact exploited by diversity combining. In diversity combining the replicas of same information signal is combined together to obtain high SNR. The Hybrid Diversity combining techniques have been carried out to reduce the effects of fading owing to its good performance and low implementation complexity [39].

A novel technique for increasing the detection range of a fully passive multiresonator based chipless RFID tag has been proposed using the Diversity technique at the reader receiver. Analysis is carried out to find the signal to noise ratio at the output of the diversity receiver using maximal ratio combining (MRC) technique. Bit error rate (BER) is analyzed for Rayleigh fading over the channel [40].

Performance analysis of multiband orthogonal frequency division multiplexing (OFDM) based ultra wideband (UWB) system in the presence of log-normal fading channels has been widely discussed in the reference paper [41].

In hybrid selection/maximal ratio combining the receiver selects the L branches with the largest signal-to-noise ratios from N available diversity branches and performs maximal ratio from N available diversity branches and performs maximal ratio combining. A penalty is incurred with respect to maximal ratio combining which can be defined as the increase in signal-to-noise ratio required for hybrid combining to achieve the same symbol error probability as maximal ratio combining [42].

The emerging ultrawideband (UWB) system offers a great potential for the design of high speed short-range wireless communications. In order to satisfy the growing demand for higher data rates, one possible solution is to exploit both spatial and multipath diversities via the use of multiple-input multiple-output (MIMO) and proper coding techniques [43].

Emerging very high-data-rate wireless communications requires that traditional diversity systems be adapted so that some performance is sacrificed for complexity reduction. This paper investigated the recently-developed absolute threshold generalized selection combining (AT-GSC) and showed that AT-GSC has poor bit-

error rate (BER) performance when the average branch signal-to-noise ratio (SNR) is comparably lower than the preset threshold. This paper therefore develops a new diversity combining scheme, referred to as switching GSC (S- GSC) [44].

Diversity is an effective technique to improve wireless communication performance. In this paper, a dual hybrid diversity scheme is proposed in which connected branches are switched in order to determine whether a dual branch should be combined via maximal ratio combining (MRC) in multi-branch. This scheme provides improved performance along an additional diversity branch available, without requiring signal power. Also, it achieves additional performance gain by adaptive switching thresholds [45].

An approach to the performance analysis of hybrid MRCS (Selection Maximal Ratio Combining) diversity system operating over Rician fading channels is presented in the reference paper. Hybrid MRCS combining method has a simple implementation, where maximal ratio combined signals are chosen on a selection combining basis. Closed form expressions are provided for standard first and second order statistical measures for the signal at the output of the combiner, ie PDF (probability density function), CDF (cumulative distribution function), LCR (level crossing rate). Capitalizing on them standard performance measures like ABEP (Average Bit Error Probability) over some modulation techniques and AFD (Average Fade Duration) are efficiently evaluated and discussed in the function of various system parameters.

The outage probability and Average Bit Errir Rate (ABER) are the parameters which are used for the performance analysis of MRC/EGC Hybrid combining technique- the fact has been analyzed in the reference paper [46].

In order to improve the performance of wireless transmissions, in addition to multi-channel propagation, error correction codes are used. Golden Code has some advantages, such as: maximum rate and diversity or coding gain. In this paper it is proposed an approach of using this code to mitigate the impulsive noise effects in a

MIMO communication system. The Middleton Class-A noise was considered. The simulation was done for different values of the impulsive noise model parameters and showed that the probability density function depends on index impulse and on gaussian factor and the number of noise sources has no influence [47].

The Orthogonal Frequency Division Multiplexing (OFDM) with high data rate, high spectral efficiency and its ability to mitigate the effects of multipath makes them most suitable in wireless application. Impulsive noise distorts the OFDM transmission and therefore methods must be investigated to suppress this noise. In this paper, a State Space Recursive Least Square (SSRLS) algorithm based adaptive impulsive noise suppressor for OFDM communication system is proposed. And a comparison with another adaptive algorithm is conducted [48].

Orthogonal frequency division multiplexing (OFDM) is a form of multicarrier transmission technique widely used in the modern wireless network to achieve high-speed data transmission with good spectral efficiency. However, in impulsive noise environment BER performances of these systems, originally designed for a Gaussian noise model, are much degraded. In this paper, a new symmetric-alpha-stable (SαS) noise suppression technique based conjointly on adaptive modulation, convolutional coding (AMC) and Recursive Least Square (RLS) filtering is presented. The proposed scheme is applied on OFDM system in Rayleigh fading channel. The transmissions are analyzed under different combinations of digital modulation schemes (BPSK, QPSK, 16-QAM, 64-QAM) and convolutional code rates (1/2, 2/3, 3/4). Simulation results show that proposed hybrid technique of the author provides effective impulsive noise cancelation in OFDM system and exhibits better BER performance [49].

The prevalence of impulsive electromagnetic interference, atmospheric or ignition noise necessitates thorough analysis of their effects on the performance of diversity combining schemes. In this paper, Middleton's class A model is adopted for the noise distribution, and analyze the performance of different diversity combining techniques over fading channels with statistically dependent impulsive noise on each branch. We

systematically analyze the performance of maximum ratio combining (MRC), equal gain combining (EGC), selection combining (SC), and post-detection combining (PDC) under the impulsive noise model, and derive insightful upper bounds. We show that even under impulsive noise, the diversity order is retained for each combining scheme. However, there is a fundamental tradeoff between diversity gain and coding gain [50].

Among the manmade sources dominant source of impulsive interference occurs in the electricity supply industry. These noises can cause significant degradation of the performance of conventional wireless communication systems. This paper introduces a concept of impulsive noise reduction utilizing the Empirical Mode Decomposition (EMD) framework, where noisy signal is decomposed adaptively into oscillatory components called Intrinsic Mode Functions (IMFs) by means of a process called sifting. The EMD denoising involves filtering or thresholding each IMF and reconstructs the estimated signal using the processed IMFs. To simulate the denoising phenomenon, input information signals, impulsive noises and EMD algorithms were generated in Matlab. The input signals were degraded by adding impulsive noise and then empirical mode decomposition was performed on the noisy signals. Simulation results suggest that a signal corrupted by impulsive noise can be considerably recovered by the EMD method [51].

1.7 Objectives of this Research

The objectives of this thesis research are:

a. To develop an analytical model of BER for an OFDM Wireless Communication System with Hybrid Receive Combining Techniques over Rayleigh fading channel and to evaluate BER performance.

b. To formulate an analytical model and evaluate BER for the above systems considering Rayleigh fading channel, and Middleton Class A and Symmetric Alpha Stable impulsive noise models.

c. To develop an analytical model to evaluate the impact of impulsive noise on BER performance of an OFDM OSTBC MIMO wireless communication system.

d. To simulate OFDM OSTBC MIMO wireless communication system considering impulsive noise and Rayleigh fading and to verify analytical result.

e. To find out an appropriate mitigation technique to overcome the effect of impulsive noise.

1.8 Possible Outcome of this Research

This thesis is unique in nature and shall bring forth the following results:

a. This study will help in the development of an analytical tool to evaluate the effect of impulsive noise on BER performance.

b. It will also help in designing an OFDM OSTBC MIMO wireless communication system.

1.9 Outline of the Thesis

This thesis paper comprises of seven chapters. The contents of the respective chapters are outlined below:

Chapter 1 is the introductory column of the entire study covering the wireless communication system, history, limitations, propagation, fading, literature review, objective, and possible outcome of the research along with the thesis layout.

Chapter 2 describes the analysis of OFDM SIMO Wireless communication system with hybrid receive combining and MRC Techniques over Rayleigh fading channel. It broadly covers the comparison of BER performance for different basic diversity combining techniques considering Gaussian noise under Rayleigh fading environment.

Chapter 3 includes the BER analysis of OFDM SISO and SIMO System considering Impulsive noise model over Rayleigh fading channel. This description involves Poisson's Noise model, Middleton Class A noise model and SαS noise model for analyzing effect of Gaussian noise and Impulsive noise on wireless communication performance under Rayleigh fading scenario.

Chapter 4 describes the impact of Impulsive noise on BER performance of an OFDM OSTBC MIMO wireless communication system. In this chapter, coding is considered for the performance analysis and coding efficiency is compared with reference paper.

Chapter 5 describes the simulation model for wireless communication link with Impulsive noise. Simulation is carried using MATLAB considering different basic and hybrid receive combining techniques under Impulsive noise.

Chapter 6 discusses performance analysis of different impulsive noise mitigation techniques and their comparison.

Chapter 7 contains the conclusion of the work with few recommendations for future works.

CHAPTER 2

ANALYTICAL MODEL OF SIMO WIRELESS SYSTEM WITH HYBRID DIVERSITY

2.1 Introduction

Diversity has long been recognized as an effective technique for combatting the detrimental effects of channel fading. The diversity combining techniques are used to improve the performance of receiver having multiple antennas. In order to overcome the performance degradation of communication systems over a fading channel, the receiver diversity is usually employed. The Maximal Ratio Combining (MRC), Equal Gain Combining (EGC) and Selection Combining (SC) are various diversity combining techniques. MRC requires the individual signals from each path to be time-aligned, co-phased, optimally weighted by their own fading amplitude, and then summed. In Selection Combining (SC), the signal in the branch with highest signal to noise ratio (SNR) is selected among all the signals in all the branches. The signals in all the branches are combined by multiplying with equal weights in Equal Gain Combining. MRC provides the maximum performance improvement relative to all other combining techniques by maximizing the signal-to-noise ratio (SNR) of the combined signal. However, MRC also has the highest complexity of all combining techniques since it requires knowledge of the fading amplitude in each signal branch. Hence, alternative techniques such as EGC and SC are often used in practice because of their reduced complexity relative to the optimum MRC scheme [52]. Hybrid diversity combining techniques have been receiving great interest in recent days by considering various aspects like low power consumption and higher diversity gain [53].

2.2 System Block Diagram

2.2.1 Hybrid SC-EGC for Rayleigh Fading Channel

Proposed system model of hybrid receive diversity (SC-EGC) at the reader receiver is given in Fig. 2.1 below. The system is composed of a reader (Interrogator) and a tag (Transponder) each equipped with an antenna serving the purpose of both transmitter and receiver simultaneously with the help of duplexers. When the interrogation signal

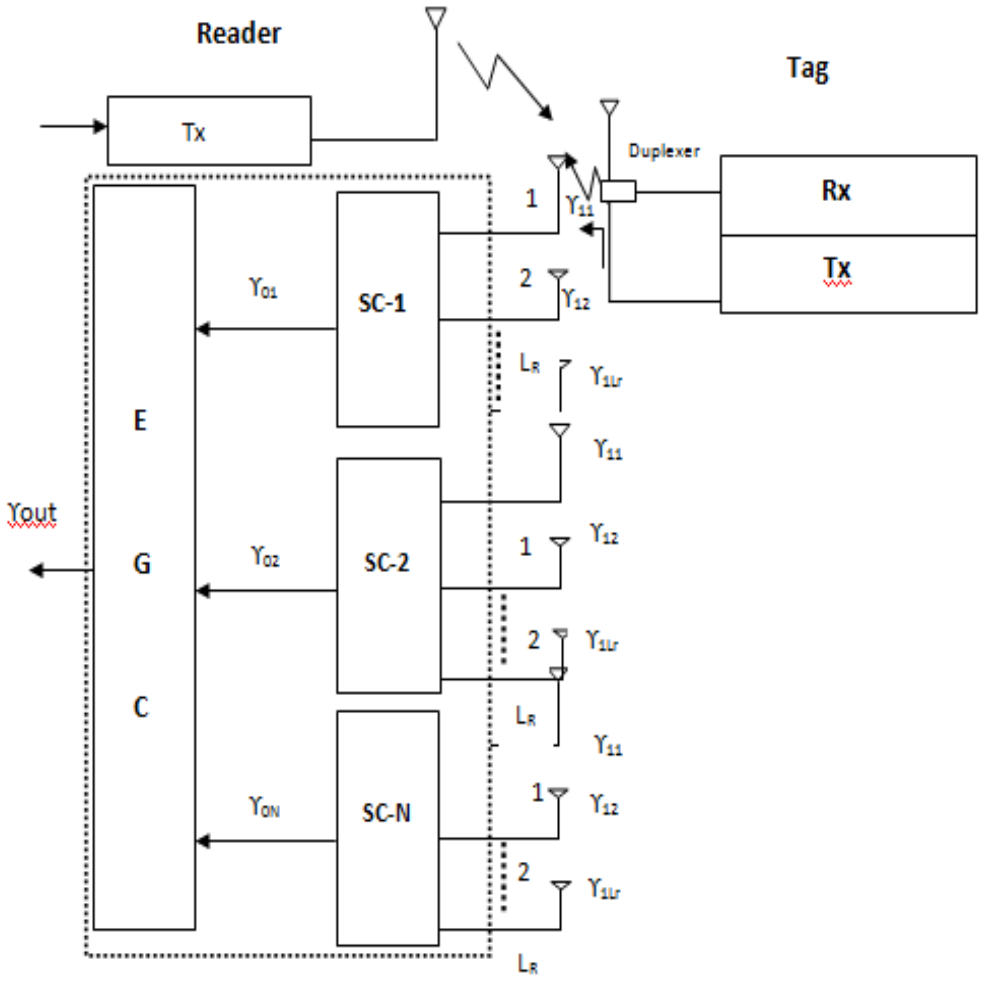

Fig.2.1 The proposed system model with hybrid diversity at the reader receiver

from the reader reaches the tag, it is received using the receiving antenna of the tag and propagates further on towards the multi resonating circuit imprinted on the tag. The multi resonating circuit encodes data bits using cascaded spiral resonators, which introduce attenuation and phase jumps at particular frequencies of the spectrum. After passing through the multi resonating circuit, the signal contains the unique spectral signature of the tag and is transmitted back to the reader receiver by the transmitting tag antenna [54].

2.2.2 Hybrid SC-MRC for Rayleigh Fading Channel

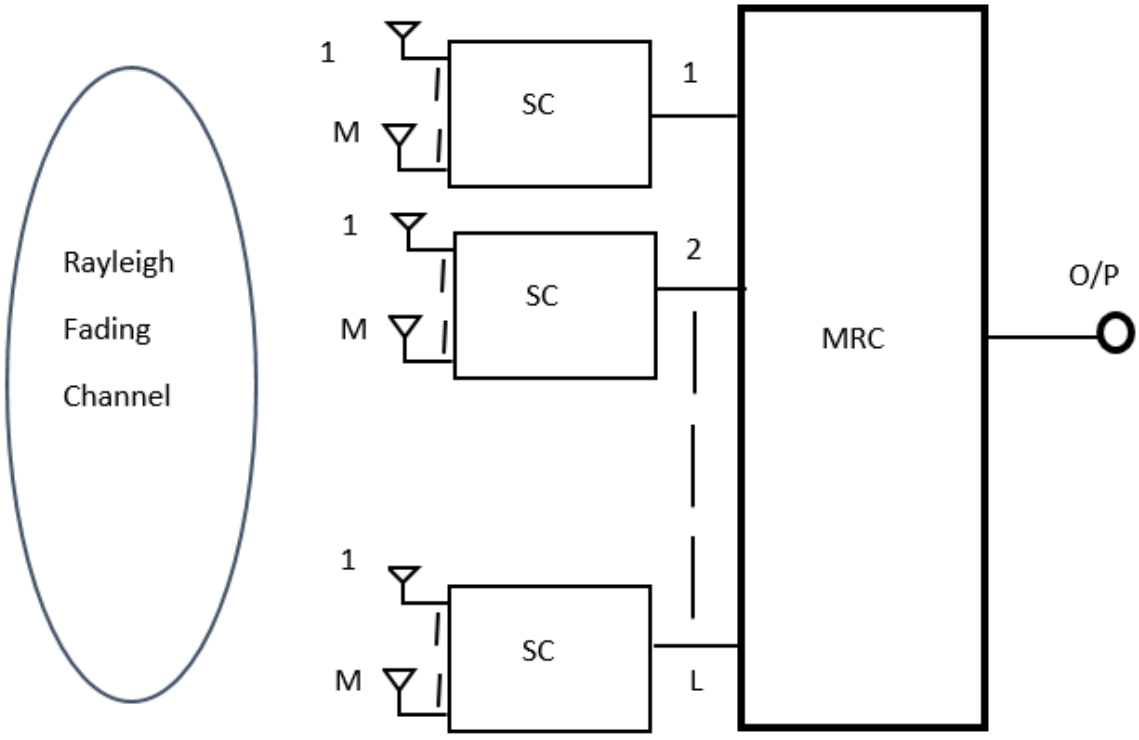

Fig. 2.2 Hybrid SC-MRC System for Rayleigh Fading Channel

In the hybrid SC/MRC System over Rayleigh Fading shown in the Fig.2.2, there are L numbers of selection combiners each having M number of input branches. Each of the M branches receive the signal from individual antennas kept sufficiently apart to

have negligible correlation among the receiver branch signals. The output of each of the L selection combiners is fed to a differential detector block. Finally, the output of all the differential detectors are processed using MRC diversity combining [55].

2.2.3 Hybrid MRC-SC for Rayleigh Fading Channel

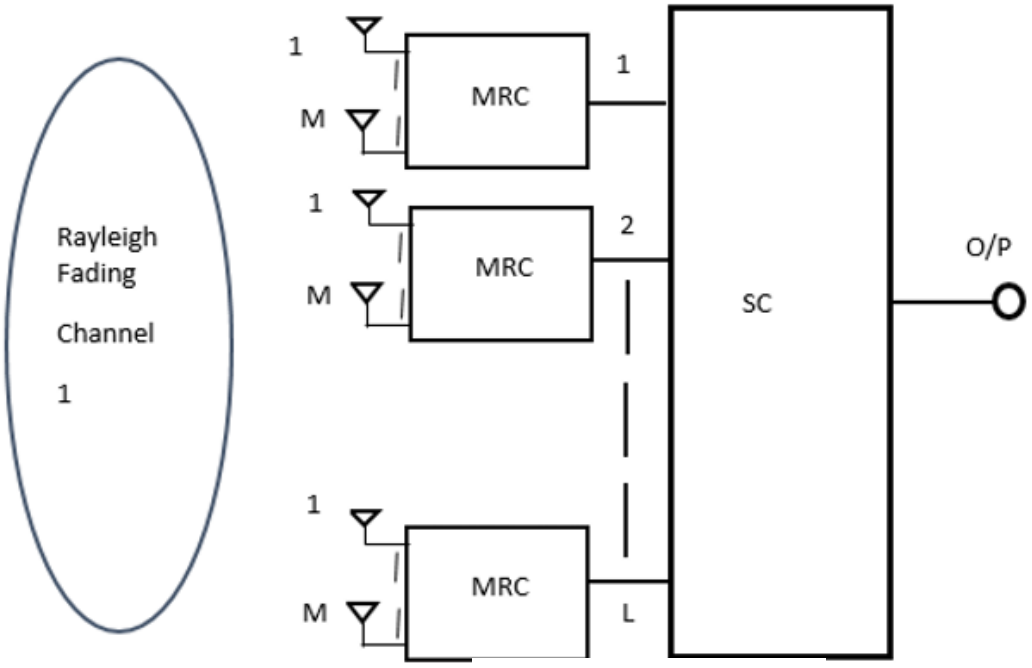

Fig. 2.3 Hybrid MRC-SC System for Rayleigh Fading Channel

In the hybrid MRC/SC System over Rayleigh Fading shown in the Fig.2.3, signal is received by L numbers of MRC having M diversity branches. The M received signals are weighted and combined to give maximum SNR. From L such systems, the one with the highest SNR is selected using SC having L diversity branches [56].

2.3 Analysis

2.3.1 Analysis for Hybrid SC-EGC System for Rayleigh Fading Channel

The transmitted BPSK signal from the reader can be represented as

$$s(t) = \sqrt{2P_{TX}}\cos\omega_c t \times \sum_{k=0}^{\infty} a_k p(t - k_p) \quad (2.1)$$

where a_k represents the k-th bit, P_{TX} is the transmitted power per bit and p(t) is the pulse shape for the data bit, T_p is the bit period. The signal received by the tag at a distance d_1 is given by

$$r_1(t) = \sqrt{2P_{TX}} \times e^{-\propto d_1} \times \cos[\omega_c t - \beta d_1]\sqrt{G_1(f)} \quad (2.2)$$

where (α+jβ) represents the propagation constant $G_1(f)$. The signal re-transmitted by the tag with some processing is given by

$$e_2(t) = \sqrt{2P_{TX}G_t}e^{-\propto d_1}\cos(\omega_c t - \beta d_1) \times \sqrt{G_1} \quad (2.3)$$

where G_t is the gain incorporated by the processing unit of the tag at the carrier frequency. The signal received by the reader antenna can be represented as:

$$r(t) = \sqrt{2P_{TX}G_t}e^{-\propto d}\cos(\omega_c t - \beta d) \times \sqrt{G_1(f).G_2(f)} \quad (2.4)$$

Where, $d=2d_1$, is the round-trip distance for reader to tag. The overall gain for the round-trip propagation can be represented as $G(f)= G_1(f).G_2(f)$

$$G(f) = \frac{P_{RX}}{P_{TX}} = \frac{1}{2}G_0\eta_{TX}\eta_{RX}\left(\left(\left(\frac{f}{f_c}\right)^{-2(k+1)}\right)/\left(\frac{d}{d_0}\right)^n\right) \quad (2.5)$$

where, f_{min} is the minimum frequency, f_{max} is the maximum frequency, f_c is the reference frequency, P_{RX} is the receive power, G_0 is the path loss in reference distance in dB, η_{TX} is the antenna transmit efficiency, η_{RX} is the antenna receive efficiency, k is the decaying factor, n is the path loss exponent. Let, Υ_{ij} is the SNR at the j-th input of i-th selection combiner and can be represented as

$$\gamma_j^i = \frac{p_{rj}^i}{N_0} T_b \quad \text{i=1: } L_c \text{ , j=1:} L_r$$

where p_{rj}^i is the average power received at the input of i-th SC which can be obtained from eqn (2.4), L_r and L_c represent the number of antenna for SC and EGC respectively. N_0 is the noise power spectral density [57].

$$P(\gamma_j^i = x) = \frac{1}{\Gamma_c} exp\left(-\frac{x}{\Gamma_c}\right)$$

Let us define the SNR of the output of i-th Selection Combiner (SC) as

γ_0^i=Max$\{\gamma_j^i\}$ j=1:L_r

Then pdf of the output SNR of i-th SC can be represented as

$$p(\gamma_0^i) = \frac{L_\gamma}{\Gamma_c} exp\left[\gamma_0^i / \Gamma_c\right]\left[1 - exp\left(-\frac{\gamma_0^i}{\Gamma_c}\right)\right]^{L_\gamma - 1} \quad (2.6)$$

where $\Gamma_c = \gamma_b E[\alpha_l^2]$ is the mean SNR per bit of each diversity channel.

The overall output SNR of the EGC is then given by

$$\gamma_{out} = \sum_{i=1}^{N} \gamma_{0i} \quad (2.7)$$

The conditional bit error rate can be evaluated as

$$P_b(\gamma_{out}) = \frac{1}{2} erfc[\frac{\sqrt{\gamma_{out}}}{\sqrt{2}}] \quad (2.8)$$

The average BER can be obtained as

$$BER = \int P_b(\gamma_{out}).f_{\gamma_{out}}(\gamma_{out}) d\gamma_{out} \quad (2.9)$$

The pdf of γ_{out} can be obtained as

$$p(\gamma_{out}) = p(\gamma_0^1) \otimes p(\gamma_0^2) \otimes \ldots\ldots\ldots\ldots \otimes p(\gamma_0^N) \quad (2.10)$$

where, $\otimes$ denotes convolution.

2.3.2 Analysis for Hybrid MRC-SC System for Rayleigh Fading Channel

In hybrid MRC-SC system, signal is received by L number of MRC having M diversity branches. The M received signals are weighted and combined to give maximum SNR. From L such system, the one with the highest SNR is selected using SC having L diversity branches. The system model is presented in Fig. 2.3. Considering Rayleigh fading channel, MRC having M diversity branches the output SNR is given by [58]:

$$f_{MRC}(\gamma) = \frac{\gamma^{M-1} e^{\frac{-\gamma}{\vec{\gamma}}}}{\vec{\gamma}^{M}\Gamma(M)} \tag{2.11}$$

Where γ = instantaneous SNR

$\underset{\gamma}{\rightarrow}$ = average SNR

$\Gamma(M)$ = Gamma Function

The Rayleigh distribution is often used to model multipath fading with no direct line-of-sight (LOS) path. Its PDF is given by [59]

$$P_{\alpha}(\alpha) = \frac{2\alpha}{\Omega} e^{-\frac{\alpha}{\Omega}} \tag{2.12}$$

Where, $\alpha \geq 0$, $\propto$ is channel fading amplitude, a random variable (RV), $\Omega = \bar{\alpha}^2$ (mean - square).

The CDF of the MRC receiver can be obtained using 2.11 as

$$F_{MRC}(\gamma_0) = \frac{1}{\bar{\gamma}^{M}\Gamma(M)} \int_0^{\gamma_0} \gamma^{M-1} e^{-\frac{\gamma}{\bar{\gamma}}} \, d\gamma \tag{2.13}$$

Eqn 2.13 can be further simplified as follows:

$$F_{\gamma MRC}(\gamma_0) = \frac{1}{\Gamma(M)} \, g\left(M, \frac{\gamma_0}{\vec{\gamma}}\right) \tag{2.14}$$

The inputs of EGC and MRC outputs. In EGC, the signals are equally weighted by their amplitude. In other words, the branch weights are all set to unity. By multiplying MRC outputs each with equal weights and then carrying L fold convolution of PDF of output SNR of MRC, PDF of hybrid MRC-EGC system can be obtained using eqn 2.14:

$$F_{\gamma MRC}(\gamma_0) = \frac{1}{\Gamma(M)} g(M, \frac{\gamma_0}{\bar{\gamma}}) \tag{2.15}$$

In SC diversity, signal having the highest SNR is sent to detector for the purpose of detection. The inputs to the SC system are the MRC outputs. Hence, the CDF of the output of MRC/SC receiver can be obtained as $F_{(MRC.SC)}(\gamma) = \prod_{i=1}^{L} F_{\gamma i}(\gamma_i)$ putting the expression of eqn 2.15 we get [59]

$$F_{(MRC.SC)}(\gamma) = \prod_{i=1}^{L} \left[\frac{1}{\Gamma(M)} g\left(M, \frac{\gamma_i}{\bar{\gamma}}\right)\right]. \tag{2.16}$$

Considering fading parameters as same and approximately equal average SNR in each branch, the CDF of SC receiver in this can be obtained as [59],

$$F_{(MRC,SC)}(\gamma) = \left[\frac{1}{\Gamma(M)} g(M, \frac{\gamma}{\bar{\gamma}})\right]^L \tag{2.17}$$

The PDF of the output SNR of the hybrid MRC/SC receiver can be obtained by differentiating eqn 2.17 with respect to γ. The resulting expression after simplification is

$$f_{MRC,SC}(\gamma) = \prod_{i=1}^{L-1} \sum_{n=0}^{\infty} \frac{L(\eta)^{M_i+M+n}}{\{\Gamma(M)\}} \frac{e^{-2\eta\gamma}}{M_i(M_i+1)n} \gamma^{M_i+M+n-1} \tag{2.18}$$

Where $\eta = \frac{1}{\bar{\gamma}}$ and $(x)_n$ is Poch hammer symbol. M_i is diversity branches for different value of i.

For identical fading parameter the expression of P_{out} can be obtained from 2.17 as

$$P_{out\ MRC,SC(\gamma_{th})} = \left[\frac{1}{\Gamma(M)} g\left(M, \frac{\gamma_{th}}{\bar{\gamma}}\right)\right]^L \tag{2.19}$$

An expression for the ABER can be obtained by averaging the conditional bit error rate (BER), $p_e(\varepsilon|\gamma)$ [58], for the modulation scheme used, over the PDF of the SC output SNR. Mathematically it can be given as

$$P_e(\bar{\gamma}) = \int_0^{\infty} p_e(\varepsilon|\gamma) f_{MRC,SC}(\gamma) d\gamma \tag{2.20}$$

For binary coherent modulations, the expression for the conditional BER can be given as $p_{e,ch}(\varepsilon/\gamma) = Q(\sqrt{2\alpha\gamma})$, where $\alpha = 0.5,1$ for coherent frequency shift-keying (CFSK) and coherent phase shift-keying (CPSK) modulation, respectively. Putting $p_{e,ch}(\epsilon/\gamma_{SC})$ and $f_{\gamma_{SC}}(\gamma_{SC})$ from eqn 2.18 together into and solving the integral, an expression for the ABER for identical fading parameter can be obtained as [58]

$$P_{e.ch}(\bar{\gamma}) = \frac{L\sqrt{\alpha}}{2\sqrt{\pi}} \frac{1}{\{\Gamma(M)\}^L} \sum_{n=0}^{\infty} \frac{(\eta)^{M_i+M+n}}{M_i(M_i+1)n} \quad \frac{\Gamma(M_i+M+n\_0.5)}{(M_i+M+n)(\alpha+2\eta^{M_i+M+n+0.5}}$$

$$2F_i(1, M_i + M + n + 0.5; M_i + M + n + 1; \frac{2\eta}{\alpha+2\eta}) \tag{2.21}$$

where $2F_i$ (a;b;c;z) is a hypergeometric function.

2.3.3 Analysis for Hybrid SC-MRC System for Rayleigh Fading Channel

SC is the simplest form of diversity combining whereby the received signal from one of N diversity branches is selected. The output SNR of SC is [60]

$$\gamma_{SC} = \max\{\gamma_i\} \tag{2.22}$$

The mean and variance of the combiner output SNR for SC becomes [61]

$$\Gamma_{SC} = \Gamma \sum_{n=1}^{N} \frac{1}{n}, \tag{2.23}$$

$$\sigma_{SC}^2 = \Gamma^2 \sum_{n=1}^{N} \frac{1}{n^2}, \tag{2.24}$$

respectively. Therefore, the average SNR gain of SC is

$$G_{SC} = 10\, log_{10} \left\{\sum_{n=1}^{N} \frac{1}{n}\right\}, \tag{2.25}$$

In MRC, the received signals from all diversity branches are weighted and combined to maximize the SNR at the combiner output. The output SNR is given by [62]

$$\gamma_{MRC} = \sum_{i=1}^{N} \gamma_{(i)} \tag{2.26}$$

Therefore, the average SNR gain of MRC is

$$G_{MRC} = 10\ log_{10}\{n\} \tag{2.27}$$

and normalized standard deviation of the MRC is

$$\sigma_{n,MRC} = 10log_{10}\left\{\frac{1}{\sqrt{N}}\right\}, \tag{2.28}$$

The instantaneous output SNR of H-SC/MRC is [63]

$$\gamma_{SC/MRC} = \sum_{i=1}^{L} \gamma_{(i)} \tag{2.29}$$

where $1 \leq L \leq N$,

The mean and the variance of the combined output SNR can be easily obtained as

$$\Gamma_{SC/MRC} = L\left(1 + \sum_{n=L+1}^{N} \frac{1}{n}\right)\Gamma, \tag{2.30}$$

$$\sigma^2_{SC/MRC} = L\left(1 + L\sum_{n=L+1}^{N} \frac{1}{n^2}\right)\Gamma^2\ , \tag{2.31}$$

respectively. Therefore, the average SNR gain of H-SC/MRC in dB is [64]

$$G_{SC/MRC} = 10log_{10}\left\{L\left(1 + \sum_{n=L+1}^{N} \frac{1}{n}\right)\right\}, \tag{2.32}$$

and normalized standard deviation of the combined output SNR in dB is [65]

$$\sigma_{n,SC/MRC} = 10log_{10}\left\{\frac{\sqrt{\left(1+L\sum_{n=L+1}^{N}\frac{1}{n^2}\right)}}{\sqrt{L\left(1+\sum_{n=L+1}^{N}\frac{1}{n}\right)}}\right\}, \tag{2.33}$$

2.4 Results and Discussion

2.4.1 BER Performance

Following the analytical approach, BER performance results for a UWB system are evaluated for residential as well as industrial environment. The building structures of residential and industrial environments are characterized by small units, with indoor walls of reasonable thickness. Here the transmission power is assumed to be 100mw. Other parameters are assumed as, f_{min}= 3GHz, f_{max}=10 GHz, f_c=5GHz, BW=$\frac{1}{Tp}$, n=4.58, G_0= -40db, d_0=1 meter, G_t=1.0, η_{TX}=.80, η_{RX}=.20 and k=1.53. These parameters have already been used in previous analysis in a research work and have been accepted as standardized model by IEEE 802.15.4a [53]. The plots BER versus distance d in case of an indoor residential environment for a fixed transmission power is shown in Fig 3.1. The maximum achievable distance d_{max} for a given BER of 10^{-5} with N_r=1 are shown in the Table-1 for different value of L_r. From Fig 2 it is clearly evident that, for a particular BER (for example 10^{-5}) a combination of 5 antennas help achieving better distance compared to that is achieved by a single receiving antenna.

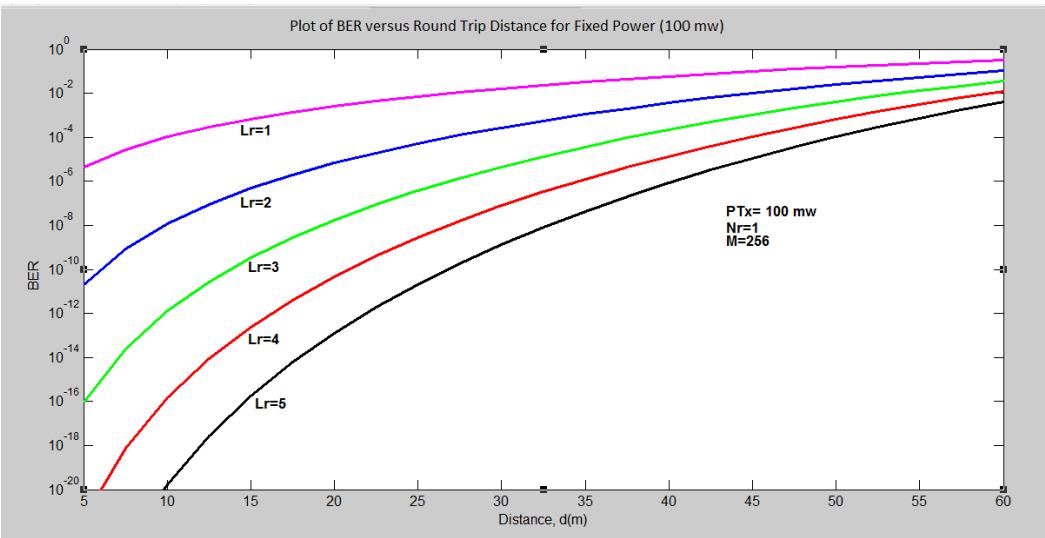

Fig 2.4 BER versus Round Trip Distance for different number of antennas (Indoor residential environment for fixed power, N_r=1)

TABLE I
Maximum distance vs Number of Antenna
(Indoor residential environment- for fixed BER=10^{-5} for N_r=1)

L	d_{max} (P_{TX}=100mw)	d_{max} (P_{TX}=150mw)	d_{max} (P_{TX}=200mw)
1	5	6	7
2	22	23	24
3	32	33	36
4	40	43	47
5	46	48	52

2.4.2 BER Versus Maximum Distance for Different Number of Antennas

The plots of maximum allowable distance, d_{max} for a given BER of 10^{-5} for different

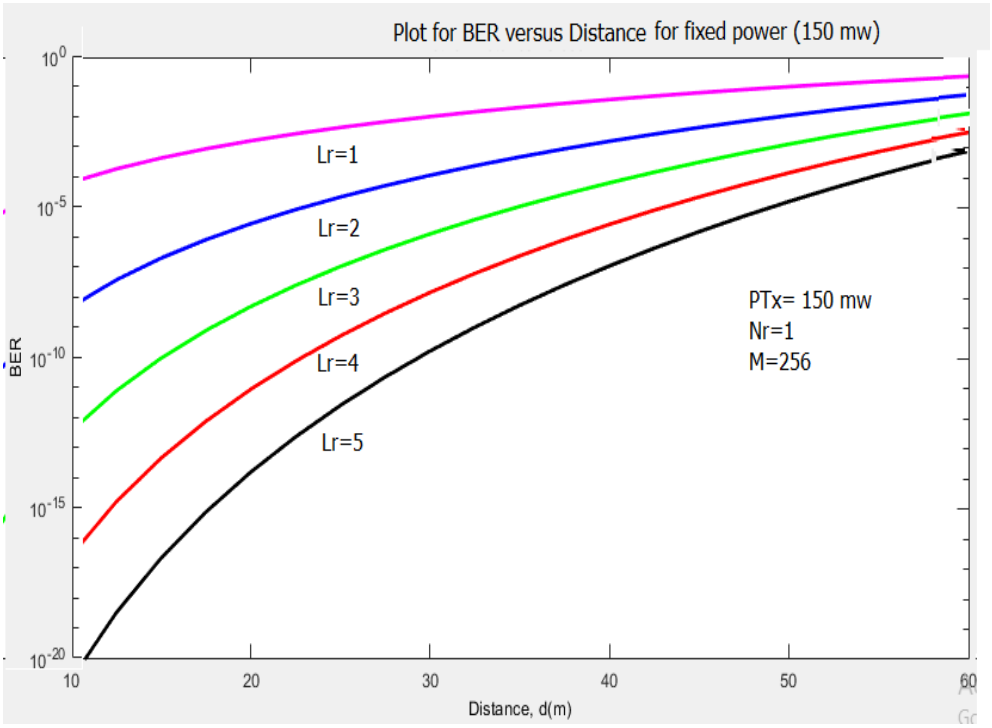

Fig 2.5 BER versus Maximum distance for different number of antennas for BER= 10^{-5} and N_r=1

number of antennas for a fixed BER (10^{-5}) and different transmit power with Nr=1 is shown in Fig 3.2. From Fig.3.2, it is clear that with increase of transmit power and number of antenna higher distance can be achieved compared to single antenna system.

In Fig 2.6 below, the allowable distance vs BER for N_r=1 in case of an industrial environment is Presented. For a fixed BER i.e BER=10^{-5} or 10^{-6} data has been taken for different number of antennas for fixed power of 100mw, 150 mw and 200 mw. The detail data is shown in Table II. From Table II and III it is clearly evident that, for a

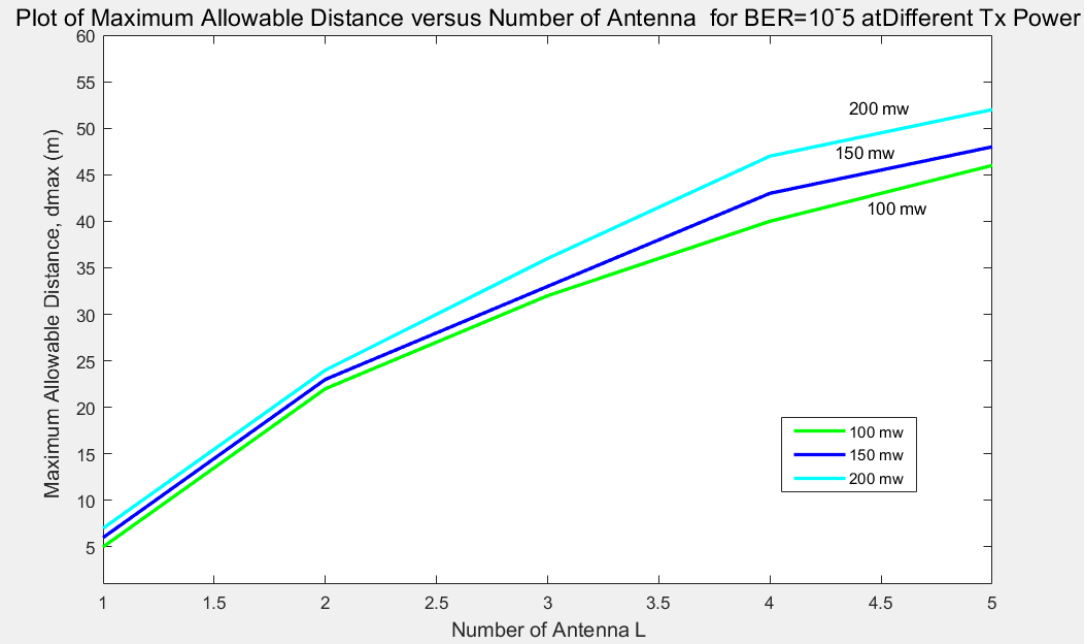

Fig 2.6.Maximum Allowable roundtrip distance vs Number of Antenna (industrial environment- For 100 mw, 150 mw and 200 mw power, N_r=1)

particular BER (for example 10^{-5} or 10^{-6}) a combination of 5 antennas help achieving better distance compared to that is achieved by a single receiving antenna.

TABLE II

Distance versus BER (Industrial Environment- for fixed BER= 10^{-4} to 10^{-8} and N_r=1

BER	Distance in Meter (m) for different L				
	L=1	L=2	L=3	L=4	L=5
10^{-4}	10	26	42	50	54
10^{-5}	06	22	34	42	48
10^{-6}	-	15	27	35	42
10^{-7}	-	12	23	30	38
10^{-8}	-	10	20	28	36

2.4.3 Results and Discussion

An analytical approach has been made to find the performance comparison of SC-MRC, SC-EGC and MRC-SC hybrid diversity combining system. A comparison of BER improvement has been made with another two Hybrid Diversty namely SC/MRC and MRC/SC Diversity combining [66] and [67]. Result for all the three systems are shown below:

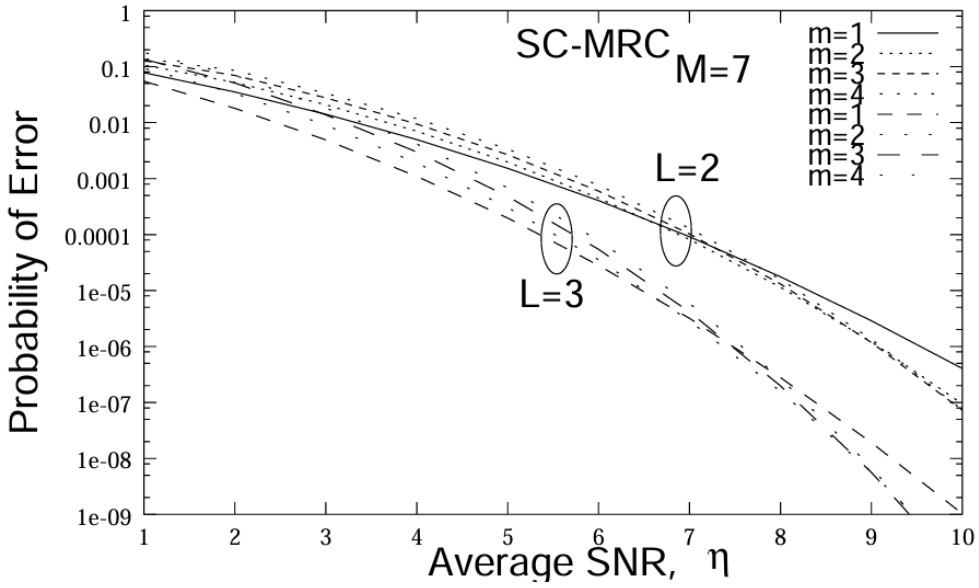

Fig: 2.7 BER Curves for SC/MRC

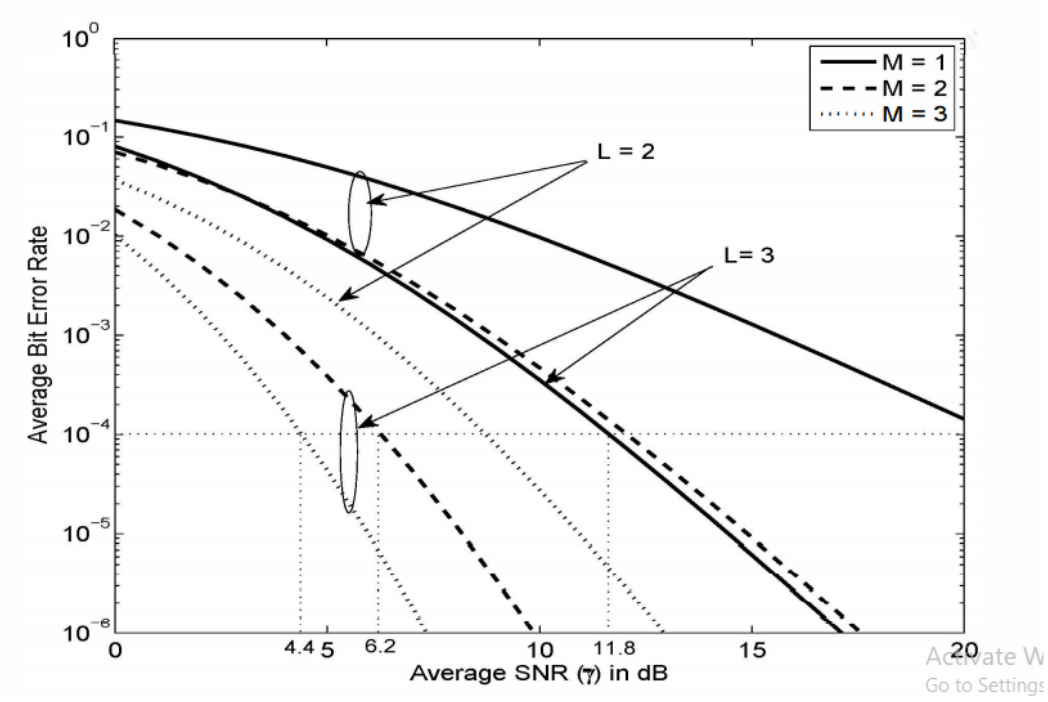

Fig: 2.8 BER Curves for MRC/SC

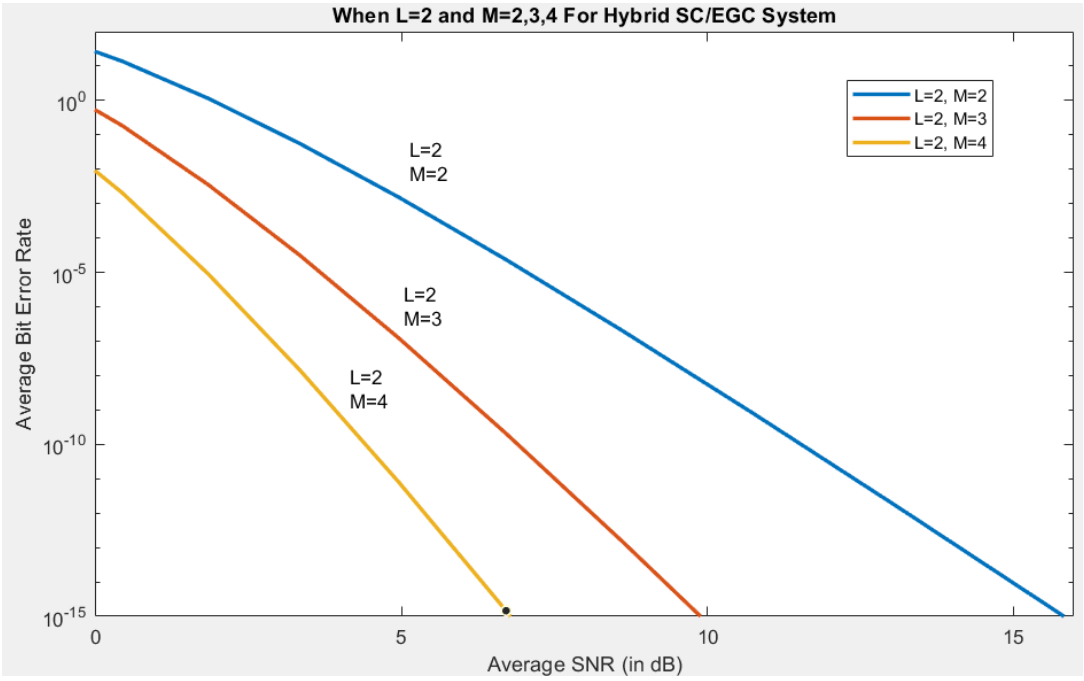

Fig: 2.9 BER Curves for SC-EGC for L=2 and M=2,3,4

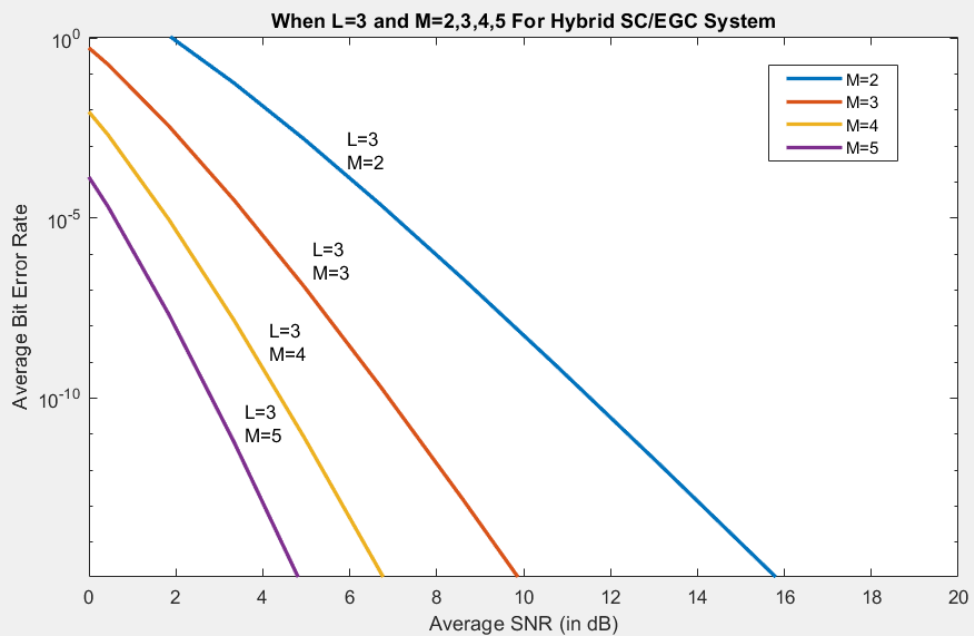

Fig: 2.10 BER Curves for SC-EGC for L=3 and M=2,3,4

2.5 Comparison

Comparison have been mare for BER performance for SC/MRC,MRC/SC and SC/EGC Diversity Scheme with reference [66] and [67]. A table for SNR in dB has been shown for BER of 10^{-4} , 10^{-5} and 10^{-6} in table III, IV and V respectively.

TABLE III

SNR required for maintaining ABER of Non-coherent Modulation Equal to 10^{-4}

Hybrid Technique	M=2 L=2	M=3 L=2
SC/MRC SNR (in dB)	6.8	5.8
SC/EGC SNR (in dB)	8.4	6.1
MRC/SC SNR (in dB)	12	8.2

TABLE IV

SNR required for maintaining ABER of Non-coherent Modulation Equal to 10^{-5}

Hybrid Technique	M=2 L=2	M=3 L=2
SC/MRC SNR (in dB)	8.0	6.5
SC/EGC SNR (in dB)	10.4	7.6
MRC/SC SNR (in dB)	15.3	11.2

TABLE V

SNR required for maintaining ABER of Non-coherent Modulation Equal to 10^{-6}

Hybrid Technique	M=2 L=2	M=3 L=2
SC/MRC SNR (in dB)	9.0	7.7
SC/EGC SNR (in dB)	12.5	8.2
MRC/SC SNR (in dB)	16.7	12.9

TABLE VI

SNR required for maintaining ABER of Non-coherent Modulation Equal to 10^{-9}

Hybrid Technique	M=2 L=2	M=3 L=2	M=2 L=3	M=3 L=3	M=2 L=4	M=3 L=4
MRC/EGC SNR (in dB)	-	-	-	-	-	-
SC/EGC SNR (in dB)	11.0	5.5	6.0	3.0	6.4	2.5

TABLE VII

SNR required for maintaining ABER of Non-coherent Modulation Equal to 10^{-10}

Hybrid Technique	M=2 L=2	M=3 L=2	M=2 L=3	M=3 L=3	M=2 L=4	M=3 L=4
MRC/EGC SNR (in dB)	-	-	-	-	-	-
SC/EGC SNR (in dB)	12.0	7.4	12.0	7.4	7.5	3.0

The system models are considered for Rayleigh fading environment. For this research work SNR in dB is also shown for BER of 10^{-9} and 10^{-10} . In the comparison analysis it is found that SC-MRC work better than SC-EGC but SC-EGC works better than MRC-SC. Though SC-MRC works better than SC-EGC but considering receiver complexity SC-EGC is less complex than that of SC-MRC. For all the diversity combining system, SNR required for having an acceptable level of performance decreases with increase in the number of diversity branches.

2.6 Summary

In this chapter, following the theoretical analysis, performance results are evaluated for a wireless communication system with single transmitter and multiple space diversity receiver over a Rayleigh fading channel. Results are evaluated in terms of bit error rate (BER) versus signal to noise ratio (SNR) in dB with the number of receiving antenna as a parameter. Analysis is also developed for BPSK signal to find the Bit Error Rate reader receiver with multiple selective combiners followed by EGC. It is observed that there is substantial improvement in range of a RFID system at a given BER and a single transmit power.

In this paper, newly introduced hybrid diversity techniques SC-EGC and SC-MRC under AWGN noise using BPSK modulation have been inspected. Rayleigh fading

channel is used to prove the performance analysis of the hybrid diversity scheme. From the output analysis, BER versus SNR graph has been used to determine the rigidity of data transmission from transmitter to receiver. Signal received by SC-MRC shows better performance than the basic diversity schemes (SC, EGC, MRC). Whereas for every increase in antenna in the reception side SC-EGC shows better robustness in contrast to SC-MRC with less complexity. For higher diversity order SC-EGC is the preferable combining scheme for SIMO transmission with a slight trade-off between diversity BER gain with complex model construction.

Hence, the first objective of the thesis is achieved which is “to develop an analytical model of BER for an OFDM Wireless Communication System with Hybrid Receive Combining Techniques over Rayleigh fading channel and to evaluate BER performance”.

CHAPTER 3

BER ANALYSIS OF OFDM SISO AND SIMO SYSTEMS

3.1 Introduction

Impulsive noise consists of relatively short duration "on/off" pulses [68]. Impulsive, non-Gaussian noise is prevalent in many communication environments due to a variety of sources, such as man-made electromagnetic interference, atmospheric noise, or ignition noise [69-70]. A widely accepted model for impulsive noise is Middleton's model with three distinct classes [71]. Middleton Class A model is valid when the bandwidth of noise is less than that of the receiver front-end and interference waveforms produce negligible transients at the receiver. If the noise bandwidth exceeds receiver front-end bandwidth and interference wave-forms result in significant transients, Class B model becomes valid. Class C, on the other hand, is considered as a mixture of Class A and B models [72]. Middleton Class A model has been widely used in analyzing the performance of communication systems under impulsive noise [73].

SIMO-OFDM is an intelligent approach for improving system capacity, spatial multiplexing and diversity coding [74]. The SIMO-OFDM system is a development in which the receiver receives a main carrier signal including multi sub-carrier signals orthogonally to each other that propagate through the transmission channel. There are many factors affect the performance of SIMO-OFDM. These factors include different types of noise and also the effect of the fading on the transmission channel. Most evaluations of SIMO and OFDM systems were considered in an ideal Gaussian noise environment [75].

3.2 System Block Diagram

3.2.1 System Block Diagram of AWGN Noise Model

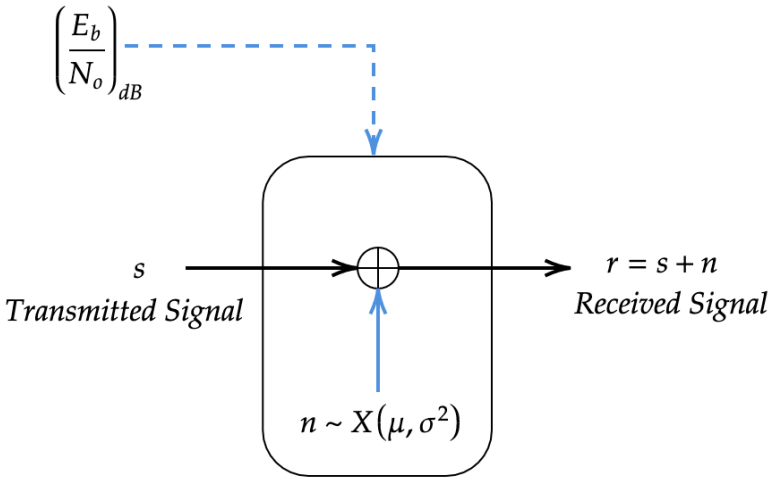

Fig 3.1 Block diagram of AWGN Noise Model

3.2.2 Impulsive Noise Models – Middleton Class A

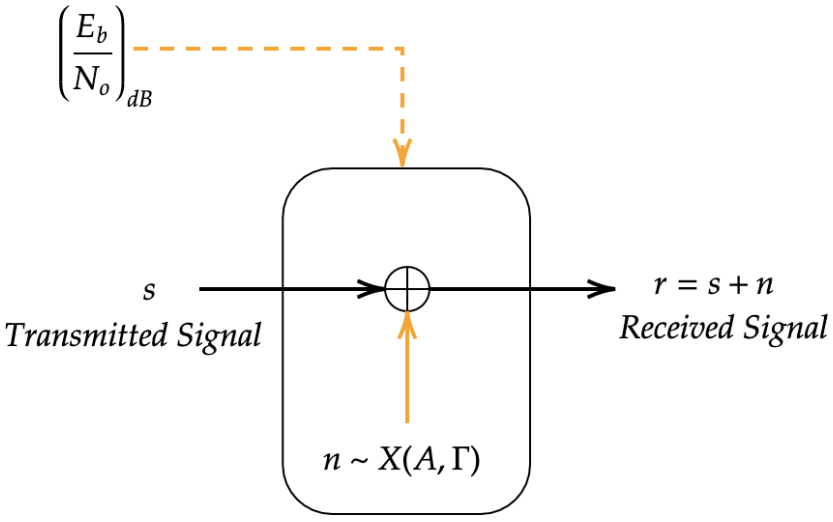

Fig 3.2 Block diagram of Middleton Class A Impulse Noise Model

3.2.3 Impulsive Noise Models S$-\alpha-S$ Model

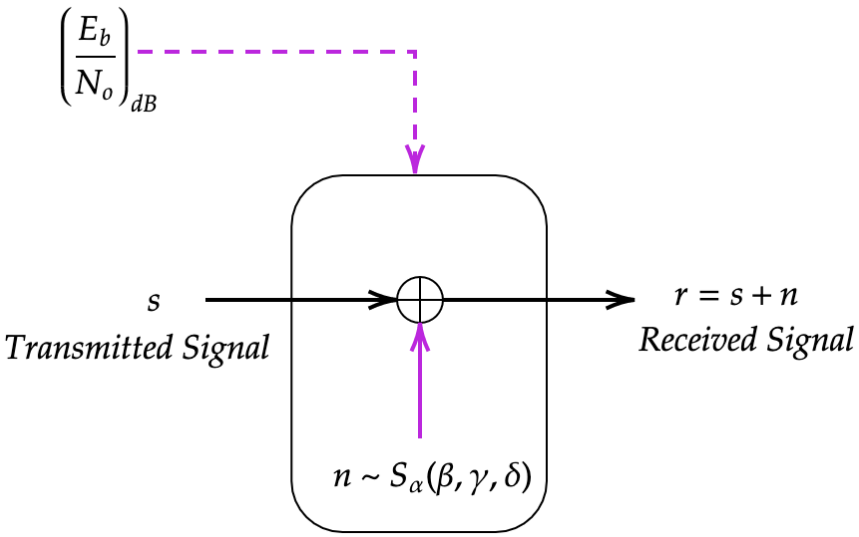

Fig 3.3 Block diagram of Symmetric Alpha Stable Impulse Noise Model

3.2.4 SIMO-OFDM System Block Diagram

OFDM (Orthogonal Frequency Division Multiplexing) technology is a kind of multi-carrier modulation (MCM) technology. The basic idea is to transform the high-speed data streams into a low rate of N sub-way data flows, and then to modulate N roads orthogonal sub-carriers [76]. Finally, transmit these data parallelly. In this way data flow rate is the 1/N of the original's rate, and the symbol period expands N-fold, [77] which is much larger than the channel maximum delay, and eliminates inter-symbol interference. The OFDM technology divided a wideband frequency selective channel into N narrowband flat fading channel, thus it has a strong resistance to multipath fading and anti-carrier interference. The combinations of MIMO and OFDM technology is widely considered to be the most effective means of improving spectral efficiency and system throughput. And it is the key physical layer technology of the fifth generation wireless mobile communication system.

Despite its advantages, OFDM-based MIMO systems suffer from non-Gaussian and nonlinear impulsive noise, which is commonly seen in wireless systems, caused by the switches of electric devices, ignition noise in vehicles, or strong bursty radio frequency emission, etc [78].

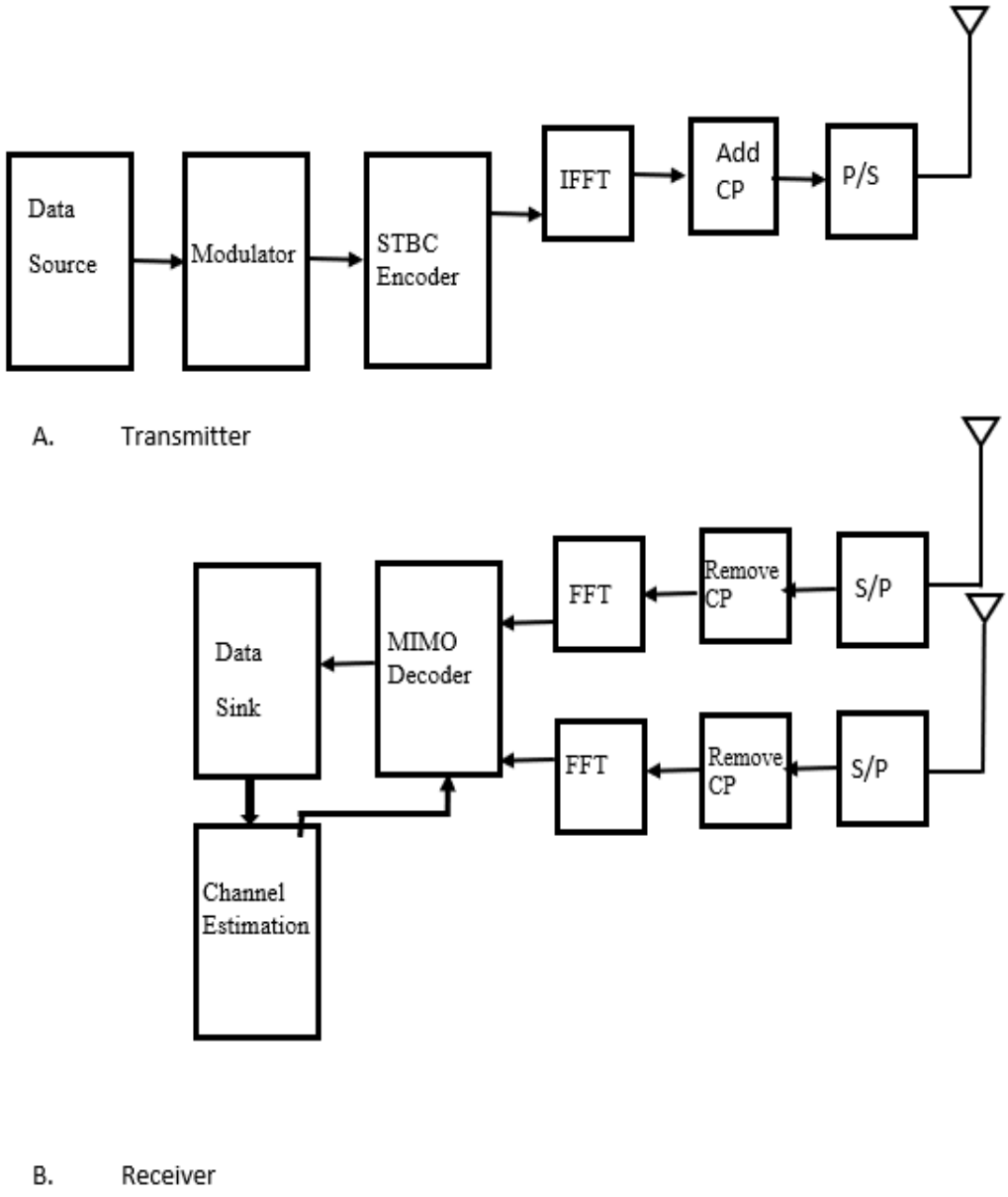

Fig 3.4 Block diagram of SIMO OFDM system (Transmitter and Receiver)

3.3 Analysis

3.3.1 Signal and Noise Power

Considering binary PSK modulation with single input single output with N-OFDM sub-carrier, the complex encircle of OFDM signal can be expressed as [79],

$$v(t) = \sqrt{\frac{2E_s}{T_s}} \sum_{k=0}^{\infty} \sum_{n=0}^{N-1} \alpha_{k,n} \varphi_n(t - kT_s)$$

$$= \sum_{n=0}^{N-1} v_n(t) \qquad (3.1)$$

where, E_s is the energy over a transmitted OFDM symbol, T_s is the symbol period $\alpha_{k,n}$ carries the information to be sent over the k-th symbol interval $t \in [kT_s,\ kT_s + T_s]$ and n-th sub-band (n=0, 1, 2, ….N-1), N being the number of OFDM subcarrier, $v_n(t)$ is the complex envelop of the signal transmitted in the n-th sub-band is given by [80] ,

$$v_n(t) = \sqrt{E} \sum_{k=0}^{\infty} \alpha_{k,n} \varphi_n(t - kT_s) \qquad (3.2)$$

where $\{\varphi_n(t)\}_{n=0}^{N-1}$ is a set of complex orthogonal wave form and is given by

$$\varphi_n(t) = \left\{ exp\left[j2\pi \langle n - \tfrac{N-1}{2} \rangle \, {}^{t}/_{T_s} \right] \right\}, t \in [0, T_s] \qquad (3.3)$$

$$t \notin [0, T_s]$$

Each waveform in the set $\{v_n(t)\}_{n=0}^{N-1}$ corresponds to a distinct (n-th) subcarrier with frequency

$$f_n = f_c + \frac{2n-(N-1)}{2T_s}. \qquad (3.4)$$

We consider binary phase shift keying (BPSK) for which $\alpha_{k,n} = \pm 1$, the received signal for the n-th OFDM subcarrier can be expressed as [81]:

$$r_n(t) = \sqrt{\frac{2E_s}{T_s}} \sum_{k=0}^{\infty} \alpha_{k,n} \varphi_n(t - kT_s) \otimes h_c(t) + n(t)$$

$$= v_n(t) \otimes h_c(t) + n(t) \quad (3.5)$$

$$= v_{0,n}(t) + n(t)$$

where, $h_c(t)$ is the impulse response of the wireless signal channel and n(t) represents the total signal consisting of background noise $n_b(t)$ and impulsive noise $n_{imp}(t)$,and E_b is the energy of an received OFDM symbol. Fourier Transform of $v_{0,n}(t)$ can be expressed as:

$$V_0, n(f_1) = V_n(f_1).H_n(f_1) \quad (3.6)$$

$$V_0(f_n) \otimes H^*(f_n) = V(f_n).|H(f_n)|^2 \quad (3.7)$$

The received OFDM signal is processed at the receiving end to remove the cyclic prefix and then all the sub-band modulated carriers of OFDM signal are separated by serial to parallel operation followed by FFT. The sub-band channel signals are passed through matched filter transfer function $H^*(f_n)$ and the output of matched filter is given by [82],

$$y_n(t) = \sqrt{\frac{2E_s}{T_s}} \sum_{k=0}^{\infty} a_{k,n} \varphi_n(t - kT_s) + n_0(t)$$

$$= \sqrt{\frac{2E_s}{T_s}} \sum_{k=0}^{\infty} a_{k,n} \varphi_n(t - kT_s) + n_0(t) \quad (3.8)$$

where, H(f_n) is given by

$$h_2(t) = \alpha \left[sin \frac{4\pi}{T_{AC}} t + \beta \right] h_c(t)$$

$$= \alpha h_c(t) Sin \frac{4\pi}{T_{AC}} t + \alpha\beta h_c(t)$$

and

$H_2(f) = F\{h_2(t)\}$

The signal at the output of coherent BPSK demodulator corresponding to n-th band is given by,

$$Z_n(t) = \sqrt{\frac{2E_s}{T_s}} \sum_{k=0}^{\infty} a_{k,n}\varphi_n\,(t - kT_s).\,|H(f_n)|^2 + n_0(t) \tag{3.9}$$

The variance of output $n_0(t) is\ given\ by,$

$$\sigma_{0,m}^2 = \sigma_m^2.\,|H(f_n)|^2 \tag{3.10}$$

The signal to noise ratio (SNR) at the output of coherent BPSK demodulator is then given by [83],

$$\gamma_{n.m} = \frac{\left|\sqrt{\frac{2E_s}{T_s}}\ .\ |H(f_n)|^2\right|^2}{\sigma_m^2.\ |H(f_n)|^2}$$

$$= \frac{A_0^2}{\sigma_m^2}.\,|H(f_n|^2 = \frac{|A_{0n}|^2}{\sigma_m^2} \tag{3.11}$$

where, $$A_0 = \sqrt{\frac{2E_s}{T_s}} = \sqrt{2P_s}\ \text{ and } A_{0n} = A_0 \tag{3.12}$$

and P_s is average signal power over an OFDM symbol interval and,

$$\sigma_m^2 = \sigma_b^2 + \sigma_{imp}^2 = \sigma_b^2(1+\frac{1}{\Gamma}) \tag{3.13}$$

Where,

$$\boldsymbol{\Gamma} = \frac{\sigma_G^2}{\sigma_I^2} \tag{3.14}$$

σ_G^2 and σ_I^2 represent the zero mean and variance for Gaussian noise and

Impulsive noise respectively

The bandwidth of an OFDM sub-channel is expressed by $\Delta f = B/N$ when B is the channel bandwidth and N is the number of OFDM sub-carriers. The SNR for i-th OFDM sub-carriers for L=1 considering the Middleton Class A noise Model is given by [84],

$$\gamma_{n,m} = \frac{A_0^2 . |H(f_1)|^2}{\sigma_m^2}$$

$$= \frac{2P_s . |H(f_1)|^2}{\sigma_b^2 \left[\frac{\left(\frac{m}{A}+\Gamma\right)}{\Gamma}\right]}$$

$$= \gamma_b . \frac{2 . |H(f_1)|^2}{\left[\frac{\left(\frac{m}{A}+\Gamma\right)}{\Gamma}\right]} ; as\ \gamma_b = \frac{A_0^2/2}{\sigma_b^2} = \frac{P_s}{\sigma_b^2} = \frac{2|H(f_1)|^2}{\left(\frac{m}{A}+\Gamma\right)/\Gamma} . \gamma_b = \frac{2\Gamma|H(f_1)|^2}{\left(\frac{m}{A}+\Gamma\right)} . \gamma_b \quad (3.15)$$

3.3.2 BER Analysis

3.3.2.1 SISO OFDM with Poisson's Noise Model

The background noise is assumed to be white Gaussian Noise (AWGN) with zero mean and variance σ_w^2. The arrival of impulsive noise follows a Poisson process with a rate of λ units per second, so that the event of k arrivals in t seconds has the probability distribution,

$$P_k = e^{-\lambda t}(\lambda t)^k / k! \quad \text{K=0, 1, 2} \quad (3.16)$$

The distribution time of the impulsive noise T_{noise} and time period is T. P_i is defined as the total average occurrence of the impulsive noise duration in time T and P_0 is the average duration without impulsive noise in time T, in which duration only AWGN is present. The probability distribution is [85],

$$P_i = \left[\sum_{k=0}^{\infty} e^{-\lambda T} \frac{(\lambda T)^2}{k!} (K T_{noise})\right] / T$$

$$= \lambda T_{noise} \left[\sum_{k=1}^{\infty} e^{-\lambda T} \frac{(\lambda T)^{k-1}}{(k-1)!}\right]$$

$$= \lambda T_{noise} \left[\sum_{k=0}^{\infty} e^{-\lambda T} \frac{(\lambda T)^k}{k!} \right]$$

At high value of k,

$$\sum_{k=0}^{\infty} e^{-\lambda T} \frac{(\lambda T)^k}{k!} = 1$$

$$P_i = \lambda T_{noise} \tag{3.17}$$

If the BER under impulsive noise is P_{b1} and BER under AWGN is $P_{b2,}$ the BER of a single carrier BPSK is given by [86],

$$P_b = P_{b1} + P_{b2}$$

where P_{b1} is BER under impulsive noise and P_{b2} is BER under AWGN

(3.18)

with impulsive noise

$$P_{b1} = \lambda T_{noise}[P_{bi}] \text{ , where } P_{bi} \text{ is BER under Impulsive noise} \tag{3.19}$$

with AWGN

$$P_{b2} = (1 - \lambda T_{noise})\,[P_{bw}] \text{ , where } P_{bw} \text{ is BER under AWGN} \tag{3.20}$$

So, we can write, BER in BPSK under impulsive noise as,

$$P_b = \lambda T_{noise}[P_{bi}] + (1 - \lambda T_{noise})\,[P_{bw}]$$

for L=1,

$$P_{bi} = \frac{1}{2}\, erfc\left[\sqrt{\frac{E_b/N_0}{1+\mu_1}}\right] \tag{3.21}$$

where, μ_1 is the ratio of impulsive noise to additive white Gaussian noise (AWGN).

$$P_{bw} = \frac{1}{2}\, erfc\left[\sqrt{\frac{E_b}{N_0}}\right] \tag{3.22}$$

where E_b is the signal energy per bit, N_0 is the power spectral density of the AWGN.

So, for L=1, in case of impulsive noise for n-th OFDM channel, the conditional bit error probability can be expressed as [87]:

$$P_e(\gamma_n) = \lambda T_{noise} 0.5\, erfc\left(\sqrt{\frac{\gamma_n(0)}{1+\mu_1}}\right) + (1-\lambda T_{noise})\, 0.5\, erfc\left(\sqrt{\gamma_n(0)}\right) \quad (3.23)$$

For L=1; $\gamma_n = \gamma_b = \frac{E_b}{N_0}$

3.3.2.2 SIMO OFDM with Poisson's Noise Model

Considering diversity reception as MRC (Maximal Ratio Combining) with L>1

The average bit error rate of n-th subchannel can be obtained by averaging the conditional bit error rate $P_e(\gamma_n)$ over the pdf of γ_n and average BER can be expressed as [88]:

$$BER(n) = \int_0^{\propto} P_e(\gamma_n).P(\gamma_n)d\gamma_n$$

Where, $P(\gamma_n) = \frac{\gamma_n^{L-1}}{(L-1)!\Gamma_c^L} exp\left[-\frac{\gamma_n}{\Gamma_c}\right]$ (3.24)

$\Gamma_c = 2\alpha_{\propto}^2.\gamma_b$; $\gamma_b = \frac{E_b}{N_0}$ is the average SNR per bit in each diversity channel.

using eqn (3.12),

$$BER(n) = \int_0^{\propto} \left\{\frac{1}{2}\lambda T_{noise} erfc\left(\left[\frac{\sqrt{\gamma_n}}{1+\mu_1}\right]\right) + \frac{1}{2}(1-\lambda T_{noise}) erfc\left(\left[\frac{\sqrt{\gamma_n}}{1+\mu_1}\right]\right)\right\} \times \frac{\gamma_n^{L-1}}{(L-1)!}\frac{exp\left(-\frac{\gamma_n}{\Gamma_c}\right)}{\Gamma_c^L} d\gamma_n$$

Probability of Bit Error for AWGN channel can be expressed as:

$$P_{bw} = 0.5(1-\mu_{2w})^L \sum_{l=0}^{L-1}\binom{L-1+l}{l}[0.5(1+\mu_{2w})]^l \approx \left(\frac{1}{4\Gamma_{c_w}}\right)^L \binom{2L-1}{L} \quad (3.25)$$

Probability of Bit Error for impulsive noise channel can be expressed as:

$$P_{bi} = 0.5(1-\mu_{2i})^L \sum_{l=0}^{L-1} \binom{L-1+l}{l} [0.5(1+\mu_{2i})]^l \approx \left(\frac{1}{4\Gamma_{c_i}}\right)^L \binom{2L-1}{L}$$

$$; \binom{n}{\gamma} = n_{C_\gamma} = \frac{n!}{\gamma!(n-\gamma)!} \tag{3.26}$$

where, $\mu_{2w} = \sqrt{\frac{\Gamma_{cw}}{1+\Gamma_{cw}}}$

and $\mu_{2i} = \sqrt{\frac{\Gamma_{ci}}{1+\Gamma_{ci}}}$

Average SNR per bit in OFDM for each diversity channel for MRC in case of AWGN is:

$$\Gamma_{cw} = 2\sigma_\alpha^2 \frac{E_b}{N_0}$$

Average SNR per bit in OFDM for each diversity channel for MRC in case of impulsive noise is:

$$\Gamma_{ci} = 2\sigma_\alpha^2 \frac{E_b/N_0}{1+\mu_1} = \frac{\Gamma_{cw}}{1+\mu_1}, \mu_1 = \mu = \frac{\sigma_i^2}{\sigma_g^2} = \frac{1}{\Gamma}$$

Assuming $0.5(1+\mu_2) \approx 1$ and $0.5(1-\mu_2) \approx \frac{1}{4\Gamma_c}$, furthermore

$$\sum_{i=o}^{L-1} \binom{L-1+l}{l} = \binom{2L-1}{L}$$

So, the BER in diversity reception is given by,

$$P_b \approx (\frac{1}{4\Gamma_c})^L \binom{2L-1}{L} \tag{3.27}$$

where, Γ_c is the SNR in OFDM and is given by,

$$\Gamma_c = 2\sigma_\alpha^2 . \frac{E_b}{N_m}$$

$$= \frac{E_b/N_0}{1+\mu_2 \lambda T_{noise}} \tag{3.28}$$

where $\mu_2 = \sqrt{\frac{\Gamma_c}{1+\Gamma_c}}$

The overall BER can be written as [89]:

$$P_b \cong \lambda T_{noise} P_{b_i} + (1 - \lambda T_{noise}) P_{bw}$$

$$\cong \left[\lambda T_{noise} \left(\frac{1}{4\Gamma_{cw}}\right)^L + (1 - \lambda T_{noise}) \left(\frac{1}{4\Gamma_{ci}}\right)^L\right] \binom{2L-1}{L} \tag{3.29}$$

Note: $\binom{2L-1}{L} = \frac{(2L-1)!}{L!(L-1)!} \Rightarrow \binom{n}{\gamma} = {}_nC_\gamma = \frac{n!}{\gamma!(n-\gamma)!}$

3.3.2.3 SISO OFDM with Middleton Class A Noise Model

The Middleton Class-A noise model stands out as prominent choice for representing impulsive noise in various scholarly works. This noise model is characterized by two key parameters: A (impulsive factor) and ***Γ*** (Gaussian Noise Factor). These parameters govern the distribution shape and behaviour of the noise model, offering a versatile tool for tailoring impulsive noise characteristics. The probability density function (PDF) of the Middleton Class-A noise model is described by the equation [90]:

$$f_z(z) = e^{-A} \sum_{m=0}^{\infty} \frac{A^m}{m!\sqrt{2\pi\sigma_m^2}} e^{\frac{z^2}{2\sigma_m^2}} \tag{3.30}$$

where

$$\sigma_m^2 = \frac{\frac{m}{A}+\Gamma}{1+\Gamma} \tag{3.31}$$

Parameters of Middleton Class A Noise Model:

A = Impulsive Index/ Overlap Index

Γ = Gaussian Factor = power ratio of the background Gaussian noise and the impulsive noise

$$\Gamma = \frac{\sigma_g^2}{\sigma_i^2}$$

Equation (3.25) further elucidates the relationship between $\boldsymbol{\Gamma}$, representing the power of Gaussian noise, and σ_g^2 and σ_i^2, representing the powers of Gaussian and Impulsive noise respectively.

The Gaussian factor $\boldsymbol{\Gamma}$ characterizes the ratio of the power of AWGN, denoted by σ_g^2, to the power of impulsive noise, denoted by σ_i^2. In essence, a higher $\boldsymbol{\Gamma}$ value signifies a predominant presence of Gaussian noise relative to impulsive noise, and conversely. The impact of impulsive noise undergoes variations with alteration in the parameter A. Throughout this analysis, the value of $\boldsymbol{\Gamma}$ remains fixed at 0.1, while A undergoes variation [83-85].

The SNR for n-th OFDM sub-channel is given by [91],

$$\gamma_{n.m} = \frac{2|H(f_n)|^2}{\left(\frac{m}{A}+\Gamma\right)/\Gamma} \cdot \gamma_b$$

$$= \frac{2\Gamma|H_n(f)|^2}{\left(\frac{m}{A}+\Gamma\right)} \cdot \gamma_b \qquad (3.32)$$

Let, $|H_n(f)|^2 = g_n$, so $\gamma_{n.m} = \frac{2\Gamma g_n}{\left(\frac{m}{A}+\Gamma\right)} \cdot \gamma_b = \eta . \gamma_b$

where, $\eta = \frac{2\Gamma g_n}{\frac{m}{A}+\Gamma}$, g_n is the effective channel gain

The average BER of n-th sub-carrier is given by

$$BER(n) = P_n(\gamma_n) = \sum_{m=0}^{\infty} \frac{e^{-A}.A^m}{m!} \cdot \frac{1}{2}\, erfc\left[\frac{\sqrt{\gamma_{n,m}}}{\sqrt{2}}\right]$$

$$= \sum_{m=0}^{\infty} C_{n,m} \cdot \frac{1}{2}\, erfc\left[\frac{\sqrt{\gamma_{n,m}}}{\sqrt{2}}\right] \; where \; C_{n,m} = \frac{e^{-A}.A^m}{m!} \qquad (3.33)$$

3.3.2.4 SIMO MRC OFDM with Middleton Class A Model

L>1 (Maximum Ratio Combining/Selection Combining) with Middleton Class A Model [92]:

BER for n-th OFDM Sub Channel = $BER\ (n) = \int_0^{\infty} P_e(\gamma_n)\,.\,f_{\gamma_i}(\gamma_b)\quad d\gamma_{n,m}$ (3.34)

Overall BER, BER= $\frac{1}{N}\sum_{n=1}^{N} BER(n)$

For Middleton Class- A noise Model:

Conditional BER for a given γ_n ,

$$P_e(\gamma_n) = \sum_{m=0}^{\infty} C_{n,m}\left[\frac{1}{2}erfc\left(\frac{\sqrt{\gamma_{nm}}}{\sqrt{2}}\right)\right] = \sum_{m=0}^{\infty} C_{n,m}\,.\frac{1}{2}\ erfc\left(\left[\frac{2\Gamma|H(f_n)|^2}{\left(\frac{m}{A}+\ \Gamma\right)}\,.\ \frac{\gamma_n}{\sqrt{2}}\right]\right)$$

$$= \sum_{m=0}^{\infty}\left(\frac{A^m}{m!}\ e^{-A}\right)\left[\frac{1}{2}\left\{erfc\left(\frac{\sqrt{2}\Gamma g_n}{\frac{m}{A}+\Gamma}.\gamma_n\right)\right\}\right]$$

$$\gamma_n = \text{Output SNR for n} - \text{th sub} - \text{channel}$$

$$f_{\gamma_n}(\gamma_n) = \text{PDF of}\ \gamma_n\ \text{at the output ofMRC Combiner}$$

$$f_{\gamma_n(\gamma_n)} = \frac{\gamma_n^{L-1}\ exp[-\gamma_n/\Gamma_c]}{(L-1)!\,\Gamma_c^L} \qquad \gamma_n > 0\ ;For\ MRC$$

where $\Gamma_c = 2\ \sigma_\alpha^2\ .\frac{E_b}{N_0} = 2\sigma_\alpha^2.\gamma_b$

$f_{\gamma_n}(\gamma_n) = \frac{L}{\Gamma_c}\exp\left(\frac{\gamma_n}{\Gamma_c}\right)\left[1 - exp\ \left(-\frac{\gamma_n}{\Gamma_c}\right)\ \right]^{L-1}$ for SC

Average BER for n-th OFDM subchannel can be expressed as:

$$BER(n) = \int_0^{\infty} P_e\ (\gamma_n)\,.\,f(\gamma_n)\,d\gamma_n$$

$$where\ P_e\ (\gamma_n) = \sum_{m=0}^{\infty} \frac{A^m}{m!}\ e^{-A}\ .\frac{1}{2}\ erfc\left[\beta_{m,n}\gamma_n\right]$$

$where\ \beta_{m,n} = \frac{\sqrt{2}\,\Gamma g_n}{\left(\frac{m}{A}+\Gamma\right)}$, here g_n is the effective channel gain

$$f(\gamma_n) = \frac{\gamma_n^{L-1}}{(L-1)!\,\Gamma_{c,0}^{L}}\ exp\left[-\frac{\gamma_n}{\Gamma_c}\right]\quad where\ \Gamma_c = 2\sigma_\alpha^2.\gamma_b\ ,$$

$$\gamma_b = \frac{E_b}{N_0}$$

$$BER(n) = \int_0^{\infty}\sum_{m=0}^{\infty}\frac{A^m.e^{-A}}{m!}\ .\ \frac{1}{2}\ erfc\left[\beta_{m,n}\,.x\right].\frac{x^{L-1}}{(L-1)!\Gamma_c^L}\ exp\left[-\frac{x}{\Gamma_c}\right]dx$$

$$= \sum_{m=0}^{\infty}\frac{A^m e^{-A}}{m!}\ .\frac{1}{2}\int_0^{\infty} erfc\left(\beta_{m,n}\ .\ x\right)\ .\ \frac{x^{L-1}}{(L-1)!\,\Gamma_c^L}\exp\left(-\frac{x}{\Gamma_c}\right)dx \qquad (3.35)$$

3.3.2.5 BER Analysis of SISO OFDM with SαS Model for α=2

$P(z_n)$ = Probability of Output voltage z_n

Let, $z_n = v_0 =$ output voltage for '0' transmitted

$p(v_0) = \frac{1}{2\sqrt{\pi}}\ exp\left[-\frac{(v_0+A_0)^2}{4}\right]$ for '0' transmitted

$p(v_1) = \frac{1}{2\sqrt{\pi}}\ exp\left[-\frac{(v_0-A_0)^2}{4}\right]$ for '1' transmitted

$$prob\{{}^{1}/_{0}\} = prob\{\text{"0" } transmitted, \text{"1" } received\}$$

$$= \int_0^{\infty} p(v_0)\ dv_0 = \int_0^{\infty}\frac{1}{2\sqrt{\pi}} exp\left[-\frac{(v_0+A_0)^2}{4}\right]dv_0$$

Let, $\frac{v_0+A_0}{2} = x\ \ \rightarrow dv_0 = 2dx$

$$v_0 = 0,\ \ x = \frac{A_0}{2}$$

$$v_0 \rightarrow \propto, x \rightarrow 0$$

$$p(1/0) = \int_{A_0/2}^{\infty} \frac{1}{\sqrt{\pi}} exp(-x^2)dx = \frac{1}{2} erfc\left[\frac{A_0}{2}\right] \quad (3.36)$$

$$p(0/1) = \frac{1}{2} erfc\left(\frac{A_0}{2}\right)$$

Let us define SNR as

$$\gamma = \frac{A_0^2}{\sigma_g^2+\sigma_i^2} \rightarrow A_0$$

$$where, \sigma_g^2 = \text{variance of Gaussian noise}$$

$$\sigma_i^2 = \text{variance of Impulsive noise}$$

Let, $\Gamma = \frac{\sigma_g^2}{\sigma_i^2}$

$$\gamma_0 = \gamma\left[1+\frac{1}{\Gamma}\right] and\ \gamma = \frac{A_0^2/\sigma_g^2}{1+\frac{\sigma_i^2}{\sigma_g^2}} = \frac{\gamma_0}{1+\frac{1}{\Gamma}}$$

$$A_0^2 = \gamma_0 = \left[1+\frac{1}{\Gamma}\right]$$

$$A_0 = \left[\frac{\Gamma+1}{\Gamma}\right]^{\frac{1}{2}}$$

$$BER(\gamma) = \frac{1}{2} erfc\left\{\left[\frac{\sqrt{\gamma}}{2}.\left[\frac{\Gamma+1}{\Gamma}\right]^{\frac{1}{2}}\right]\right\} = \frac{1}{2} erfc\left[\frac{\sqrt{\gamma}}{2}.\sqrt{\frac{1}{1+\frac{1}{\Gamma}}}\right] = \frac{1}{2} erfc\left[\frac{\sqrt{\gamma}}{2\sqrt{1+\frac{1}{\Gamma}}}\right] \quad (3.37)$$

3.3.2.6 BER Analysis of SIMO MRC OFDM with SαS Model for α=2

$$p_e(\gamma) = \frac{1}{2} erfc\left[\frac{\gamma}{2}\right] = Conditional\ BER$$

PDF of γ at the output of MRC

$$p(\gamma) = \frac{\gamma^{L-1}}{(L-1)!\,\Gamma_c^L}\ exp\left[-\frac{\gamma}{\Gamma_c}\right]$$

Average BER for n-th OFDM channel:

$$BER(n) = \int_0^{\infty} p_e(\gamma).p(\gamma)\,d\gamma$$

$$= \int_0^{\infty} \frac{1}{2} erfc\left[\frac{\sqrt{\gamma}}{2\sqrt{1+\frac{1}{\Gamma}}}\right].\frac{\gamma^{L-1}}{(L-1)!\Gamma_c^L}\ exp\left[-\frac{\gamma}{\Gamma_c}\right] d\gamma \qquad (3.38)$$

3.3.2.7 BER Analysis of SISO OFDM with SαS Model for 0<α < 1

$$f_{x_n}(x_n) = pdf\ of\ x_n(impulsive\ noise)$$

$$f_{x_n}(x_n) = \frac{1}{\pi x_n}\sum_{k=1}^{\infty}\frac{(-1)^{k-1}}{k!}\Gamma(\alpha k+1)x_n^{-\alpha k}.sin\left(\frac{k\alpha\pi}{2}\right) \quad 0<\alpha<1 \qquad (3.39)$$

$$Ber = \frac{1}{2}\left[p_e({}^0/_1) + p_e\,{}^1/_0\right]$$

Voltage at the receive output

$$v_0 = -A_0 + x_n \quad --'0'$$

$$v_0 = +A_0 + x \quad --'1'$$

$$p(v_0) = f_{x_n}(x_n)\big|x_n = v_0 + A_0$$

$$= \frac{1}{\pi(v_0+A_0)}\sum_{k=1}^{\alpha}\frac{(-1)^{k-1}}{k!}\Gamma(\alpha k+1)(v_0+A_0)^{-\alpha k}.sin\left(\frac{k\alpha\pi}{2}\right) \quad 0<\alpha<1$$

$$p({}^1/_0) = \int_0^{\infty} p(v_0)dv_0$$

$$= \int_0^{\infty}\frac{1}{\pi(v_0+A_0)}\sum_{k=1}^{\infty}\frac{(-1)^{k-1}}{k!}\,\Gamma(\alpha k+1)(v_0+A_0)^{-\alpha k}.sin\left(\frac{k\alpha\pi}{2}\right)dv_0 \quad 0<\alpha$$

$$<1$$

Let, $v_0 + A_0 = x$

$dv_0 = dx$

Then, $v_0 = 0, \quad x = A_0$

$v_0 = \propto, \quad x = \propto$

$$p(^1/_0) = \int_{A_0}^{\propto} \frac{1}{\pi x}. \sum_{k=1}^{\propto} \frac{(-1)^{k-1}}{k!} \Gamma(\alpha k + 1). x^{-\alpha k}. sin\left(\frac{k\alpha\pi}{2}\right) dx$$

So, $p(^1/_0) = \int_{\gamma=^{A_0}/_{\sigma_g}}^{\propto} \frac{1}{\pi(y.\sigma_g)} \sum_{k=1}^{\propto} \frac{(-1)^{k-1}}{k!} \Gamma(\alpha k + 1). (y\sigma_g)^{-\propto k}. sin\left[\frac{k\alpha\pi}{2}\right] {}^{\sigma}/_{y}\, dy$

$$BER(\gamma_0) = p(^1/_0)$$

$$= \int_{\gamma\sqrt{\gamma_0}}^{\propto} \frac{1}{\pi y}. \sum_{k=1}^{\propto} \frac{(-1)^{k-1}}{k!} \Gamma(\alpha k + 1)(y)^{-\propto k} \sigma_g^{(-\alpha k)} sin\left[\frac{k\alpha\pi}{2}\right] dy$$

Note: Let, $\frac{x}{\sigma_g} = y$

$dx = \sigma_g dy$

where $x \to A_0$

$y = {}^{A_0}/_{\sigma_g}$

where $x \to \propto \quad y \to \propto$

$$BER(\gamma) = \int_{y=\sqrt{\left(\gamma.\frac{1+\Gamma}{\Gamma}\right)}}^{\propto} \frac{1}{\pi y} \sum_{k=1}^{\propto} \frac{(-1)^{k-1}}{k!}. \boldsymbol{\Gamma}(\propto \mathrm{k} + 1)\mathrm{y}^{(-\propto \mathrm{k})}. \sigma_{\boldsymbol{g}}^{-\alpha \mathrm{k}} \sin\left(\frac{k\alpha\pi}{2}\right) dy \quad 0 < \propto < 1$$

3.3.2.8 BER Analysis of SISO OFDM with SαS Model for $1<\alpha<2$

$$f_{x_n}(x_n) = \frac{1}{\pi\alpha} \sum_{k=0}^{\propto} \frac{(-1)^{k-1}}{2k!} \boldsymbol{\Gamma}\left(\frac{2\mathrm{k}+1}{\alpha}\right), \mathrm{x}_\mathrm{n}^{2\mathrm{k}} \qquad 1 < \alpha < 2 \qquad (3.40)$$

Rx Output Voltage:

$$v_0 = -A_0 + x_n \qquad 0 \ transmitted$$

$$v_1 = A_0 + x_n \qquad 1 \ transmitted$$

$$p(v_0) = f_{x_n}(x_n) = \frac{1}{\pi\alpha}\sum_{k=0}^{\infty}\frac{(-1)^{k-1}}{2k!}\boldsymbol{\Gamma}\left(\frac{2\mathrm{k}+1}{\alpha}\right).(v_0 + A_0)^{2k} \qquad 1 < \alpha < 2$$

$$p(^1/_0) = \int_0^{\infty} p(v_0)\, dv_0$$

$$= \int_0^{\infty}\frac{1}{\pi\alpha}\sum_{k=0}^{\infty}\frac{(-1)^{k-1}}{2k}\Gamma\left(\frac{2k+1}{\alpha}\right).(v_0 + A_0)^{2k}\ dv_0$$

Let, $v_0 + A_0 = x$

$dv_0 = dx$

when $v_0 = 0 \quad x = A_0$

$v_0 = \propto \qquad x = \propto$

$$p(^1/_0) = \int_{A_0}^{\infty}\frac{1}{\pi\alpha}\sum_{k=0}^{\infty}\frac{(-1)^{k-1}}{2k!}\Gamma\left(\frac{2k+1}{\alpha}\right).x^{2k}dx$$

$$\frac{A_0}{\sigma_g} = \sqrt{\gamma_0} \ \ as \ \frac{A_0^2}{\sigma_g^2} = \gamma_0$$

Let, $\frac{x}{\sigma_g} = y$

Then $dx = \sigma_g.dy$ when $x = 0 \qquad y = 0$

$$x = A_0 \qquad y = {}^{A_0}/_{\sigma_g}$$

$$p(1/0) = \int_{y=A_0/\sigma_g=\sqrt{\gamma_0}} \frac{1}{\pi\alpha} \sum_{k=0}^{\infty} \frac{(-1)^{k-1}}{2k!} . \Gamma\left(\frac{2k+1}{\alpha}\right) (\sigma_g\, y)^{2k} dy$$

$$BER(\gamma_0) = \int_{y=\sqrt{\gamma_0}}^{\infty} \frac{1}{\pi\alpha} \sum_{k=0}^{\infty} \frac{(-1)^{k-1}}{(2)(k!)} \Gamma\left(\frac{(2k+1)}{\alpha}\right) (\sigma_g\, y)^{2k} dy$$

3.4 Result and Discussion

Following the theoretical analysis Bit Error Rate Performance results for SISO OFDM with Poisson's noise model are evaluated as depicted in Fig. 3.5 as BER versus received power P_s (dBm) with λT_s as a parameter for μ=0.85, BW=1250 MHz and N=1024.

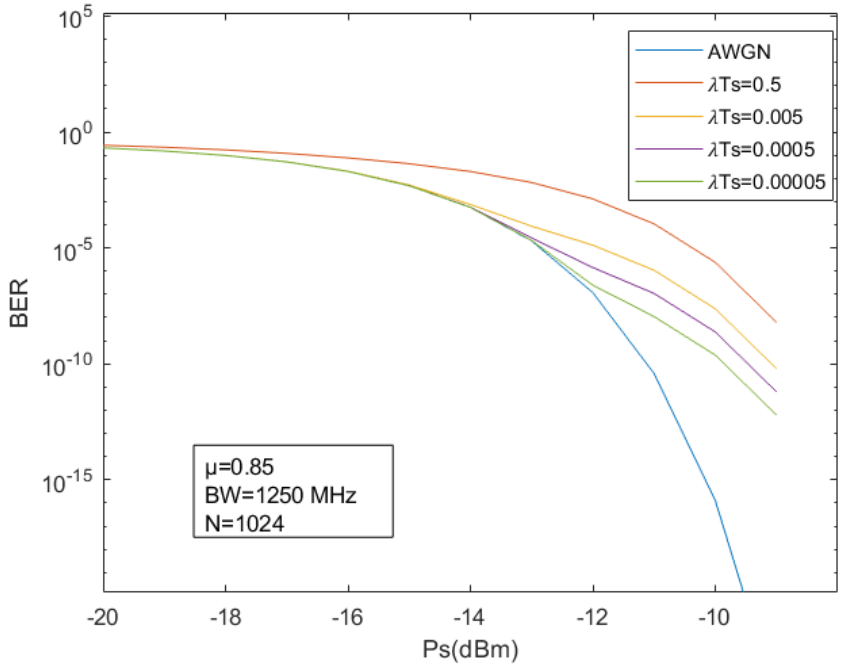

Fig. 3.5 : BER Vs Received Power for SISO OFDM System for different values of λT_s (μ=0.85, BW=1250 MHz, N=1024) with Poisson's Noise Model

From Fig. 3.5 it is revealed that BER performance is highly affected due to impulsive noise in presence of Gaussian noise.

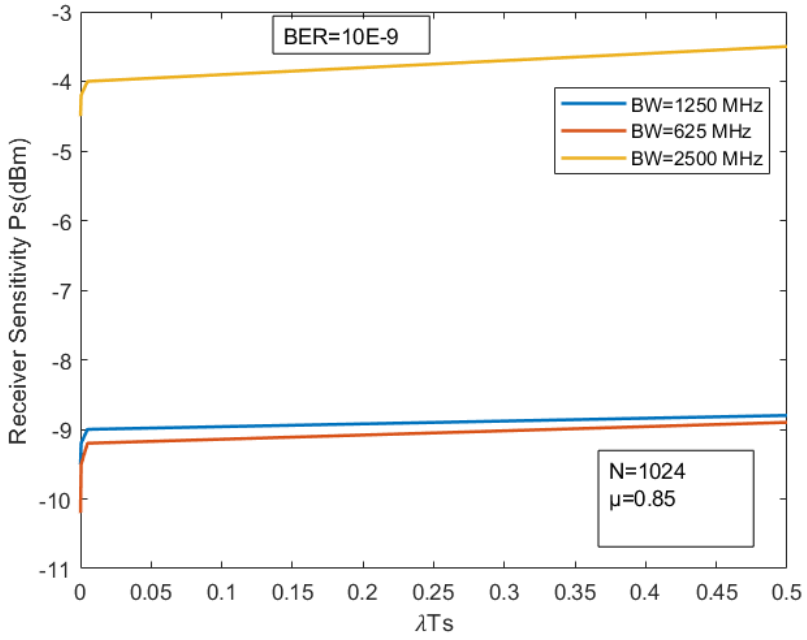

Fig.3.6: Receiver Sensitivity Vs λTs under various Bandwidth (625 MHz, 1250 MHz, 2500 MHz) values for SISO OFDM Poisson's Noise Model

The receiver sensitivity for BER 10^{-9} is also plotted in Fig. 3.6 as a function of λTs at a given BW and μ. The BER performance curve without impulsive noise is also depicted in Fig. 3.5. It clearly indicates the degradation of BER performance due to impulsive noise over that of Gaussian noise. Comparison of receiver sensitivity P_s(dBm) at BER=10^{-9} for OFDM SISO system without and with impulsive noise gives the power penalty due to impulsive noise as plotted in Fig. 3.7. It is noticed that power penalty is 1 dB, 2 dB and 4 dB corresponding to λTs=0.5, 0.005, 0.0005 respectively. Higher duration impulsive noise results in higher power penalty at a given BER. The similar power penalty for other values of μ and BW are also depicted in Fig. 3.7 Penalty is higher at high system BW.

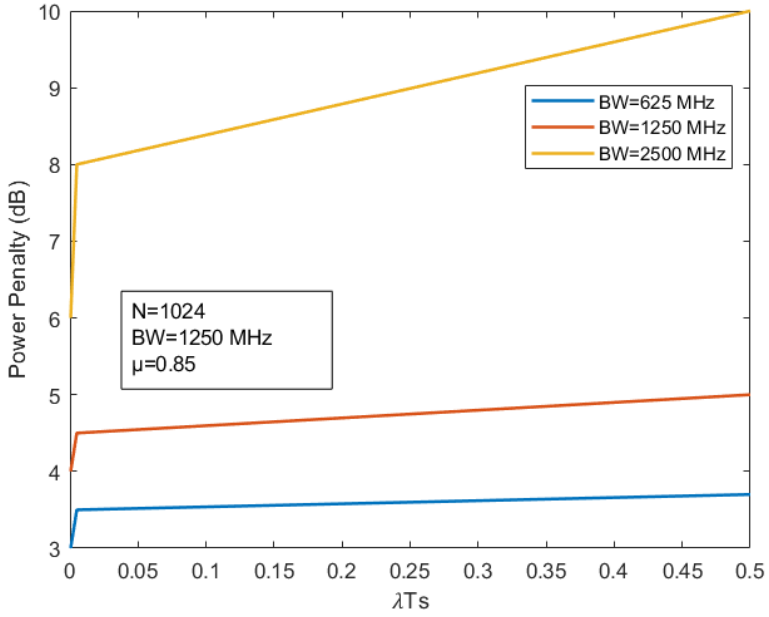

Fig. 3.7: Power Penalty Vs λTs for SISO OFDM System for different values of BW 9625 MHz, 1250 MHz, 2500 MHz) with Poisson's Noise Model

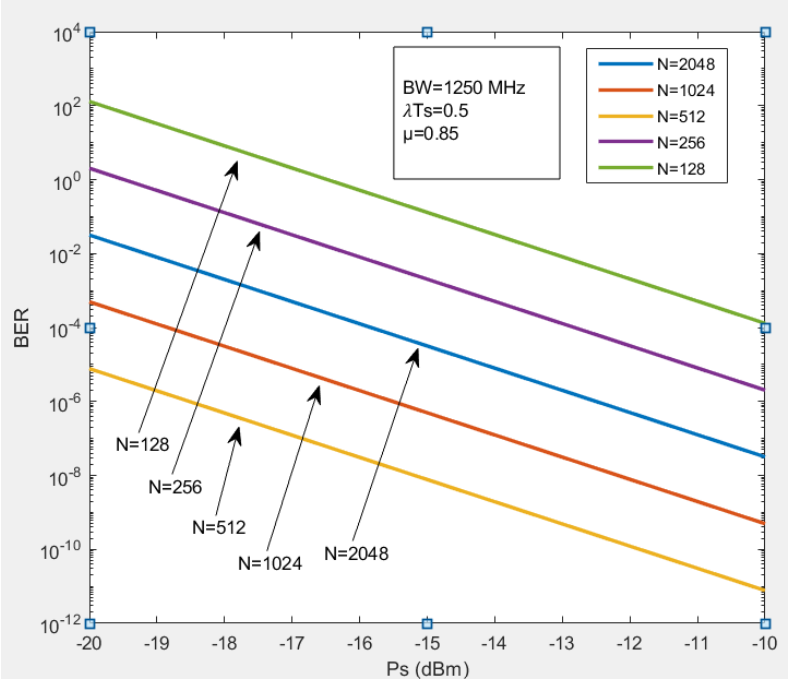

Fig: 3.8 BER Vs Received Power for SISO OFDM System for different values of N (λTs=0.5, μ=0.85, BW=1250 MHz) with Poisson's Noise Model

BER performance for SISO OFDM with impulsive noise is also plotted in Fig. 3.8 as a function of received signal power Ps(dBm) with number of OFDM subchannel, N as a parameter. The figure clearly depicts that higher number of OFDM sub-channel results in improvement is receiver sensitivity due to less effect of impulsive noise over a subchannel due to reduced subchannel bandwidth.

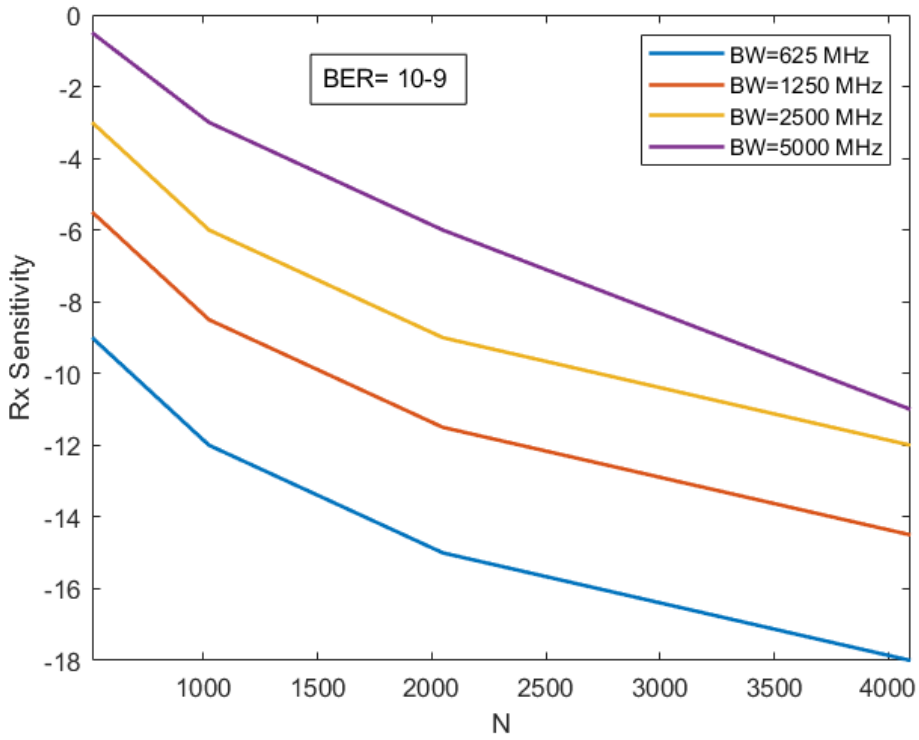

Fig.3.9: Receiver Sensitive vs Number of Subchannel N for SISO OFDM Poisson Noise Model (λTs=0.5, μ=0.85)

The plots of receiver sensitivity at a BER=10^{-9} as a function of number of OFDM subchannel N are depicted in Fig. 3.9 for different system Bandwidth BW at a given value of λTs and μ. The improvement in receiver sensitivity clearly depicted at a given BER with increase in the number of subchannel N for given values of other system parameters and BER=10^{-9}.

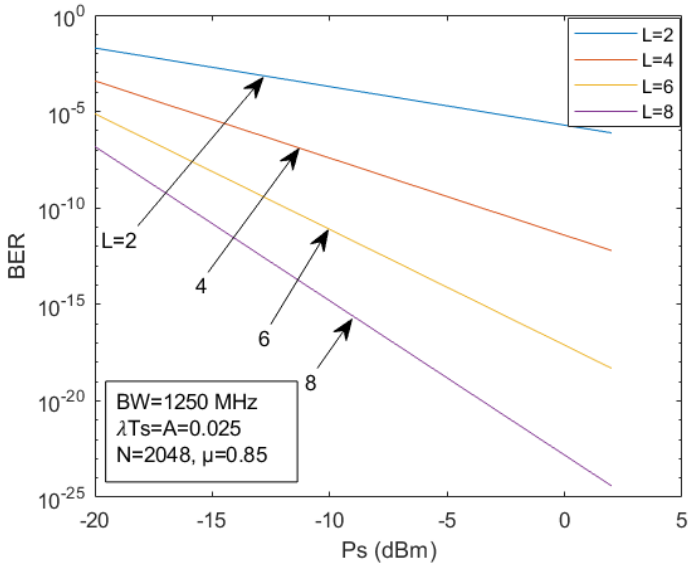

Fig: 3.10 BER Vs Received Power for SIMO OFDM System for different values of L (λTs=0.025, μ=0.85, BW=1250MHz, N=2048) with Poisson's Noise Model

The BER performance results for different values of number of receiving antennas are shown in Fig. 3.10 for λTs=0.025, N=2048, μ=0.85 for SIMO OFDM with MRC with number of receiver antenna L=2, 4, 6 and 8. It is observed that there are significant improvement in receiver sensitivity with increase in number of receiving antenna, L.

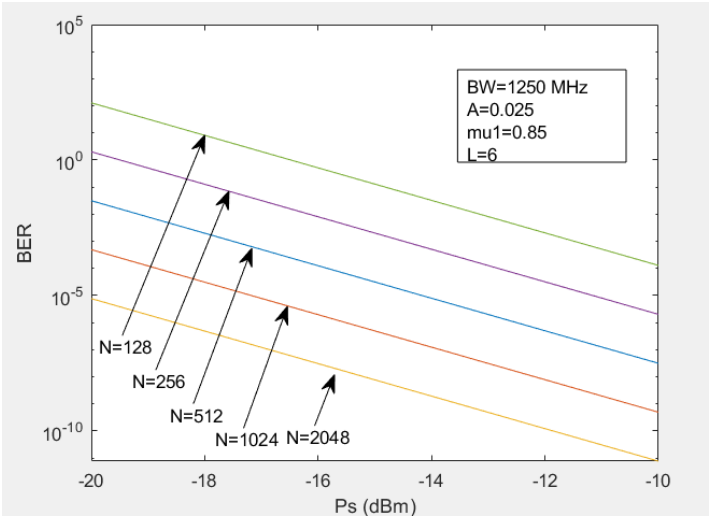

Fig. 3.11: BER Vs Received Power for SIMO OFDM System for different values of N (λTs=A=0.025, mu1=0.85, BW=1250 MHz) with Poisson's Noise Model

Similar BER performance results are also depicted in Fig. 3.11 as BER versus Ps(dBm) with number of OFDM subchannel N as a parameter with L=6. From Fig. 3.10 and Fig. 3.11 it is clearly observed that there are significant improvement in receiver sensitivity with reduction in the amount of power received to achieve a given BER with increase in L due to diversity in reception and also due to increase in number of OFDM subchannel. Which results in less channel bandwidths and less effect of impulsive noise.

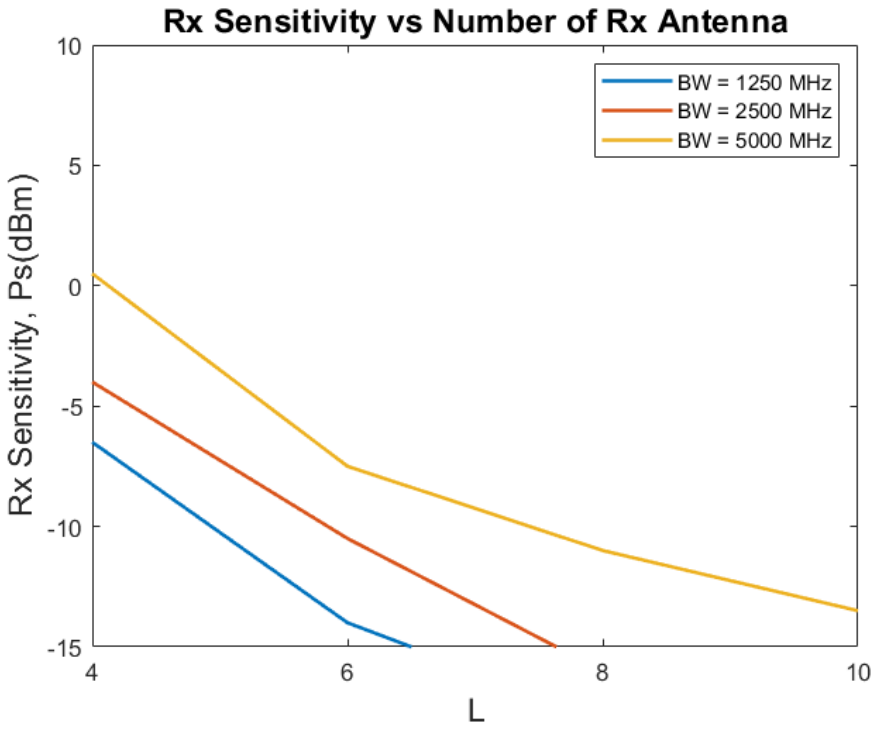

Fig. 3.12: Receiver Sensitivity Vs Number of Receiving Antenna L for SIMO OFDM Poisson's Model (λTs=A=0.025, μ=0.85)

The receiver sensitivity at BER=10^{-9} is plotted in Fig. 3.12 as a function of number of receiving antenna, L with BW as a parameter for λTs=0.025, μ=0.85.

The BER performance result of a SISO OFDM wireless link in presence of Gaussian noise and impulsive noise are evaluated base on the analysis presented in Sec III

considering Middleton Class A noise model for impulsive noise. Fig. 3.13 depicts the plots of BER versus received power Ps (dBm) with are highly degraded because of

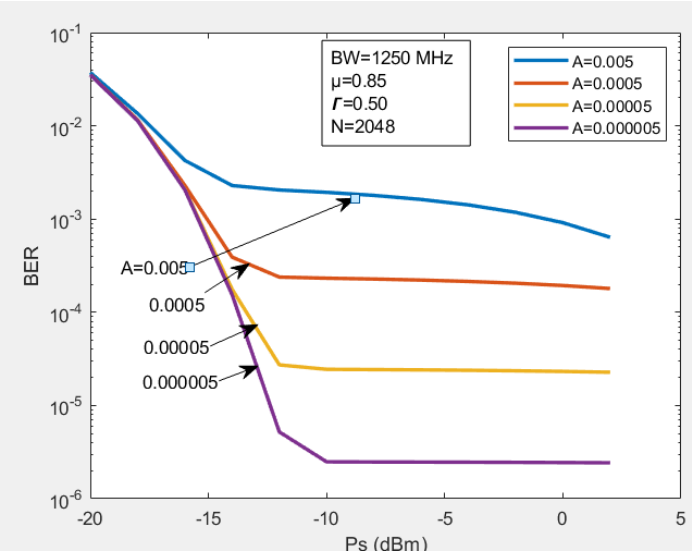

Fig. 3.13: BER Vs Received Power for SISO OFDM System for different values of Impulsive Noise Index A with Middleton Noise Model

impulsive noise and there occurs BER floors due to impulsive noise. The level of BER depends on the impulsive noise index A. At high value of A, BER floor occurs

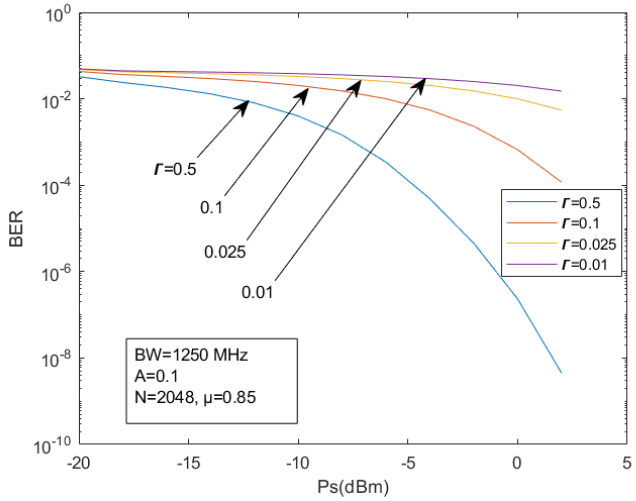

Fig. 3.14: BER vs Received Power for SISO OFDM System for different values of Γ (A=0.1, μ=0.85, N=2048, BW=1250 MHz) with Middleton Noise Model

at a Similar BER performance curves are also shown in Fig 3.14 for several values of ratio of gaussian noise power to impulsive noise power Γ for a given value of N=2048, A=0.1, μ=0.85, BW=1250 MHz. It is observed that BER performance deteriorates significantly at smaller values of Γ which indicates higher impacts of impulsive noise.

The BER performance results for different values of number of OFDM subchannel N are shown in Fig. 3.15 with μ=0.85, BW=1250 MHz, Γ=0.01 and A=0.5. It is found that BER

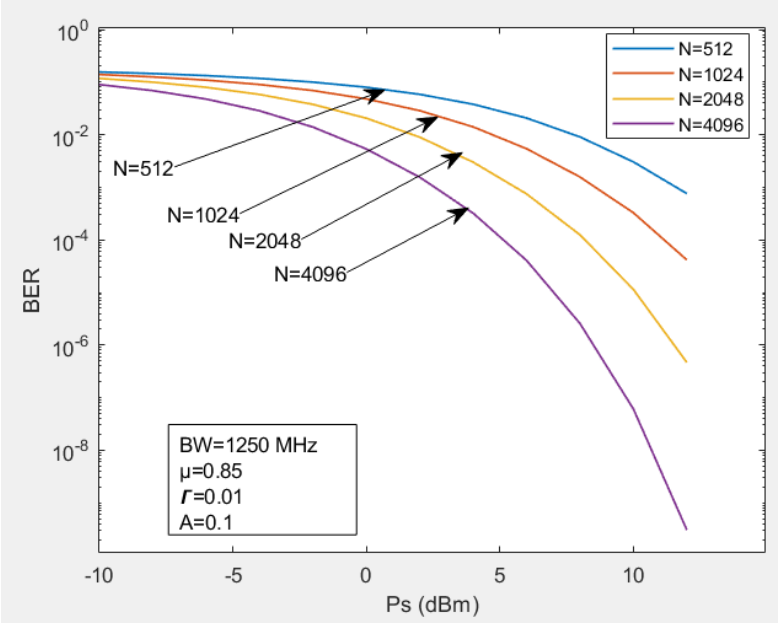

Fig. 3.15: BER Vs Received Power for SISO OFDM System for different values of N (A=0.5, μ=0.85, Γ=0.01, BW=1250 MHz) with Middleton Noise Model

performance can be highly improved by increasing the number of OFDM subchannel N for 512 to 4096. For example, receiver sensitivity at BER-10^{-9} is found to be Ps= 18 dBm corresponding to N=1024. The corresponding value of Ps are 14 and 12 dBm for N=2048 and 4096 respectively. The receiver sensitivity at BER=10^{-6} is found to be 15 dBm, 12 dBm and 8 dBm for N=1024, 2048 and 4096 respectively. Thus, there is improvement in receive sensitivity of about 3 to 4 dB due to increase in number of OFDM sub-channel for N=1024 to 4096.

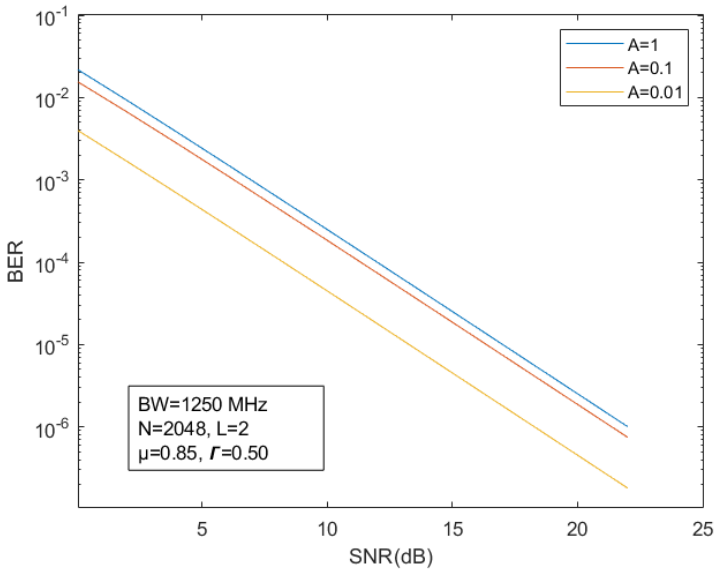

Fig. 3.16: BER vs SNR for SIMO OFDM System for different values of Impulsive Noise Index A (BW=1250 MHz, Γ= 0.50, μ=0.85, L=2 and N=2048) with Middleton

The plot of BER vs SNR is shown in Fig. 3.16 where Impulsive Noise Index A is considered as a parameter. Here A varies from 0.0001 to 0.01. Due to the effect of impulsive noise, the receiver performance is highly degraded.

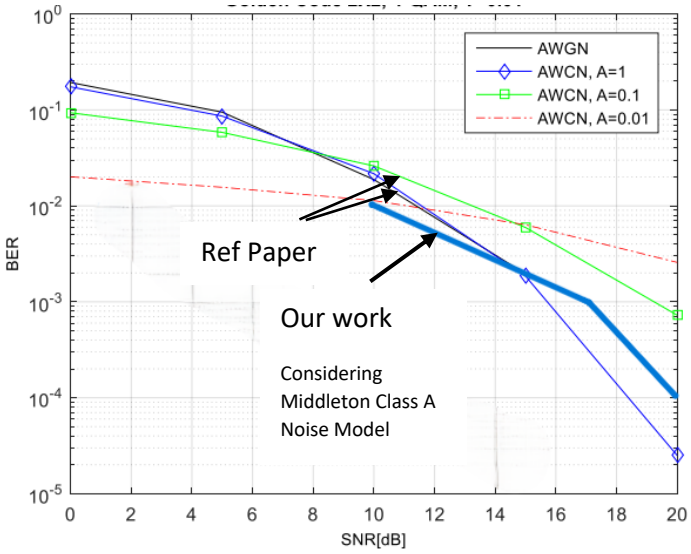

Fig. 3.17: Golden Code performance for AWCN Channel

TABLE I

Comparison of Reference Paper and Our Work

BER SNR (dB)		10^{-2}	10^{-3}	10^{-4}
Ref Work		12.5	20	22
Our Work N=256	L=2	10	17	20
	L=3	7	10	13.5
	L=4	4	6	10

The plot of BER vs SNR for a 2X2 MIMO receiver affected by Rayleigh fading and impulsive noise described by Middleton Class A model is shown in Fig. 17 at BER of 10^{-3}, for impulsive index value of A=0.01, the SNR is found 20 dB.

A comparison curve of our work where BER values are evaluated for same parameter as in Ref Paper [1] considering Middleton Class A noise model which is depicted in Fig. 17. In Table I a comparison of SNR value against different BER value is shown for ref paper as well as our work. Here the results are found in good conformity with the ref paper.

The plot of BER vs SNR for a 2X2 MIMO receiver affected by Rayleigh fading and impulsive noise described by Middleton Class A model is shown in Fig. 3.17 at BER of 10^{-3}, for impulsive index value of A=0.01, the SNR is found 19 dB.

The dependency of BER performance on impulsive noise index A is depicted in Fig. 3.18 which shows the plots of BER versus Ps (dBm) and l-th impulsive noise index as a parameter. Here A varies for 0.00005 to 0.5. Due to the effect of impulsive noise index, the receiver performance is highly degraded and there is significant increase in BER at both value of A for given signal power Ps. At a BER 10^{-9}, the system suffers power penalty of approximately 6 dB where A is increased from 0.00005 to 0.5, for N=2048, μ=0.85, Γ=0.05, BW=1250 MHz, number of receiving antennas L=2.

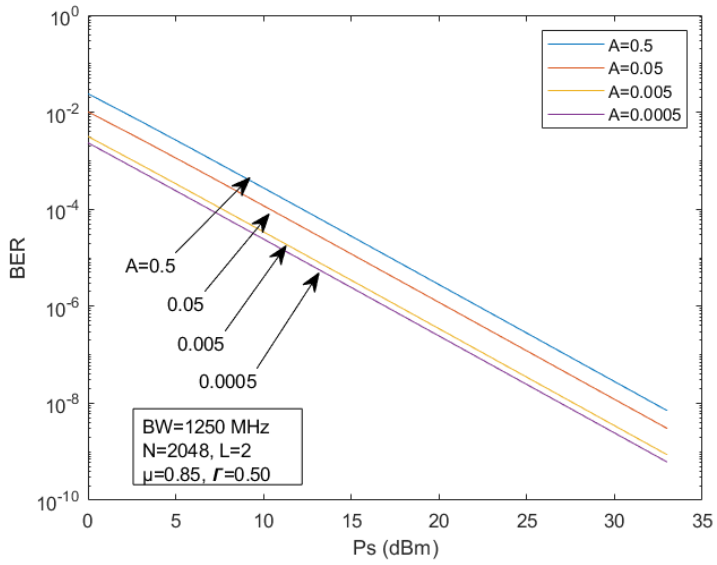

Fig. 3.18: BER Vs Received Power for SIMO OFDM System for different values of A (N=2048, Γ=0.50, μ=0.85, BW=1250 MHz) with Middleton Noise Model

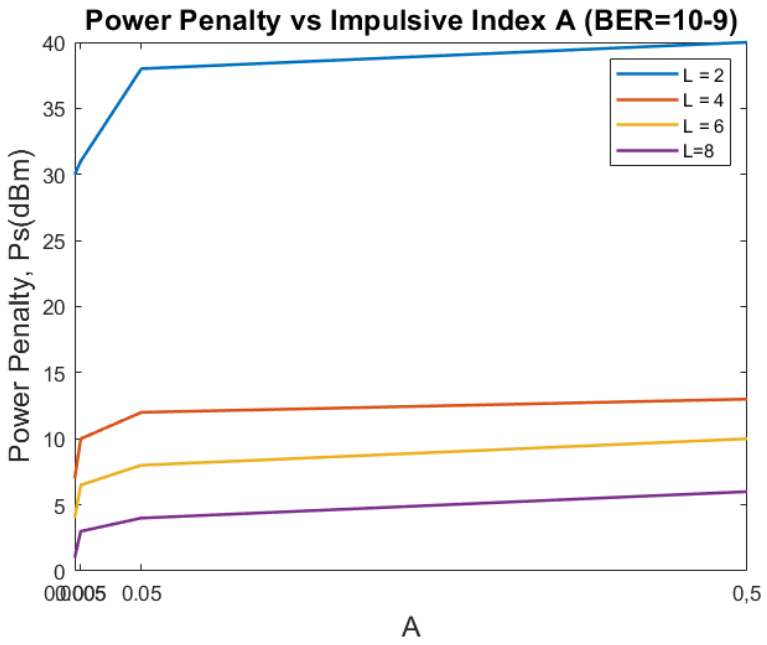

Fig. 3.19: Power Penalty (dB) Vs Impulsive Noise Index A for SISO OFDM with Middleton Noise Model

The plots of power penalty to achieve a given BER 10^{-9}, due to effect of impulsive noise are depicted in Fig. 3.19 as a function of impulsive noise index A for μ=0.85, Γ=0.5, BW=1250 MHz for L=2, 4, 6, 8. It is noticed that there is significant reduction in power penalty due to impulsive noise at a given BER with increase in the number of receiving antennas. It is found that power penalty is 5 dB, 5 dB and 20 dB corresponding to A=0.005, 0.05 and 0.5 for L=2. The corresponding power penalty values are found to be reduced to –dB, -- dB and – dB when L is increased to 8.

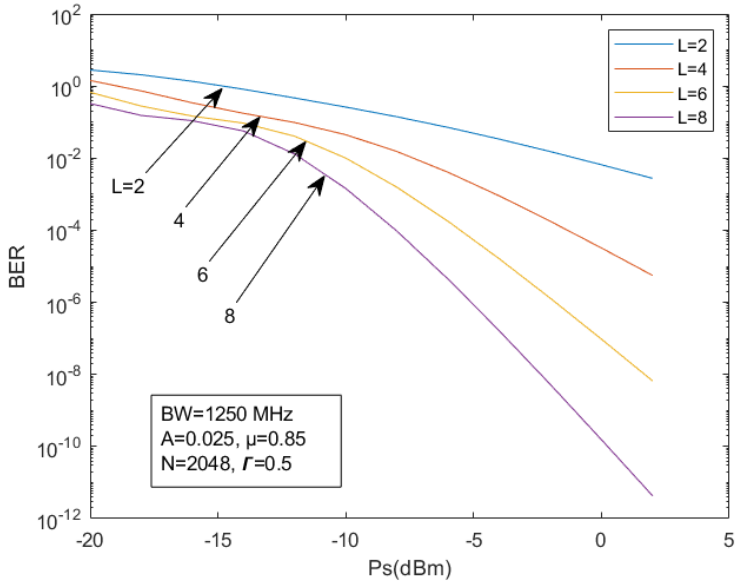

Fig. 3.20 BER Vs Received Power for SIMO OFDM System for different values of L (A=0.025, Γ=0.5, μ=0.85, BW=1250 MHz) with Middleton Noise Model

The BER performance with L as a parameter are also shown in Fig 3.20 for Γ=0.5, A=0.025, BW=1250 MHz. The plots revealed that there is a significant improvement in receiver sensitivity at higher values of number of receiving antenna L.

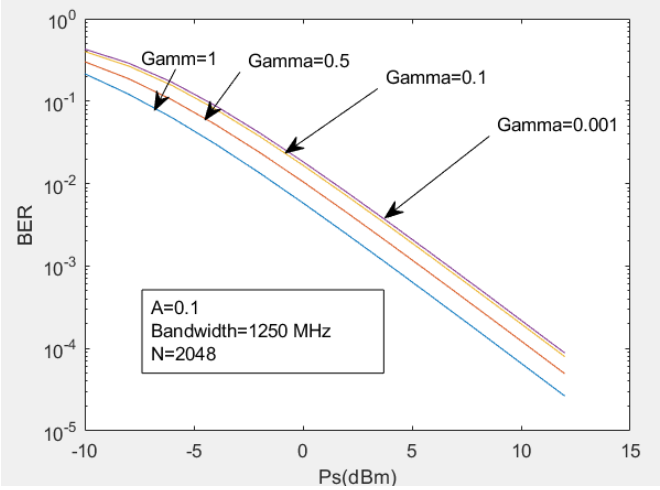

Fig. 3.21: BER Vs Received Power for SISO OFDM System for different values of Γ (A=0.1, N=2048, μ=0.85, BW=1250 MHz) with Middleton Noise Model

BER performance degradation due to impulsive noise is also depicted in Fig. 3.21 as BER vs Ps (dBm) with ratio of Gaussian noise to impulsive noise Γ as a parameter. Impulsive noise is prominent at smaller values of Γ and their 1significant degradation in performance due to increase of Γ at a given L=2.

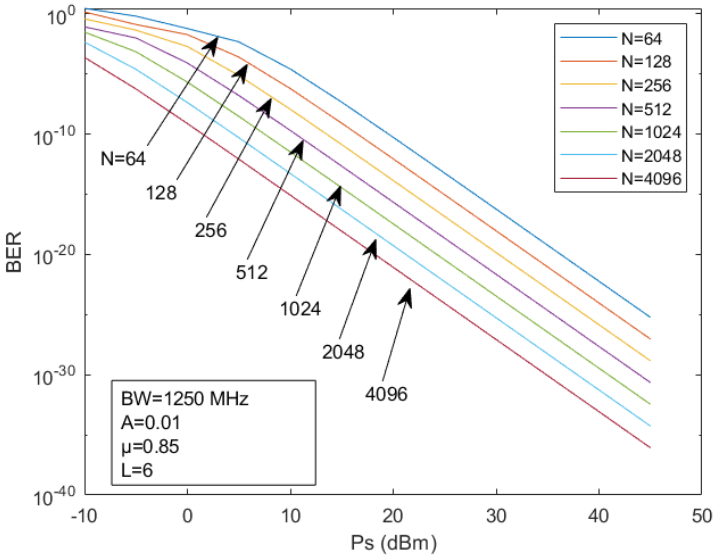

Fig. 3.22: BER Vs Received Power for SIMO OFDM System= for different values of N (A=0.01, Γ=0.1, μ=0.85, BW=1250MHz) with Middleton Noise Model

BER performance improvement due to high number of OFDM sub-carriers in a SIMO OFDM MRC wireless link are depicted in Fig. 3.22 where BER is plotted as a function of received power Ps (dBm) with number of OFDM Sub-channel N as a parameter corresponding to number of receiving antenna L=2, A=0.0005, BW=1250 MHz, Γ=0.50. It is noticed that to achieve a given BER of 10^{-9}, there is less amount of received power required with increase in the number of sub-channel N and improvement in receiver sensitivity is high at high values of N.

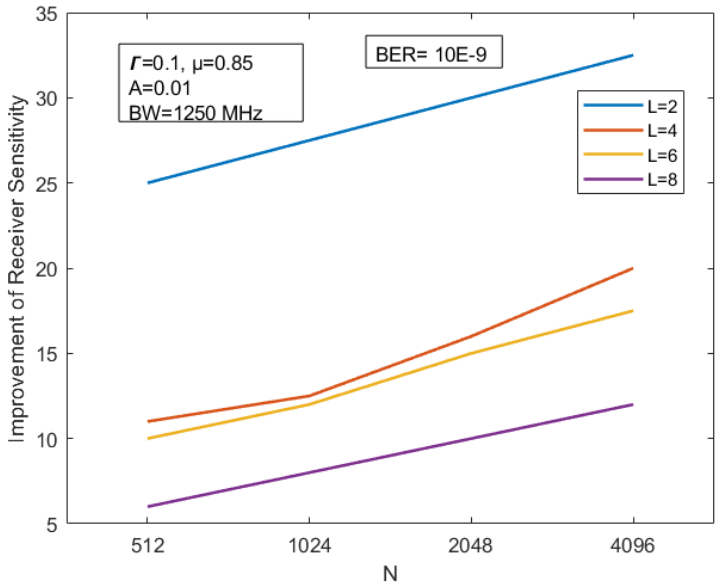

Fig. 3.23: Improvement of Receiver Sensitivity (dB) Vs Number of Subcarrier for SIMO OFDM Middleton Noise Model

The improvement in receive sensitivity over OFDM-SIMO, N=512 is shown in Fig 3.23 for values of N=1024, 2048 and 4096 and L=2,4,6 and 8. Improvement in receiver performance can be obtained by increasing the number of OFDM subcarriers as well as the number of receiving antenna, L. The variation of Receiver Sensitivity with number of subchannel N is shown in Fig. 3.24 with Γ as a parameter, which reveals that improvement does not change significantly with Γ. Receiver sensitivity at BER=10^{-9} as a function of number of subchannel L is shown in Fig. 3.25 for several values of system Bandwidth BW.

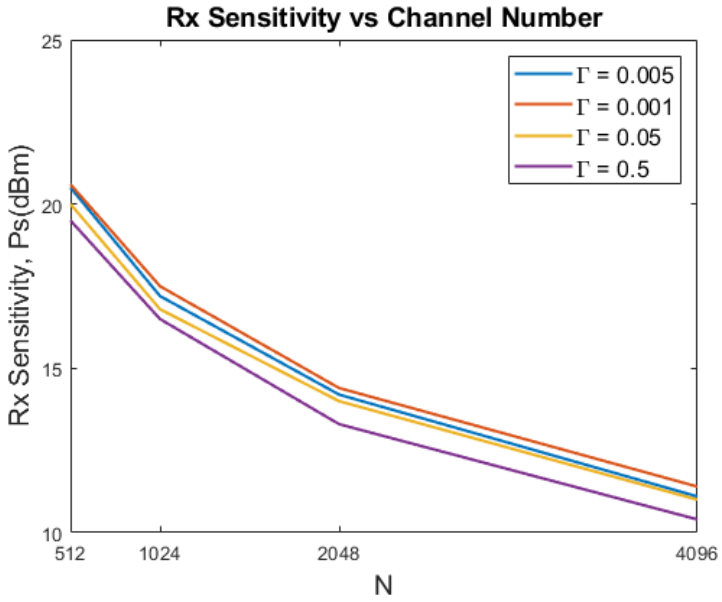

Fig. 3.24: Receiver Sensitivity Under Various ***Γ*** value for SIMO OFDM System for different values of N (A=0.005, μ=0.85, BW=1250 MHz) with Middleton Noise Model

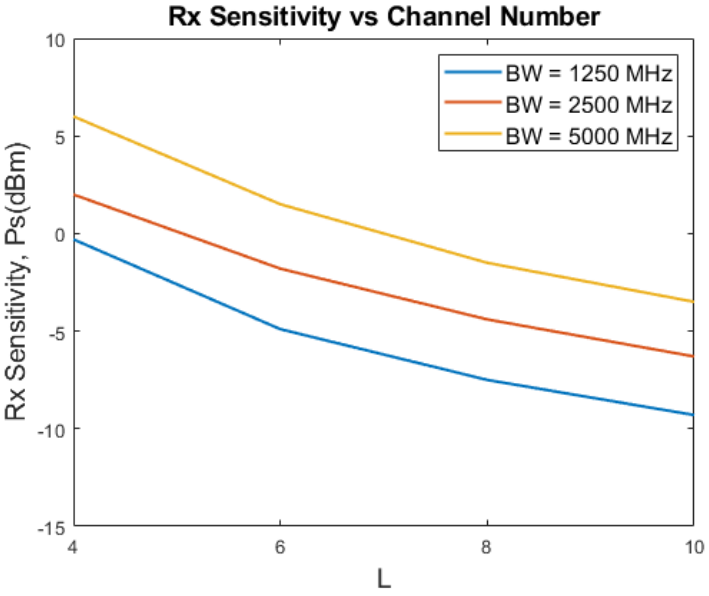

Fig. 3.25: Receiver Sensitivity under various Bandwidth (1250 MHz, 2500 MHz and 5000 MHz) foe SIMO OFDM System for different values of L (A=0.005, μ=0.85) with Middleton Noise Model

At higher BW effect of Impulsive noise is more prominent. Improvement still occurs due to increase in number of subchannel N.

3.5 Summary

In this chapter, a theoretical analysis is presented to find analytical expressions for average bit error rate considering the combined influence of Impulsive noise and Additive white Gaussian noise on the SISO and SIMO MRC OFDM wireless communication links over a Rayleigh fading channel. It is noticed that the level of BER depends on the impulsive noise index A and at high value of A, BER floor occurs at a high level which cannot be covered by increasing signal power. It is also observed that BER performance deteriorates significantly at smaller values of Gaussian Noise Factor Γ which indicates higher impacts of impulsive noise. Results are evaluated numerically and are found to be in good conformity with simulation results reported earlier. It is found that the system suffers significant power penalty in receiver sensitivity at a given bit error rate due to impulsive noise depending on the ratio of Gaussian to impulsive noise. However, penalty can be significantly reduced by increasing the number of OFDM subcarriers and number of receiver antennas. It is noticed that to achieve a given BER of 10^{-9}, there is less amount of received power required with increase in number of subchannel N and improvement in receiver sensitivity is high at high value of N. Further, at higher bandwidth, the effect of impulsive noise is more prominent. Improvement still occurs due to increase in number of subchannel N. For example, there is an improvement in receive sensitivity of about 3 to 4 dB due to an increase in number of OFDM sub-channel for N=1024 to 4096. Finally, it is shown that improvement in receiver performance can be obtained by increasing the number of OFDM sub-carriers as well as the number of receiving antenna, L. Hence, the second objective of the thesis is achieved. which is “to formulate an analytical model and evaluate BER for the above systems considering Rayleigh fading channel, and Middleton Class A and Symmetric Alpha Stable noise models”.

CHAPTER 4

OFDM OSTBC MIMO WIRELESS SYSTEM

4.1 Introduction

Orthogonal Frequency Division Multiplexing (OFDM) has been adapted to high data rate wireless data transmission system because of its high spectrum efficiency and its resistance to multi-path fading. Besides the above advantages, intersymbol interference (ISI) and inter-carrier interference (ICI) give intolerable degradation to the bit error rate (BER) performance over fading channels. The ISI, which is caused by the delay spread, can be easily neglected when multi-path delay is within a guard interval (GI), while the ICI, which is caused by the Doppler frequency shift, cannot be canceled without ideal estimation at a receiver [86].

In OFDM systems with differential phase shift keying (DPSK) it is possible to apply differential modulation either in the time or frequency domain depending on the condition of the fading channels such as the Doppler frequency shift and the delay spread. Besides the ICI, the BER performance in those systems is influenced by time or frequency correlation between the adjacent symbols. Generally, the symbol period in OFDM system is much longer than that in single carrier systems in order to reduce the effect of the delay spread. Owing to this fact inter-symbol fluctuation at the time domain caused by the Doppler frequency shift is led to be larger while inter-carrier fluctuation in the frequency domain caused by the delay spread is led to be small. Consequently, there exists a merit to adopt the differential modulation in the frequency domain depending on the channel condition [87].

MIMO (Multiple Input and Multiple Output) system is the latest and most popular arrangement and addition of antenna arrangement. In MIMO system limited bandwidth and power is utilized at the cost of space diversity. If the individual channel route gains between the broadcast and receive antennas fade separately, the likelihood of a well-conditioned channel state information matrix is high, and parallel spatial

channels are produced. MIMO introduces the advantages of higher data rates transmitted through different channels, time diversity for sending data packs at different time slots, frequency diversity for employing different frequency components, reduced fading and distortion, improved SNR, superior accuracy [88].

4.2 Performance Analysis

4.2.1 System Model with Description

The model of a OFDM system with STBC considered for analysis is shown in Fig 4.1.a. and Fig. 4.1.b

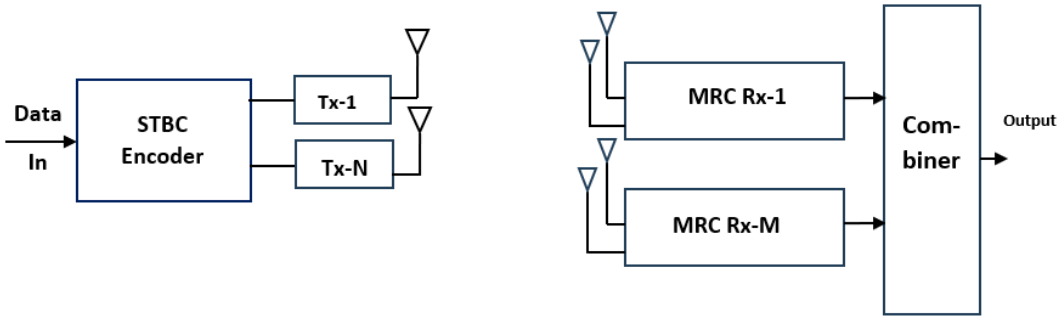

Fig. 4.1.a : Block diagram of MIMO-OFDM System with STBC (Simple)

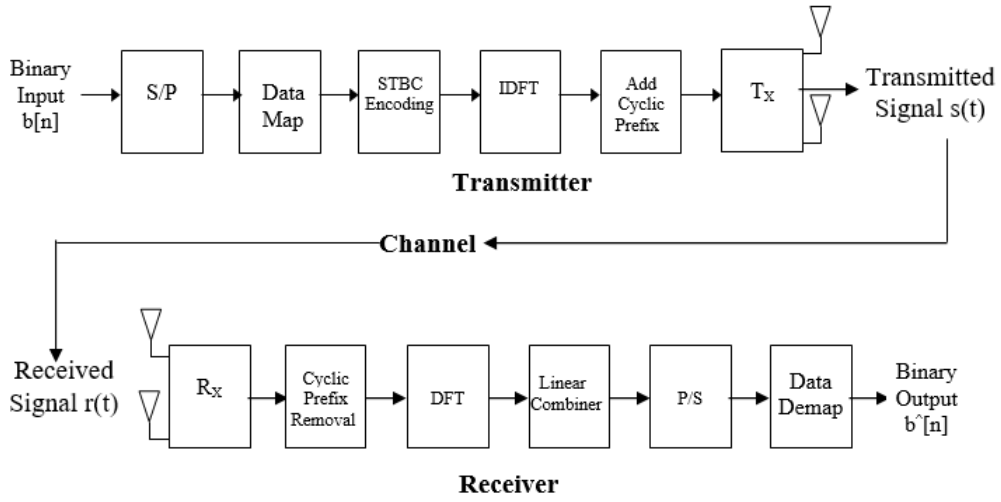

Fig. 4.1.b: Block diagram of MIMO OFDM system with STBC (detail)

The serial data stream input is formatted into the word size required for transmission by serial to parallel conversion, e.g. 2 bits/word for QPSK, and shifted into a parallel format. The data is then transmitted in parallel by assigning each data word to one carrier in the transmission. The data to be transmitted on each carrier is mapped into a Phase Shift Keying (PSK modulation) format. The data on each symbol is then mapped to a phase angle based on the modulation method. For example, for QPSK the phase angles used are 0, 90, 180, and 270 degrees. For DQPSK and DPSK (DBPSK) modulation, differential coding is performed in the time domain. The data is encoded by Space-Time Block Code (STBC) to achieve coding and diversity gain [93].

The guard period/cyclic prefix is a copy of the last part of the OFDM symbol that is prepended to the transmitted symbol and removed at the receiver before the demodulation. The length of the cyclic prefix is made longer than the experienced impulse response to avoid ISI and ICI. After the guard has been added, the symbols are then converted back to a serial time waveform. This is then the base band signal for the OFDM transmission. Cyclic Prefix (CP) is added to remove Inter-symbol Interference (ISI) and to cancel Inter-Carrier Interference (ICI).

IDFT is the Inverse discrete Fourier transform of the input signal. Using IFFT, OFDM modulation is computed on each set of symbols, resulting in time-domain samples. The Inverse Discrete Fourier transform (IDFT) is given by [94]:

$$x_n = \frac{1}{N}\sum_{k=0}^{N-1} X_k e^{\frac{2\pi i}{N}kn} \qquad \text{n=0, . . . , N-1} \tag{4.1}$$

A simple description of these equations is that the complex numbers X_k represent the amplitude and phase of the different sinusoidal components of the input "signal" x_n. The DFT computes the X_k from the x_n, while the IDFT shows how to compute the x_n as a sum of sinusoidal components $X_k \exp(2\pi ikn / N) / N$ with frequency k / N cycles per sample. The diversity in transmission is achieved by multiple transmit antennas which helps to utilize space diversity also. The channel is time-selective Rayleigh/Rician fading with AWGN.

The receiver basically does the reverse operation to the transmitter. The guard period is removed. The DFT of each symbol is then carried out to find the original transmitted spectrum. This returns N parallel streams. The phase angle of each transmission carrier is then evaluated and converted back to binary stream by demodulating the received phase. These streams are then re-combined into a serial stream, $\hat{b}[n]$ which is an estimate of the original binary stream at the transmitter.

4.3 BER Analysis with Coding

To improve transmission performance, channel coding is added. To optimize the use of the correction capacity of a particular code, soft decision is always a good solution. For this reason, convolutional coding is chosen for the system. In the presence of channel coding, an expression of the bit error probability P_e cannot be worked out exactly, showing the need for a good upper bound. It is well known that using a rate R= K/N convolutional coding and a Viterbi algorithm decoding, the bit error probability for an information symbol is bounded by as [94]

$$P_e \leq \frac{1}{K} \sum_{d=d_f}^{\infty} W(d)P(d) \tag{4.2}$$

where P(d) is the probability for the decoding algorithm to choose a path at distance d from the correct path in the decoding trellis, d_f is the free distance of the encoder and W(d), a characteristic coefficient of the encoder, is defined as [95]:

$$W(d) = \sum_{i=1}^{\infty} ia(d,i) \tag{4.3}$$

where $a(d,i)$ is the number of paths at distance d from the correct path and corresponding to i information symbols equal to '1'. In general, the a(d, i) are deduced from the transfer function of the encoder. Considering the uncoded BER to be P_{un} the value of $P(d)$ can be expressed as follows:

$$P(d) = \{4\ P_{un}\ (1 - P_{un})\}^{d/2} \tag{4.4}$$

W(d) is obtained from the code weights in Table 4.1 [95]. Substituting the unconditional BER (Pe) from Equation. (4.2) in Equation. (4.3), we can calculate the coded BER from Equation. (4.4).

Table 4.1: Weigh Spectrum of convolutional encoders

Hamming Weight d	**W(d) for R=1/2**	**W(d) for R=1/3**
10	3.6×10^{01}	-
11	0	-
12	2.11×10^{02}	-
13	0	-
14	1.404×10^{03}	-
15	0	1.1
16	1.633×10^{04}	1.6
17	0	1.9
18	7.7433×10^{04}	2.8
19	0	5.5
20	5.0269×10^{05}	9.6
21	0	1.69×10^{02}
22	3.322763×10^{06}	3.38×10^{02}
23	0	6.36×10^{02}
24	2.129291×10^{07}	1.276×10^{03}
25	0	2.172×10^{03}
26	1.3436491×10^{08}	-

4.4 Performance Analysis of a OFDM System

4.4.1 Performance with STBC:

We consider MIMO-OFDM system with P number of transmitting and two receiving antennas. There are N_s number of OFDM subcarriers. We also consider Rayleigh and Rician fading channel. Binary input data is mapped to a modulation symbols {a(i)}that are assumed to have the following properties [96]:

$$E[a(i)] = 0$$

$$E[a(i)\, a^*(j)] = \begin{cases} 1, i = j \\ 0, i \neq j \end{cases}$$

The input sequence {a(i), i=0, 1, 2 …….. (N_sP-1)} is serial-to-parallel converted into P sequences each of length N_s, as $a_p(k)= a(k+(p-1)N_s)$ where p=1, 2……P and k=0, 1, 2……(N_s –1) Each of the N_s sequences {$a_1(k)$ …….. $a_P(k)$}, k=0,1,2……,(N_s –1) is mapped to a matrix Ψ_k of size P×P by using a quasi orthogonal STBC with constellation rotation. For P=4, the 4×4 quasi orthogonal scheme is given as [96]:

$$\Psi_k = \begin{bmatrix} a_1(k) & -a_2^*(k) & e^{j\Phi}a_3(k) & -e^{-j\Phi}a_4^*(k) \\ a_2(k) & a_1^*(k) & e^{j\Phi}a_4(k) & e^{-j\Phi}a_3^*(k) \\ e^{j\Phi}a_3(k) & -e^{-j\Phi}a_4^*(k) & a_1(k) & -a_2^*(k) \\ e^{j\Phi}a_4(k) & e^{-j\Phi}a_3^*(k) & a_2(k) & a_1^*(k) \end{bmatrix}$$

where the rotation angle Φ depends on the signal constellation. Then we take the IDFT of $\Psi_1, \Psi_2, \ldots\ldots \Psi_k$ in order to form the transmitted signals as

$$S_m = \frac{1}{\sqrt{N_s}} \sum \Psi_k . e^{j(2\pi/Ns)mk},\ m=0,1\ldots\ldots(Ns-1) \qquad (4.5)$$

S_m is a P×P matrix, which represents the transmitted signals on the *m*th subcarrier. We define

$$\Psi=[\Psi_0^T,\ldots\ldots\ldots..\Psi_{Ns-1}^T]^T,\ (N_sP\times P) \tag{4.6}$$

$$S=[S_0^T,\ldots\ldots\ldots\ldots S_{Ns-1}^T]^T,(N_sP\times P) \tag{4.7}$$

where $(.)^T$ denotes transpose, then S can be written as

$$S=(U\otimes I_p)^H\Psi \tag{4.8}$$

Here $(.)^H$ denotes complex conjugate transpose, $\otimes$ denotes kronecker product, I_p is the P×P identity matrix, and U is the $N_s\times N_s$ unitary discrete Fourier transform (DFT) matrix. In frequency-selective fading channels with L resolvable paths, there exists inter block interference (IBI). To minimize this IBI, a cyclic prefix of length c_p ($c_p\geq L$) is added to each OFDM symbol. At the receiver, the cyclic prefix is discarded, leaving IBI-free, information-bearing signals.

The model of the channel with L resolvable multipath components can be expressed as [24]

$$h(\tau)=\sum_{l=0}^{L-1}\rho_l\delta(\tau-\tau_l T_s) \tag{4.9}$$

where ρ_l is the zero-mean complex Gaussian random variable, and τ_l is the delay of the *l*th path normalized with respect to T_s. The delays $\{\tau_l\}$ are assumed to be uniformly distributed over the cyclic prefix c_p. The channel has an exponential power-delay profile $\theta(\tau_l)=e^{-\frac{\tau_l}{\tau_{rms}}}$, where τ_{rms} represents the rms delay spread, which is also normalized with respect to T_s. The P symbols in each column of Ψ_k are transmitted from the P transmit antennas simultaneously during every OFDM symbol period. Considering the channel matrix H the received signals is expressed in an $N_s\times P$ matrix as:

$$R=HS+V, \tag{4.10}$$

Where, $V=[v_0,\ldots\ldots..v_{Ns-1}]^T$ $(N_s\times P)$ is the additive white Gaussian noise (AWGN) matrix whose elements are independent and identically distributed. Hence

$$E[vec(V).vec(V)^H]=\sigma^2 I_{NsP} \tag{4.11}$$

where σ^2 is the variance of the zero-mean noise samples when the transmitted symbol energy is normalized to unity. For OFDM systems over fast fading channels, channel estimation is generally carried out by transmitting pilot symbols in given positions of the frequency-time grid. We assume hereafter that channel state information (CSI) is known at the receiver. In the presence of time-selective fading, H is no longer a block-circulant matrix. Consequently, $G = UH(U \otimes I_P)^H$ is not a block diagonal matrix. This shows that time-selective fading causes ICI, which is represented by the off-diagonal blocks of G.

The received signal R is processed by multiplying it with U, forming $N_s \times P$ matrix X as $X=[x_0^T, \ldots\ldots\ldots x_{Ns-1}^T]^T = UR$,

Now from (4.14) we get

$$X=U(HS+V)=G\Psi+W \tag{4.12}$$

where $x_k =[x_1(k), \ldots\ldots x_P(k)]^T$, $w_k =[w_1(k),\ldots..w_P(k)]^T$ and $W=UV=[w_0, \ldots.w_{Ns-1}]^T(N_s \times P)$

$$x_k^T = g_{k,k}^T \Psi_k + \sum_{k'=0,k'\neq k}^{N_s-1} g_{k,k'}^T \Psi_{k'} + w_k^T, \qquad k=0,\ldots\ldots,N_s\text{-}1$$

$$\text{and } g_{k,k'} = [g_{k,k'}^{(1)},\ldots\ldots\ldots\ldots, g_{k,k'}^{(P)}]^T, \quad k, k' =0,\ldots\ldots\ldots, N_s\text{-}1 \tag{4.13}$$

$g_{k,k'}$ is the (k,k')th block of G. The signal X is received in two receiving antennas. Diversity combiner at the receiver selects the best instantaneous signal of the two antennas. The received signal can be detected through differential or coherent scheme.

SINR for quasi-orthogonal STBC-OFDM system has an expression as:

$$\text{SINR}= \frac{4\sum_{l=0}^{L-1}[N_s + 2\sum_{i=1}^{N_s-1}(N_s-1)J_0(2\pi i f_d T_s)]e^{-\frac{\tau_l}{\tau_{rms}}}}{4\sum_{k'=1}^{N_s-1}\sum_{l=0}^{L-1}[N_s + 2\sum_{i=1}^{N_s-1}(N_s-1)J_0(2\pi i f_d T_s)\cos(\frac{2\pi}{N_s}k'i)\, e^{-\frac{\tau_l}{\tau_{rms}}}] + \sigma^2} \tag{4.14}$$

4.5 Performance Analysis of Transmit Diversity of MIMO-OFDM with STBC

4.5.1 Two-Branch Transmit Diversity with One Receiver.

At a given symbol period, two signals are simultaneously transmitted from the two antennas. The signal transmitted from antenna one is denoted by s_1 and from antenna two by s_2. During the next symbol period signal $\left(-s_2^*\right)$ is transmitted from antenna one, and signal s_1^* is transmitted from antenna two where $*$ is the complex conjugate operation. This sequence is shown in Table I.

TABLE I

The Encoding and Transmission Sequence for the Two-Branch Transmit Diversity Scheme

	antenna 1	antenna 2
time t	s_1	s_2
time $t+1$	$-s_2^*$	s_1^*

The channel at time t may be modeled by a complex multiplicative distortion $\alpha_1(t)$ for transmit antenna one and $\alpha_2(t)$ for transmit antenna two. Assuming that fading is constant across two consecutive symbols, we can write

$$\alpha_1(t) = \alpha_1(t+1) = \alpha_1 = \partial_1 e^{j\theta_1}$$
$$\alpha_2(t) = \alpha_2(t+1) = \alpha_2 = \partial_1 e^{j\theta_2} \quad (4.15)$$

Noise and interference are added at the receivers. The resulting received baseband signals are

$$r_1 = r(t) = \alpha_1 s_1 + \alpha_2 s_2 + \eta_1$$

$$r_2 = r(t+1) = -\alpha_1 s_2^* + \alpha_2 s_1^* + \eta_2 \tag{4.16}$$

where r_1 and r_2 are the received signals at time t and $t+1$, η_1 and η_2 are complex random variables representing receiver noise and interference. Assuming η_1 and η_2 are Gaussian distributed, the maximum likelihood decision rule at the receiver for these received signals is to choose signal s_i if and only if (in case of s_1) [97]

$$d^2\left(r_1, \alpha_1 s_i\right) + d^2\left(r_2, \alpha_2 s_i^*\right) \le d^2\left(r_1, \alpha_1 s_k\right) + d^2\left(r_2, \alpha_2 s_k^*\right) \quad \forall i \ne k$$

choose signal s_i if and only if (in case of s_2)

$$d^2\left(r_1, \alpha_2 s_i\right) + d^2\left(r_2, \left(-\alpha_1 s_i^*\right)\right) \le d^2\left(r_1, \alpha_2 s_k\right) + d^2\left(r_2, \left(-\alpha_1 s_k^*\right)\right) \forall i \ne k \tag{4.17}$$

where $d^2(x, y)$ is the squared Euclidean distance between signals x and y calculated by the following expression:

$$d^2(x, y) = (x - y)\left(x^* - y^*\right) \tag{4.18}$$

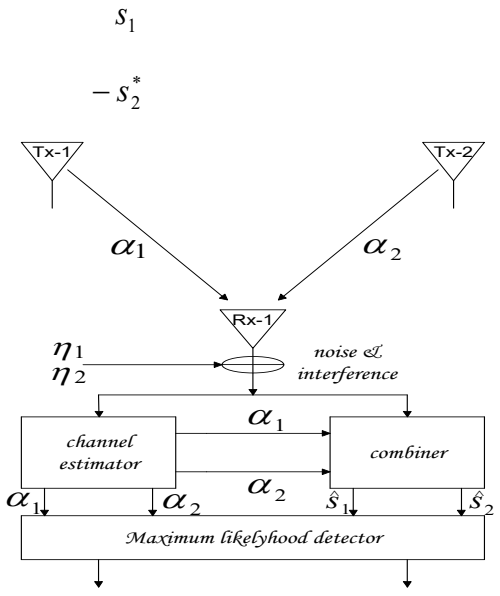

Fig 4.2 Two-Branch Transmit Diversity with One Receiver

The combiner shown in Figure 4.2 builds the following two combined signals that are sent to the maximum likelihood detector:

$$\hat{s_1} = \alpha_1^* r_1 + \alpha_2 r_2^* = \alpha_1^* \left(\alpha_1 s_1 + \eta_1\right) + \alpha_2 \left(\alpha_2 s_1^* + \eta_2\right)^* = \left(\partial_1^{\,2} + \partial_2^{\,2}\right) s_1 + \alpha_1^* \eta_1 + \alpha_2 \eta_2^*$$

$$\hat{s_2} = \alpha_2^* r_1 - \alpha_1 r_2^* = \alpha_2^* \left(\alpha_2 s_2 + \eta_1\right) - \alpha_1 \left(-\alpha_1 s_2^* + \eta_2\right)^* \tag{4.19}$$

Expanding (3.17) and using (3.18) and (3.19) and some manipulation, we get

choose signal s_i if (in case of s_1)

$$\left(\partial_1^{\,2} + \partial_2^{\,2} - 1\right) \left|s_i\right| + d^2\left(\hat{s_1}, s_i\right) \le \left(\partial_1^{\,2} + \partial_2^{\,2} - 1\right) \left|s_k\right| + d^2\left(\hat{s_1}, s_k\right) \;\forall\; i \neq k$$

choose signal s_i if (in case of s_2)

$$\left(\partial_1^{\,2} + \partial_2^{\,2} - 1\right) \left|s_i\right| + d^2\left(\hat{s_2}, s_i\right) \le \left(\partial_1^{\,2} + \partial_2^{\,2} - 1\right) \left|s_k\right| + d^2\left(\hat{s_2}, s_k\right) \;\forall\; i \neq k \tag{4.20}$$

For PSK signals (equal energy constellations) $\left|s_i\right|^2 = \left|s_k\right|^2 = E_s \quad \forall\; i,k$ (4.21)

where E_s is the energy of the signal. Therefore, for PSK signals, the decision rule in (4.26) may be simplified to

choose signal s_i if (in case of s_1) $\quad d^2\left(\hat{s_1}, s_i\right) \le d^2\left(\hat{s_1}, s_k\right) \;\forall\; i \neq k$

choose signal s_i if (in case of s_2) $\quad d^2\left(\hat{s_2}, s_i\right) \le d^2\left(\hat{s_2}, s_k\right) \;\forall\; i \neq k$ (4.22)

The maximal-ratio combiner may then construct the signal $\hat{s_1}$ and $\hat{s_2}$, as shown in Figure 4.5, so that the maximum likelihood detector may produce $\tilde{s_1}$ and $\tilde{s_2}$, which is a maximum likelihood estimate of s_1 and s_2.

4.6 MIMO-OFDM:

STBC-OFDM with transmitting diversity is transformed into MIMO-OFDM by addition of receiving diversity. The block diagram of a MIMO system is shown in Fig 4.3.

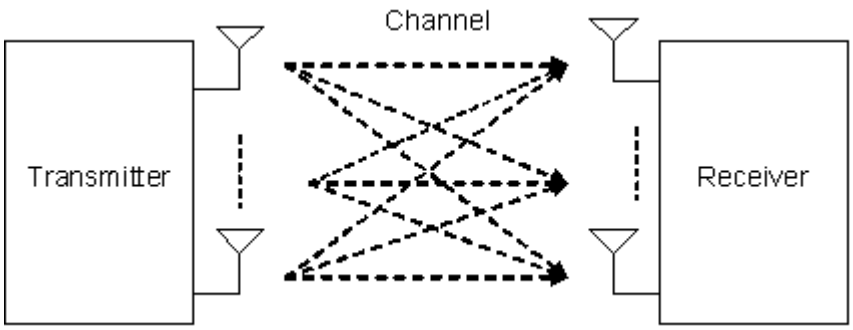

Fig. 4.3 Block diagram of a MIMO system

To utilize the receiving diversity scheme diversity combining is required. For selective diversity combining the instantaneous processed bit SNR/SIR at the output of the combiner is given by [96]

$$\gamma = \max\{ \lambda 1, \lambda 2 \} \tag{4.23}$$

Here λ is the instantaneous SIR at each receiving antenna and γ is the the instantaneous SIR of the combined branch. For a single antenna the pdf of λ is obtained as follows

$$P_1(\lambda) = \frac{A}{(\lambda + A)^2} \tag{4.24}$$

where A denotes the average value of λ_1. The pdf of γ for the selection combining method is [94]

$$P_2(\gamma) = \frac{2A}{(\lambda + A)^2} - \frac{2A}{(2\lambda + A)^2} \tag{4.25}$$

The average Bit error probability without diversity is $Pe_1(A)$ and with diversity is Pe2(A)

$$P_{e_1}(A) = \int_{-\infty}^{\infty} P_e(\gamma) P_1(\gamma) d\gamma = \int_{-\infty}^{\infty} P_e(\gamma) \frac{A}{(\lambda+A)^2} d\gamma \tag{4.26}$$

$$Pe_2(A)=\int_{-\infty}^{\infty} Pe(\gamma)P_2(\gamma)d\gamma=\int_{-\infty}^{\infty} Pe(\gamma)\{\frac{2A}{(\lambda+A)^2}-\frac{2A}{(2\lambda+A)^2}\}d\gamma \quad (4.27)$$

$$Pe_2(A)=\int_{-\infty}^{\infty} Pe(\gamma)\{\frac{2A}{(\lambda+A)^2}-\frac{2A}{(2\lambda+A)^2}\}d\gamma=\int_{-\infty}^{\infty} Pe(\gamma)\frac{2A}{(\lambda+A)^2}d\gamma-\int_{-\infty}^{\infty} Pe(\gamma)\frac{2A}{(2\lambda+A)^2}d\gamma$$

$$=2\int_{-\infty}^{\infty} Pe(\gamma)\frac{A}{(\lambda+A)^2}d\gamma-\int_{-\infty}^{\infty} Pe(\gamma)\frac{(A/2)}{(\lambda+\frac{A}{2})^2}d\gamma=2Pe_1(A)-Pe_1(A/2)$$

So, for SIR=A, the relationship becomes:

$$Pe_2(A)=2Pe_1(A)-Pe_1(A/2) \quad (4.28)$$

For SNR=A the same result is found: $Pe_2(A)=2Pe_1(A)-Pe_1(A/2)$

From the expressions we can conclude that for SINR=A the same relationship will hold. In this case, $Pe_1(A)$ represents BER for average SINR=A with single receiving antenna and $Pe_2(A)$ represents BER for average SINR=A with diversity combining of two receiving antennas. Substituting the unconditional BER of STBC-OFDM with single receiving antenna we obtain the unconditional BER for MIMO-OFDM with two receiving antennas [95-96]. The expression mentioned in Section 4.3 can be used to calculate the conventional coded BER for MIMO-OFDM systems.

In this chapter we have presented the analytical method for evaluating OFDM, STBC-OFDM and MIMO-OFDM in presents of three impairments. We can notice that our coding offers a considerable performance gain of 6 dB at 8 dB for all the values of α. We have analyzed the performance of convolutional code versus non-Gaussian impulsive noise modeled as a stable alpha distribution in the OFDM system. We then provided a BER comparison between different modulation schemes and convolutional coding, as a result we saw that CC boosts the quality of OFDM transmission.

4.7 Result and Discussion

Following the theoretical analysis, Bit Error Rate performance results for MIMO OFDM with Middleton Class A noise model are evaluated as depicted in Fig. 4.4 as

BER versus received power Ps (dBm) with A as a parameter for μ=0.85, BW=1250 MHz, N=256, T=Γ=0.01.

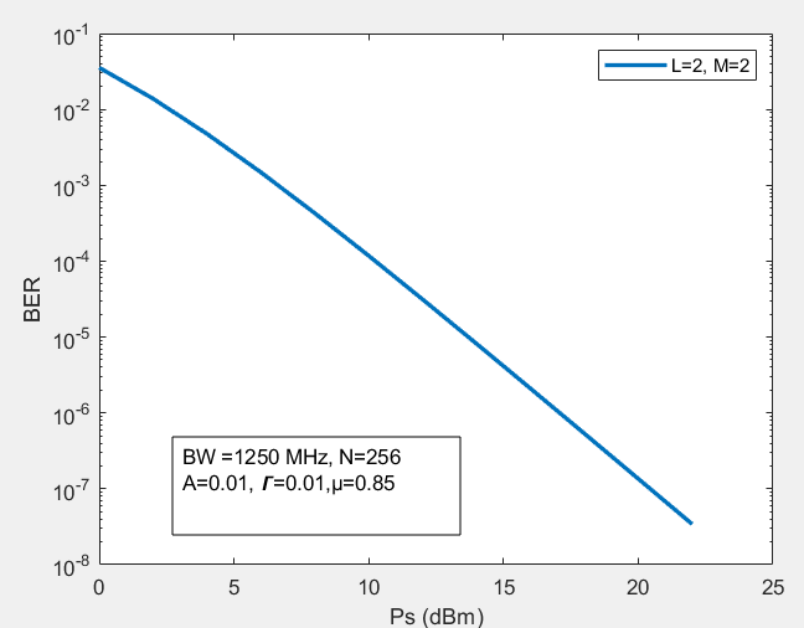

Fig. 4.4 BER vs Ps(dBm) or SNR (dB) for L=2 and M=2 (2X2 MIMO)

In Fig. 4.5 the comparison of performance for Golden Code and our result for 2 transmitting and 2 receiving antennas affected by Rayleigh fading and impulsive noise described by Middleton Class-A model are depicted. Here in this figure, up to 8dB SNR value (except for A=0.01 where SNR=12 dB), the Golden Code leads to better performance in Additive White Class A (AWCN) channel and after 9 dB, the AWCN channel has a low BER. At A=1, the BER is closer to AWGN. The performance is better for impulsive noise, for low SNR value. The plot of BER vs SNR for a 2X2 MIMO receiver affected by Rayleigh fading and impulsive noise described by Middleton Class A model is shown in Fig. 4.4 and Fig. 4.5 at BER of 10^{-3}, for impulsive index value of A=0.01, the SNR is found 20 dB.

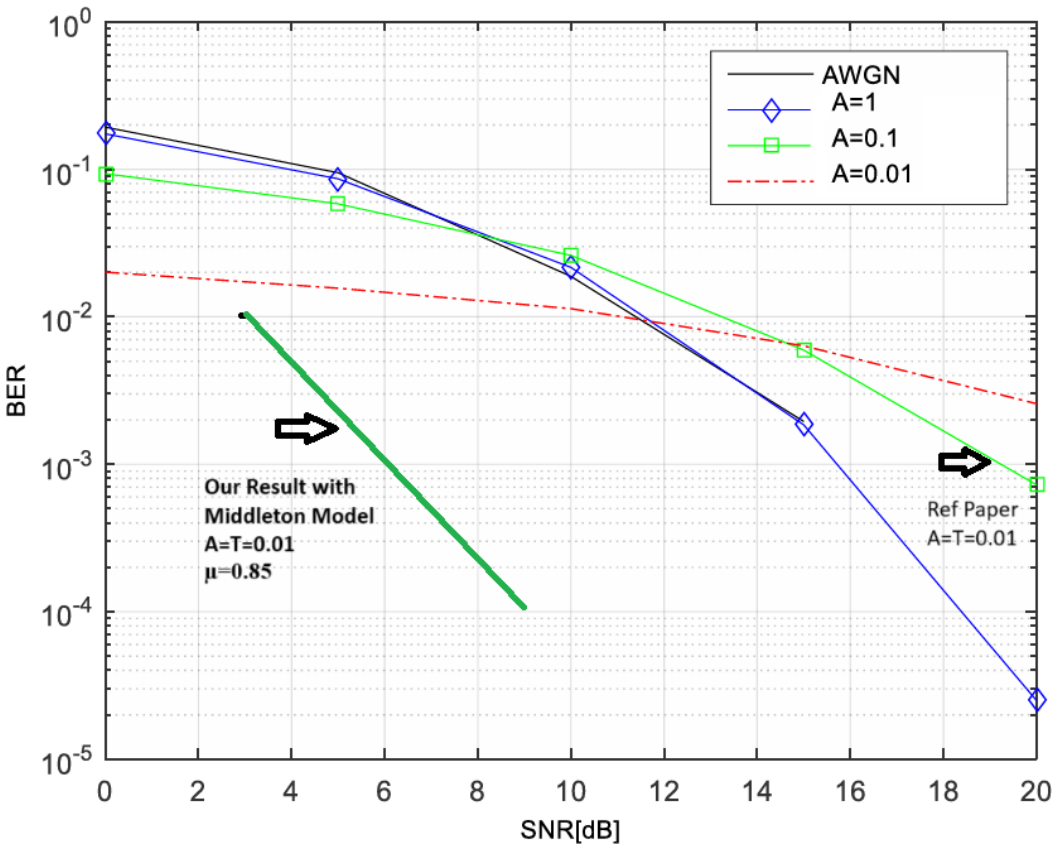

Fig. 4.5: Comparison of performance for 2X2 MIMO Golden Code (Ref Paper) and 2X2 MIMO Middleton Class A model of Our Work

TABLE III

Comparison of our work for MIMO OFDM with Ref Paper (A=0.1)

BER SNR (dB)		10^{-2}	10^{-3}	10^{-4}
Ref Work		12.5	20	22
Our Work N=256	L=2 M=2	3	6	9
	L=3 M=3	4	8	10
	L=4 M=4	5	9	12

A comparison curve of our work where BER values are evaluated for same parameter as in Ref Paper [1] considering Middleton Class A noise model which is depicted in Fig. 4.5 In Table I a comparison of SNR value against different BER value is shown for ref paper as well as our work. Here the results are found in good conformity with the ref paper.

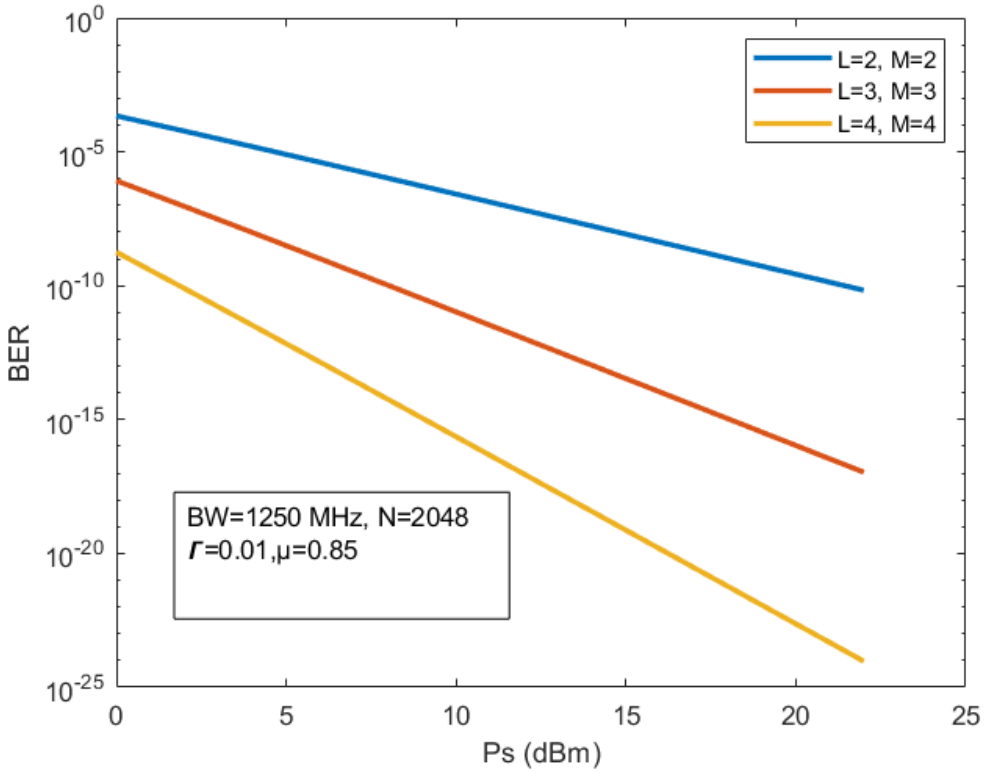

Fig.4.6 BER versus Ps (dBm) curve for MIMO OFDM for different Antenna Configuration

The BER performance results for different values on number of receiving and transmitting antennas are shown in Fig. 4.6 for BW=1250 MHz, Γ=0.01, μ=0.85, and N=2048 for MIMO OFDM with MRC with number of TX and Rx antennas. It is observed that there are significant improvement in receiver sensitivity with increase in Tx and Rx antennas, L and M.

4.8 Summary

In this chapter, the study systematically assessed the efficiency of Maximal Ratio Combining (MRC) Techniques in mitigating the impact of impulsive noise on wireless communication system with and without receive diversity over a Rayleigh fading channel. BER and SNR response of a wireless communication system is a significant tool used to determine the rigidity of data transmitted through the system. In this paper, Poisson's noise model and Middleton Class A models are studied for SISO, SIMO and MIMO OFDM system by observing their PDF and noise signal. The effects were observed for MRC for varying parameters. The noises having Gaussian characteristics stand out with the best BER response, whereas impulsive noise models make poor BER response. The improvement occurs in terms of lowering the BER floor, which cannot be lowered even by increasing number of receiving antennas. Order of improvement in BER floor is around 10^{-6} to 10^{-9}. Performance improvement has been analyzed using L-th order diversity in transmitting and receiving side. It has also been analyzed that performance can be highly improved by increasing the number of OFDM subchannel N from 512 to 4096. For an example, there is an improvement in receive sensitivity of about 3 to 4 dB due to increase in number of OFDM sub-channel for N=1024 to 4096.

Finally, it is shown that improvement in receiver performance can be obtained by increasing the number of OFDM sub-carriers as well as the number of receiving antenna, L. The practical implications of these findings extend to the development of communication system that are more robust and reliable in the face of impulsive noise, thereby providing valuable guidance for future research endeavour in their domain.

Hence, the third objective of the thesis is achieved which is "to develop an analytical model to evaluate the impact of impulsive noise on BER performance of an OFDM OSTBC MIMO wireless communication system".

CHAPTER 5

SIMULATION MODEL FOR WIRELESS SYSTEM

System Block Diagram

5.1 In a wireless communication system, an impulsive noise refers to a type of interference characterized by sudden, high-amplitude disturbances that can cause significant degradation in signal quality. These disturbances can be caused by various sources including electrical equipment, atmospheric conditions, or external environmental factors. To model a wireless communication link with impulsive noise, a combination of blocks has been used that represented the different systems of communication system and the noise influences [105]. Block diagram of wireless communication link with impulsive noise is shown in figure 5.1 below:

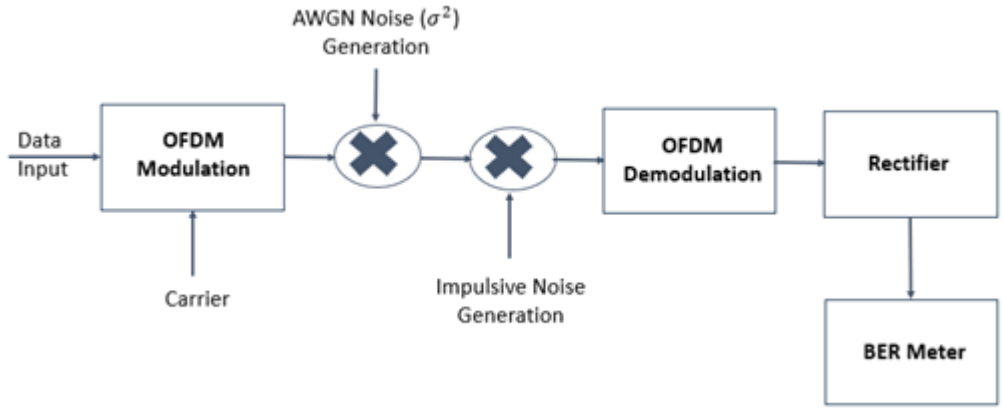

Fig. 5.1: Block Diagram of Simulation Model for Wireless Communication Link with Impulsive Noise

5.1.1 Data Input/ Information Source: This is the original data (e.g. text, voice, video) that needs to be transmitted over the communication channel. The data is typically converted to bits and then passed through a source encoder, which formats

the data appropriately for transmission. Data input block also performs error correction and channel coding (such as Turbo coding, OSTBC or LDPC codes) to increase the robustness of the transmission against error, including those induced by impulsive noise.

5.1.2 OFDM Modulator: The OFDM Modulator process the encoded data by dividing it into multiple sub-channels (or subcarriers), each of which is modulated independently. The IFFT (Inverse Fast Fourier Transform) block maps the data onto subcarriers to create the OFDM symbols. This block also handles the cyclic prefix insertion to combat multipath interference.

5.1.3 Wireless Channel: The wireless channel represents the propagation medium, where the signal is affected by various factors, including multipath fading, path loss, and impulsive noise. Impulsive noise is modeled as sudden, high-amplitude disturbances that interfere with the transmitted signal, often modeled using Poisson's Process for burst-like interference.

5.1.4 AWGN Noise Generation: AWGN is the most commonly used model for noise in communication systems, and it is represented by Gaussian random variables that have a zero mean and a constant power spectral density over all frequencies. AWGN noise is added to the transmitted signal, which simulates the random noise due to thermal effects, hardware imperfections, and environmental interference in the communication channel. In the simulation, AWGN noise is typically generated with a certain variance (σ^2), which is related to the Signal-to-Noise Ratio (SNR).

5.1.5 Impulsive Noise Generation: This block simulates the presence of impulsive noise in wireless channels. Impulsive noise is a non-Gaussian disturbance that results in sudden spikes, which can cause significant degradation of signal. In the simulation, impulsive noise can be modeled as a heavy-tailed distribution with occasional bursts of high-amplitude noise.

5.1.6 OFDM Demodulator: At the receiver side, the OFDM demodulator extracts the subcarriers, performing the FFT (Fast Fourier Transform) to convert the signal back to the frequency domain. It then removes the cyclic prefix and applies channel equalization to compensate for any distortions or multipath effects.

5.1.7 Rectifier/ Noise Removal and Equalization: This block performs noise filtering and equalization techniques (such as MMSE equalization or ZF equalization) to mitigate the effects of impulsive noise. Impulsive noise being bursty, may require advanced filtering techniques to reduce its impact on received signal. The final output is the recovered data (e.g. text, image) after demodulation. If any errors occurred during transmission, they may be detected or corrected based on the error correction code.

5.1.8 BER Meter: The BER meter compares the transmitted data (original data) with the received data after demodulation and correction to compute the bit error rate. Steps in BER calculation includes, storing original data or transmitted data in buffer, comparing received data (after demodulation and correction) with original data bit-by-bit, counting the amount of bit error by comparing the transmitted it to the received bits.

5.2 Pure Combining Techniques

After obtaining the received signal components from all fading channels, they have to be combined to decode the transmitted signal. Numerous methods are there include, Maximal ratio combining technique (MRC), Equal gain combining technique (EGC), Selective combining technique (SC).

5.2.1 Maximal ratio combining technique

Maximal ratio combining capitalizes on the spatial domain and is used to stimulate the weight of the inner product and signal vector. In an MRC the number of received signals are weighted and combined to maximize the SNR at the output of the combiner. MRC utilizes both the amplitude and phase element of the signal to maximize the

SNR. The operations materialized by MRC are, time alignment of signal branches, co-phasing, matching of channel gain and combining [106].

5.2.2 Equal Gain Combining Technique

Equal gain combining comes with the advantages equally weighted signal followed by coherent detection where phase distortion is removed. The receiver do not have to anticipate the amplitude fading, thus it is less complex than MRC. As a result a number of unacceptable inputs achieve the possibility of acceptable signal in this scheme. The equal fading channel and co phasing is generally set to unity for all diversity paths.

5.2.3 Selective combining technique

It is the simplest of all Combining with the advantage of no performance demeaning. For signal detection it chooses the ones with highest SNR among the receiver monitors of each diversity channel. A receiver module having n number of antennas are sampled and the gains are adjusted to provide an average SNR for all branches.

5.3 Simulation Result without Impulsive Noise:

The simulation is done in MATLAB which evaluates the Bit Error Rate (BER) performance of BPSK modulation under Rayleigh fading with basic diversity combining (e.g. Maximal Ratio Combining (MRC)), without impulsive noise.

Key Elements are:

- Modulation: BPSK
- Diversity: Maximal Ratio Combining (MRC)
- Noise: AWGN (no impulsive noise)

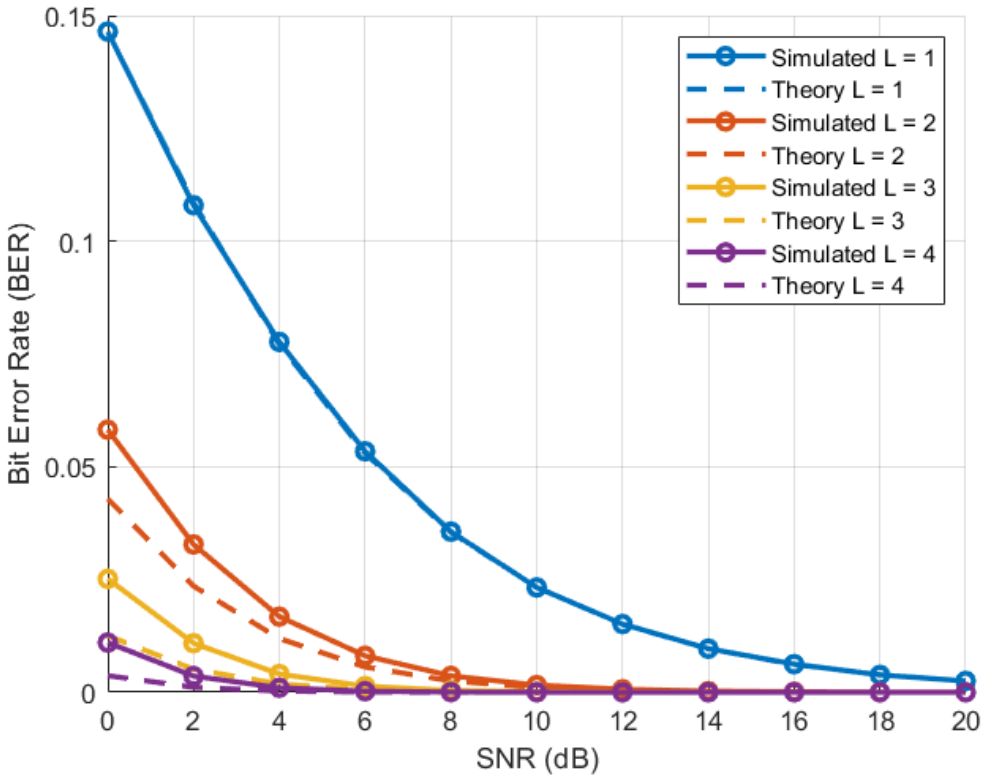

Fig. 5.2 Comparison Between Simulated and Theoretical Result (BER vs SNR Curve) for Basic Diversity Combining Technique (MRC) Without Impulsive Noise for Various L

Parameters:

- N=1e6
- Eb/N0 range in dB: EbN0_dB = 0:2:20
- Number of diversity branches: 4

5.4 Details of Simulation:

For BPSK over Rayleigh fading with Maximal Ratio Combining (MRC) of L independent branches, the theoretical BER is:

$$BER_{theory} = \frac{1}{2}\left(1 - \sqrt{\frac{\gamma}{1+\gamma}} \sum_{k=0}^{L-1} \binom{L-1+k}{k} \left(\frac{1}{4\gamma(1+\gamma)}\right)^{k}\right)$$

But this is complex to evaluate directly. For particular purpose, a simplified approximation from Simon & Alouini (for BPSK and i.i.d Rayleigh fading):

$$BER_{MRC} \approx \frac{1}{2}\left(1 - \sqrt{\frac{\gamma}{1+\gamma}}\right)^{L}$$

where, $\gamma = \frac{E_b}{N_0}$

Steps for simulations are as follows:

- Selection of parameters
- Generation of random bits and BPSK symbols
- Storage of BER
- Generation of Rayleigh fading and noise
- Transmit symbol over L branches
- Considerations for Maximal Ratio Combining
- Consideration for Demodulation
- BER Calculation
- Theoretical BER approximation
- Plot results

As each bit is independently transmitted through a random Rayleigh fading channel, there are effectively 1 million independent channel realizations per point. As such, with $N=10^6$, BER of 10^{-5} can be achieved.

5.5 Addition of Impulsive Noise to a Signal in MATLAB:

To add impulsive noise to a signal in MATLAB, the function 'imnoise' with 'salt & pepper' option can be utilized, which can add random white and black pixels to the image or signal, simulating impulsive noise. Here is an example of how to add impulsive noise to a signal in MATLAB:

```
% Generate a signal
Signal = sin(2*pi*(0:0.001:10));
% Add impulsive noise
Noisy_signal =  imnoise(signal, 'salt & pepper', 0.001);
% Plot the original and noisy signals
Subplot (2,1,1);
title ('original signal');
subplot (2,1,2);
plot (noisy_signal);
title ('Noisy signal with impulsive noise');
```

In this example, we have generated a sine wave signal and added impulsive noise with a noise density of 0.005 (i.e. 0.5% of the signal's pixels are randomly set to white or black). The resulting signals is then plotted alongside the original signal to compare them visually. The impulsive noise generated is shown below:

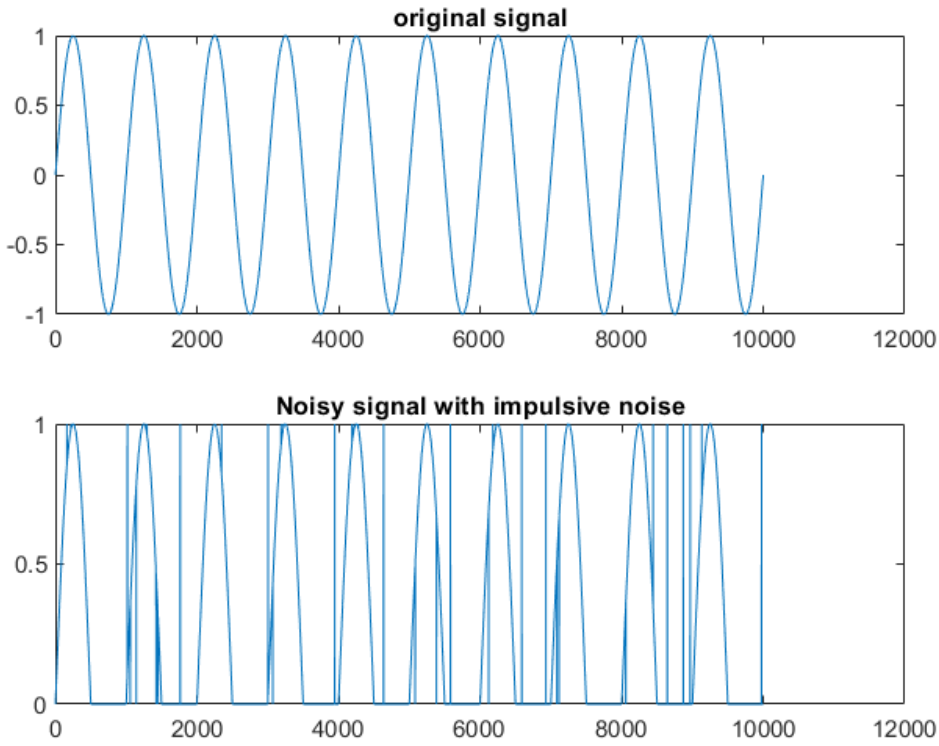

Fig. 5.3: Generated Impulsive Noise Signal through MATLAB Coding

5.6 Simulation Result with Impulsive Noise:

Transmitter:

- Generate N random bits $b_k \in \{0,1\}$
- BPSK symbols: $s_k = +1\ for\ b_k = 0, -1\ for\ b_k = 1.$

Channel:

- Each receive branch i=1,. . . , L experiences an independent flat Rayleigh fading coefficient:

$$h_{i.k} \sim CN\ (0,1)\ \Rightarrow |h_{i,k}| \sim Rayleigh(\Omega = 1),$$

- Parameter sweep: Vary A and Γ to study impulsivity impact on BER Floor and Diversity gain.

- Accuracy: Increase N or refine the impulsive model with full cluster-based Middleton A if deeper tail behaviour is needed.

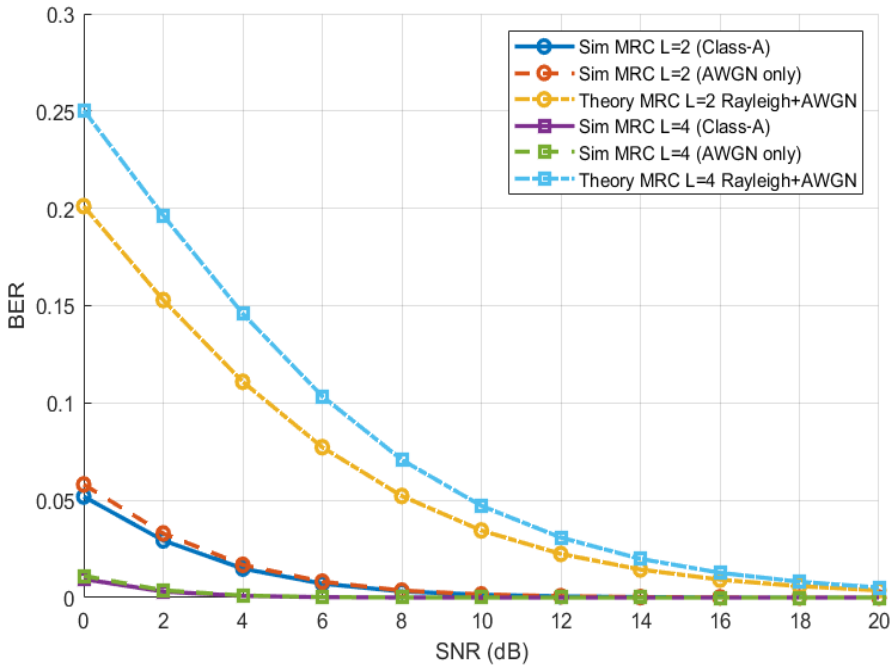

Fig 5.4 BER Performance for BPSK Modulation with MRC Rayleigh Fading channel with Impulsive Noise under Middleton Class-A Noise Model

Considering Parameters:

Table I: Consideration Parameters

Parameters	Value
Modulation	BPSK
Number of Rx Module	2
Number of Rx Antenna	4
BER	10^{-5}
Impulsive Noise Index, A	A=0.001
Noise Model	Middleton Class – A
Gamma, Γ	Γ=5

5.7 Comparison of Simulation and Theory for MRC under Middleton Class-A Noise (L=4)

- The simulation and theoretical/ analytical curves displays good conformity across most of the SNR range.
- Slight differences at very low or high SNR levels could be due to numerical exactness, limited number of Monte Carlo trials in simulation, or estimates in the theoretical model.
- The use of MRC with 4 branches suggestively improves performance related to single-branch reception.
- A conspicuous slope rise in the BER curve indicates effective diversity gain, dropping error rates sharply with growing SNR.
- The performance deprivation compared to AWGN is apparent, especially at mid to low SNRs, which supports with the impulsive nature of Class-A noise.
- The impact of impulsive noise is more noticeable at low SNR, where the noise bursts can govern signal energy even with MRC.
- The analytical model likely includes assumptions about the Class-A parameters (e.g. impulsive index A, Gaussian factor Γ).
- The close match to simulation authenticates the theoretical derivation under these parameters and confirms that MRC retains its robustness in impulsive environments.

5.8 Simulations for Different Combining Schemes

Simulation for different combining schemes under different noise models was done in MATLAB software to visualize the results. Three figures given below are the simulation results of two combining techniques namely Equal Gain Combining and Maximal Ratio Combining techniques. Along with AWGN theoretical and Middleton

Class A impulsive noise are considered for this simulation. It is observed that, according to simulation result, BER performance deteriorates with the incorporation of impulsive noise. Moreover, according to simulation, among EGC and MRC combining techniques, MRC performs better which is in conformity with the theoretical result.

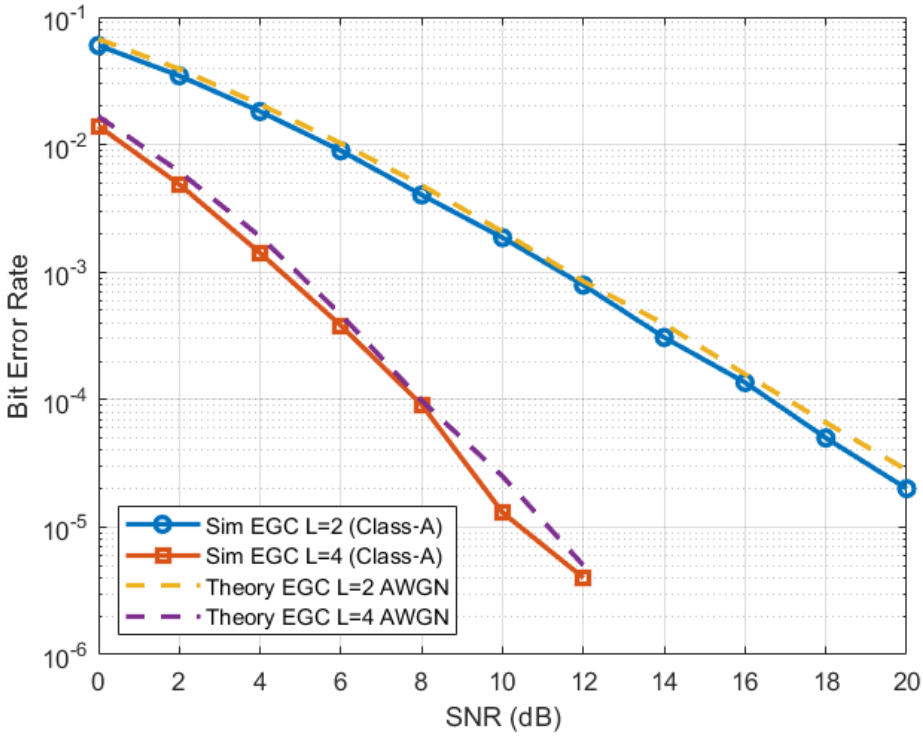

Fig 5.5: BER for BPSK with EGC over Rayleigh Fading with Middleton Class-A Noise Model

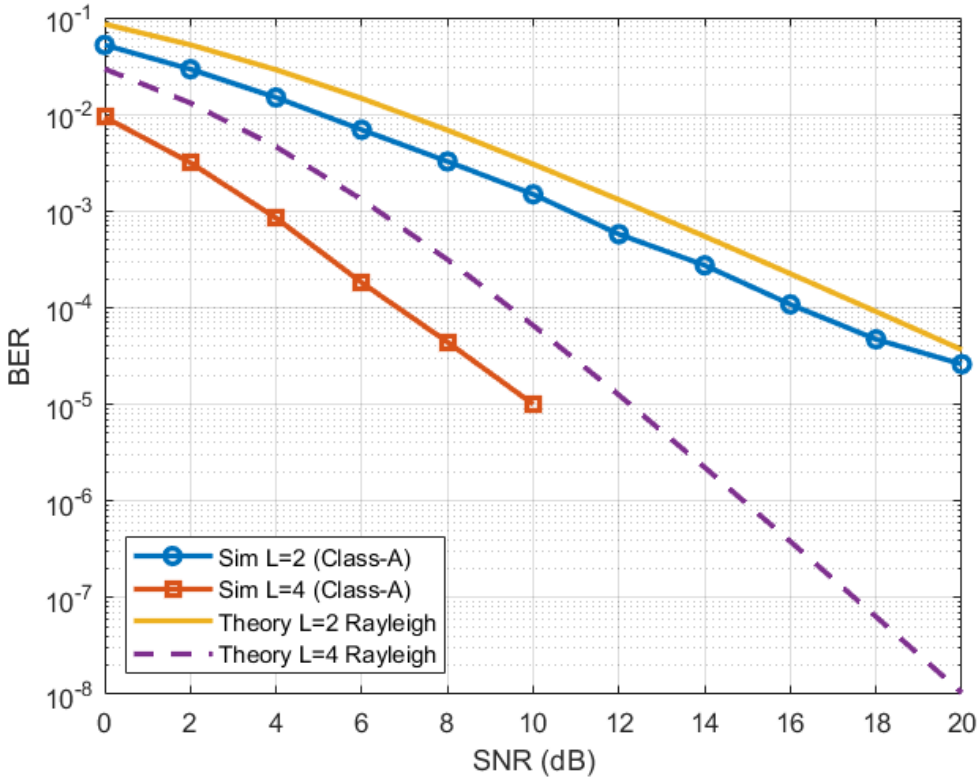

Fig 5.6: BER Performance for BPSK Modulation with MRC in Rayleigh Fading Channel under Middleton Class A Noise

For simulating the comparison of BER curve taking consideration of impulsive noise in Maximal Ratio Combining (MRC) techniques, we have considered different values of impulsive noise index. Here we have considered the value of impulsive noise index A= 0.001. The resulted simulated and theoretical BER considering impulsive noise for Hybrid MRC is shown Fig 5.6.

Analyzing different graphs (Fig 5.5 and 5.6) with considering impulsive noise, it is observed that simulated BER is better than analytical or numerical one in both the cases of diversity combining techniques. It is also observed that for different values of Impulsive Noise Index A, the simulated result is found in good conformity with the

earlier results. Moreover, as Rayleigh fading environment is considered, so, there is no line of sight (LOS) component and due to that simulated result is found better than that of analytical result.

5.9 Comparison of Analytical and Simulated Result Considering Impulsive Noise Under Middleton Class- A Model

A comparison table has been prepared for SNR values of analytical and simulated curve under different combining techniques considering fixed BER of 10^{-2} and 10^{-5} which are shown below:

Table II (L=4)

BER	Equal Gain Combining (EGC) SNR (dB)		Maximal Ratio Combining (MRC) SNR (dB)	
	Simulated	Theoretical	Simulated	Theoretical
10^{-2}	0.4	0.8	0.2	2.4
10^{-3}	4.4	5	3.9	6.2
10^{-4}	7.8	8	6.6	9.4
10^{-5}	10.4	11.2	10	12.1

A comparative analysis is done in Table II for different combining techniques considering Middleton class A. From the table (Table II) it is evident that with any type of Combining Technique MRC outperforms other technique (EGC).

5.10 Summary

In this chapter, a system model has been developed to simulate OFDM OSTBC MIMO wireless communication system considering impulsive noise and Rayleigh fading. Initially, MATLAB program has been developed considering different combining techniques and simulated result was found out considering only Rayleigh fading environment without considering impulsive noise. Later on MATLAB program was

also developed taking in consideration of impulsive noise under Middleton Class – A model. BER vs SNR graph was found out for different values of Impulsive Noise Index A and it was observed that MRC performs better than EGC in terms of SNR gain for fixed BER which verifies the theoretical or analytical result.

Hence, the fourth objective of the thesis is achieved which is “to simulate OFDM OSTBC MISO wireless communication system considering impulsive noise and Rayleigh fading and to verify analytical result”.

CHAPTER 6
IMPULSIVE NOISE MITIGATION TECHNIQUES

6.1 Introduction

Impulsive noise has arisen as an important challenge in the present day's wireless communication, especially in the context of Single Input Single Output (SISO) and Multiple Input Multiple Output (MIMO) systems. Impulsive noise is categorized by arbitrary amplitude and duration and has a substantial impact on the performance of these systems. Two popular models for impulsive noise are considered for the purpose of our thesis work which are Middleton Class A model and Symmetric alpha-stable (SαS) model. The Middleton Class – A model and SαS are widely used model in communication systems for modelling non-Gaussian and impulsive noise [102].

In this context, the analysis and comparison of these two models i.e. Middleton Class – A and Symmetric Alpha Stable on SISO and MIMO systems have received substantial attention in recent research. Researchers have proposed various techniques to mitigate the effect of impulsive noise on SISO and MIMO systems. These techniques include filtering methods, such as Adaptive Filters and Median Filtering, as well as subspace-based approaches, such as Independent Component Analysis (ICA) and Principal Component Analysis (PCA). While both models have been extensively studied, the comparison of their impact on SISO and MIMO systems remains an active research area. The performance of the different mitigation techniques can also be evaluated based on the specific impulsive noise model used. Therefore, we have done a detailed analysis and comparison of these two models which will provide valuable insights into the design of efficient mitigation techniques for SISO and MIMO systems. In this chapter we have evaluated the impact of impulsive noise on the Bit Error Rate (BER) versus Signal-to-Noise Ratio (SNR) curve with the analysis and comparison of the MCA and alpha-stable impulsive noise models on SISO and MIMO systems [103]. The BER versus SNR curve is a plot of the

probability of bit error against the signal-to-noise ratio, which is a measure of the quality of the received signal. In the presence of impulsive noise, the BER versus SNR curve can exhibit non-Gaussian behavior, such as increased error rates and error floors [104].

Various mitigating techniques has been taken into consideration to mitigate the impact of impulsive noise on the BER versus SNR curve. These techniques can improve the robustness of SISO and MIMO systems in the presence of impulsive noise and reduce the error rates on the BER versus SNR curve. Overall, the analysis and comparison of the Middleton Class-A and SαS impulsive noise models on the BER versus SNR curve of SISO and MIMO systems can provide valuable insights into the design of effective mitigation techniques for impulsive noise in communication systems which has been discussed briefly in this chapter.

6.2 Impulsive Noise Modelling

Impulsive noise modeling denotes to the method of simulating and modeling the behavior of impulsive noise in a given environment. Impulsive noise is a type of noise that is characterized by short, high-energy pulses. It is often encountered in industrial settings and can cause substantial damage to electronic equipment if it is not properly managed. The process of impulsive noise modeling involves analyzing the sources and characteristics of the impulsive noise in a given environment and then using mathematical models to simulate its behavior. This can include analyzing the frequency and time domain behavior of the noise, as well as its statistical properties such as cumulative distribution function (CDF) and probability density function (PDF). Once the impulsive noise has been modeled, it can be used to test the response of electronic equipment and to evaluate the effectiveness of different noise mitigation approaches. This information can then be used to design more effective noise mitigation systems and to improve the overall reliability of electronic equipment in noisy environments [105]. It can be modeled using various statistical methods, including the following: The Gaussian model: The Gaussian model assumes that the

impulsive noise is a Gaussian random process, but it is not effective in representing the non-Gaussian characteristics of impulsive noise. The Laplacian model: The Laplacian model is a better illustration of impulsive noise than the Gaussian model, as it considers the non-Gaussian characteristics of the noise. The GGD model: The GGD model can characterize a wide range of distributions, including Gaussian and Laplacian distributions. It is often used to model impulsive noise because it can provide a better fitting to the actual noise distribution. The Alpha-Stable distribution: The Alpha-Stable distribution is a class of distributions that can model both Gaussian and heavy-tailed noises. It is often used to model impulsive noise in wireless communication systems [106].

6.2.1 Middleton Class A

The Middleton Class A impulsive noise model is a arithmetical model used to describe impulsive noise in communication systems. The model undertakes that the impulsive noise is generated by a Poisson process, with a probability density function (PDF) that follows an exponential spreading. The Class A model is used for applications where the average number of impulses per symbol interval is less than one. The Class A impulsive noise model is characterized by two parameters: the average number of impulses per symbol interval (lambda), and the amplitude distribution of the impulses. The amplitude distribution of the impulses can be modeled using different distributions, such as Gaussian or Laplacian, depending on the characteristics of the impulsive noise in a particular system [107]. The Middleton Class A impulsive noise model is widely used in communication systems and is a useful tool for analyzing and designing systems that are susceptible to impulsive noise. Here are some mathematical expressions that describe the Middleton Class A impulsive noise model:

Poisson process: The number of impulses per symbol interval, N, follows a Poisson distribution with mean λ:

$$P(N = k) = \frac{\lambda^k e^{-\lambda}}{k!} \tag{6.1}$$

where k is a non-negative integer.

Amplitude distribution: The amplitudes of the impulses, A, are modeled as independent and identically distributed random variables with a known distribution function, f(A). For example, if the amplitude distribution is Gaussian, the PDF is:]

$$f(A) = \frac{1}{\sqrt{2\pi\sigma^2}}, e^{-\frac{A^2}{2\sigma^2}} \tag{6.2}$$

where sigma is the standard deviation of the Gaussian distribution. Received signal: The received signal, y, is given by: y = x + n where x is the transmitted signal and n is the impulsive noise. PDF of the received signal: The PDF of the received signal, f(y), can be obtained by convolving the PDF of the transmitted signal, f(x), with the PDF of the impulsive noise,

$$f(y) = \int(-\infty, \infty) f(x) * f(y - x) dx \tag{6.3}$$

This expression provides a mathematical representation of the effect of impulsive noise on the received signal. The performance of communication systems under impulsive noise con ditions can be analyzed using this expression. The class A model assumes that the noise is composed of two terms [14] N(t) = NG(t) + NI (t), (1) where NG(t) is a stationary Gaussian signal and NI (t) can be expressed as

$$N_i(t) = X_j U_j(t, \sum) \tag{6.4}$$

Where U_j denotes the jth waveform from a noise source and ∑ denotes a set of random parameters which describes the waveform scale and structure. Under certain assumptions, the PDF of the instantaneous amplitude of N(t) can be expressed as a mixture of zero-mean Gaussian terms weighted according to a Poisson process [108].

$$f_N(n) = \sum_{m=0}^{\infty} \frac{e^{-AA_m}}{m!} \frac{1}{\sqrt{2\pi\sigma_m^2}} e^{-\frac{n^2}{2\sigma_m^2}} \tag{6.5}$$

where the variances σ_m^2 can be expressed as $\sigma_m^2 = \sigma_{m,A}^2 + \Gamma_1 + \boldsymbol{\Gamma}$, where σ^2 is the power of $N(t)$, and σ_G^2 and σ_I^2 are the power of the Gaussian and impulsive terms, respectively. Its ratio is denoted by $\Gamma = {\sigma_G^2}/{\sigma_I^2}$. For the sake of simplicity, in the rest of the paper we will consider signals with σ^2 = 1, and this term will be omitted conditions.

6.2.2 Symmetric Alpha stable

Symmetric alpha-stable distributions are a type of probability distribution that are usually used to model heavy-tailed features. Unlike Gaussian or normal distributions, symmetric alpha-stable distributions have heavy tails that are categorized by slow decay. This means that they are more likely to produce extreme values, or outliers, which can make them useful for modeling real-world characteristics that have a high degree of variability. In mathematical terms, a symmetric alpha-stable distribution is defined by four parameters: the scale parameter, the location parameter, the stability parameter (α), and a skewness parameter (β). The value of α determines the tail behavior of the distribution, with α = 2 corresponding to a Gaussian distribution, and α < 2 representing a heavy-tailed distribution. The value of β determines the skewness of the distribution, with β = 0 corresponding to a symmetric distribution and β= 0 corresponding to a skewed distribution. Symmetric alpha-stable distributions have a number of properties that make them useful for modeling real-world characteristics. For example, they are self-similar, meaning that if X is a symmetric alpha-stable random variable, then for any constant c, the random variable cX is also symmetric alpha-stable. This property can make them useful for modeling phenomena that exhibit scale-invariant behavior. Symmetric alpha-stable distributions are often used to model impulsive noise in signal processing applications. Impulsive noise, also known as burst noise, is a type of noise that consists of short, intense spikes that occur randomly in time. This type of noise can be difficult to model using traditional Gaussian distributions, which are not well-suited to represent extreme values or outliers. The

value of the stability parameter alpha can be used to control the amount of heavy-tailedness in the distribution, while the value of the skewness parameter beta can be used to control the skewness of the distribution. By modeling impulsive noise as a symmetric alpha-stable distribution, it is possible to capture the heavy-tailed behavior and extreme values that are often observed in real-world impulsive noise signals [108].

6.2.3 Experimental Results and Discussions

MATLAB m. files are used to simulate the transmitter, receiver, and channel. Table 1shows different simulation parameters.

Table I. MATLAB simulation parameters

Type of Modulation	QPSK
Number of OFDM Carriers	256
Number of faded channel paths	4
Number of cyclic prefix	16
Number of Transmitted bits	2*256*5000
Type of Fading	Rayleigh Frequency Selective
Number of Pilots	2

6.3 Impulsive noise mitigation in a Single-Input Single-Output (SISO)

Impulsive noise mitigation in Single Input Single Output (SISO) systems refers to the process of eliminating or reducing the impact of impulsive noise on the signal being transmitted. There are several methods for mitigating impulsive noise in SISO systems which are discussed in subsequent paragraphs [111].

6.3.1 Wiener Filtering Detection

Wiener filtering is a signal processing technique that can be used for detecting and mitigating the impact of impulsive noise in single-input single-output (SISO) communication systems. The Wiener filter is an adaptive filter that reduces the mean-square error between the filtered signal and the original signal. In the context of

impulsive noise mitigation, the Wiener filter can be used to approximate the underlying signal by removing the impulsive noise. The filter is trained using the received signal and a reference signal, and the filter coefficients are updated over time to adapt to the changing noise conditions. The Wiener filter operates in the frequency domain and is based on a statistical model of the noise and the signal. The filter estimates the power spectral density (PSD) of the noise and the signal, and uses this information to calculate the filter coefficients that minimize the mean-square error [112]. In SISO communication systems, the Wiener filter can be implemented at the receiver and used to improve the reliability of the communication link. The filter can be trained using the reference signal and the received signal, and the filtered signal can be used to improve the performance of the demodulator. Overall, Wiener filtering can be an effective solution for detecting and mitigating the impact of impulsive noise in SISO communication systems. The method provides good results for low-level impulsive noise and is relatively simple to implement. However, the method may not be effective for high-level impulsive noise and may also introduce additional noise into the signal. The mathematical model and algorithm for Wiener filtering in a SISO communication system can be represented as follows:

Let's assume that the transmitted signal is given by x(t) and the received signal is given by y(t), where t is the time index. The reference signal, r(t), is known at the receiver. At the receiver, the received signal y(t) is correlated with the reference signal r(t) to obtain the cross-correlation function $Rxy(\tau)$:

$$Rxy(\tau) = \mathbb{E}[y(t)r(t-\tau)] \tag{6.6}$$

where $\mathbb{E}$ [y(t)r(t −τ)] represents the expectation operator and τ is the time lag. Next, the auto-correlation function of the reference signal Rrr(τ) is calculated:

$$R_{rr}(\tau) = \mathbb{E}[r(t)r(t-\tau)] \tag{6.7}$$

The Winner filter is then calculated using the cross-correlation function $R_{xy}(\tau)$ and the auto-correlation function $R_{rr}(\tau)$:

$$H(\tau) = \frac{R_{xy}(\tau)}{R_{rr}(\tau)} \quad (6.8)$$

The filtered signal z(t) is then obtained by convolving the received signal y(t) with the Wiener f ilter H(τ):

$$z(t) = y(t) * H(\tau) \quad (6.9)$$

where * represents the convolution operation. Finally, the estimated signal y(t) is obtained by adjusting the gain of the filtered signal: y(t) = g * z(t) where g is the gain factor that is adjusted to maintain a constant modulus. Overall, the mathematical model and algorithm for Wiener filtering in a SISO communication system involves the calculation of the cross-correlation function and auto-correlation function, the calculation of the Wiener filter, the convolution of the received signal with the Wiener filter, and the adjustment of the gain of the filtered signal to obtain the estimated signal [112].

6.3.2 Bayesian Detection

In Bayesian detection of impulsive noise mitigation for a Single-Input Single-Output (SISO) system, the mathematical model involves updating our prior belief about the presence of im pulsive noise in the system based on the available data.

Let's assume that the received signal at the receiver is given by:

$$y(t) = x(t) + n(t) \quad (6.10)$$

where x(t) is the transmitted signal, n(t) is the additive noise and y(t) is the received signal. The task is to detect whether n(t) is impulsive or not. We can model this problem as a hypothesis testing problem, where H0 represents the hypothesis that the noise is not impulsive and H1 represents the hypothesis that the noise is impulsive.

The Bayesian approach involves computing the likelihood of the received signal given each hypothesis and using Bayes' theorem to update our prior belief about the presence of impulsive noise. Bayes' theorem states that:

$$P(H_1|y) = \frac{P(y|H_1)P(H_1)}{P(y|H_1)P(H_1)+P(y|H_0)P(H_0)} \quad (6.11)$$

$P(H_1|y)$ is the posterior probability of H_1 given the received signal y, $P(y|H_1)$ is the likelihood of the received signal given $H_1, P(H_1)$ is the prior probability of H_1 and $P(H_0)$ is the prior probability of H_0.

We can use various statistical models to compute the likelihood of the received signal given each hypothesis [47]. For example, if we assume that the impulsive noise follows a Laplacian distribution, then the likelihood of the received signal given H1 can be computed as:

$$P(y|H_1) = \frac{1}{2b} e^{-\frac{|y-x|}{b}} \quad (6.12)$$

where b is a parameter that controls the spread of the Laplacian distribution.

Once we have computed the posterior probabilities, we can make a decision about the presence of impulsive noise by comparing the values of This is a basic mathematical model for Bayesian detection of impulsive noise mitigation in a SISO system. More sophisticated models can be developed by incorporating additional information and making different assumptions about the underlying distributions.

The mathematical model for Bayesian detection of impulsive noise mitigation in a Single Input Single-Output (SISO) system can be formulated as follows:

Hypothesis testing: The problem of detecting impulsive noise can be treated as a hypothesis testing problem. Let H_0 represent the hypothesis that the noise is not impulsive and H_1 represent the hypothesis that the noise is impulsive.

Prior probabilities: Define the prior probabilities of H_0 and H_1, $P(H_0)$ and $P(H_1)$, respectively. These can be estimated based on prior knowledge or past experience with similar systems.

Likelihood function: Define the likelihood function for the received signal, y(t), given each hypothesis. For example, if the impulsive noise is modeled as a Laplacian distribution, the likelihood function can be given by:

$$P(y|H_1) = \frac{1}{2b} exp\left(-\frac{|y-x|}{b}\right) \tag{6.13}$$

where b is a parameter that controls the spread of the Laplacian distribution, and x(t) is the transmitted signal.

Bayes' theorem: Use Bayes' theorem to calculate the posterior probabilities of H_0 and H_1 given the received signal y(t):

$$P(H_1|y) = \frac{P(y|H_1).P(H_1)}{P(y|H_1).P(H_1)+P(y|H_0).P(H_0)} \tag{6.14}$$

Decision rule: To compare the values of $P(H_1|y)$ and $P(H_0|y)$ to make a decision about the presence of impulsive noise, we can use the following decision rule:

If $P(H_1|y) > P(H_0|y)$, we can conclude that the noise is impulsive. If $P(H_1|y) < P(H_0|y)$, we can conclude that the noise is not impulsive.

This is a simplified mathematical model for Bayesian detection of impulsive noise mitigation in a SISO system. The model can be refined and made more sophisticated by incorporating additional information and making different assumptions about the underlying distributions.

6.3.3 Small signal approximation Bayesian detection

Small signal approximation is a method used in control systems to linearize a nonlinear system around a operating point, so that it can be analyzed and controlled using linear control techniques. In the context of Bayesian detection, it is used to model the behavior of a signal in the presence of impulsive noise. Impulsive noise can severely impact the performance of communication systems and cause errors in the detection

of the signal. Mitigating the effects of impulsive noise in single input single output (SISO) systems is challenging because it is difficult to accurately model the behavior of the noise. The Bayesian approach provides a way to perform optimal signal detection by modeling the signal and noise as random variables and then computing the probabilities of the signal being in different states. In the Bayesian framework, the signal and noise are modeled as random variables, and a likelihood function is used to describe the relationship between the signal and the received signal. Given the likelihood function, the Bayesian approach can be used to compute the posterior probability distribution of the signal, which represents the probability of the signal being in different states given the received signal. The small signal approximation can be used to simplify the mathematical model by linearizing the system around the operating point. This allows the signal and noise to be modeled as Gaussian random variables, which makes the computation of the posterior probability distribution and the performance evaluation simpler. The small signal approximation is only valid for small signals and may not be accurate for large signals or in the presence of strong impulsive noise. This approximation simplifies the analysis and makes it easier to compute the probabilities of the signal being in different states. The Bayesian approach provides a flexible framework for signal detection in the presence of impulsive noise, and can be used to optimize the signal detection performance in SISO systems.

6.3.4 Quantized Bayesian Detection

Quantized Bayesian detection refers to the process of detecting a signal in the presence of impulsive noise using a Bayesian approach and quantizing the posterior probability distribution of the signal. In this method, the posterior probability distribution is quantized into a finite number of levels, and the signal state is determined by mapping the quantized levels to a finite set of signal states.

The main advantage of quantized Bayesian detection is that it can reduce the computational complexity of Bayesian detection, making it more suitable for implementation in real-time systems with limited processing power. The trade-off is

that quantization introduces a quantization error, which can impact the performance of the detection system. To mitigate the effects of quantization error, the number of quantization levels and the map ping of the quantized levels to signal states should be carefully designed to minimize the impact on the performance of the detection system. In practice, the quantization error can be reduced by increasing the number of quantization levels, but this comes at the cost of increased computational complexity. In summary, quantized Bayesian detection provides a way to implement Bayesian signal detection in real-time systems with limited processing power, while balancing the trade-off between computational complexity and performance.

6.3.5 Optimal and Selection Myriad Filtering

The Myriad filter is a type of nonlinear filter that has been shown to be effective for impulsive noise mitigation in SISO systems. It is an adaptive filter that uses a set of multiple reference signals to estimate the signal corrupted by impulsive noise. The Myriad filter is designed to take into account both the temporal and spectral characteristics of the impulsive noise, making it a promising approach for impulsive noise mitigation. The design of the Myriad filter involves the selection of a set of reference signals that are used to estimate the clean signal. The optimal selection of reference signals depends on the statistical properties of the impulsive noise and the clean signal. Researchers have proposed various approaches for selecting the optimal set of reference signals, such as Principal Component Analysis (PCA), Independent Component Analysis (ICA), and subspace-based approaches. The performance of the Myriad filter in mitigating impulsive noise in SISO systems can be evaluated using the BER versus SNR curve, which measures the error rate of the system as a function of the signal to-noise ratio. Studies have shown that the Myriad filter can significantly improve the BER versus SNR curve of SISO systems in the presence of impulsive noise, compared to traditional linear filtering methods. One challenge in the design of the Myriad filter is the selection of the optimal number of reference signals. Increasing the number of reference signals can improve the estimation accuracy of the clean

signal but can also increase the computational complexity of the filter. The optimal number of reference signals can be determined based on the trade-off between estimation accuracy and computational complexity. In summary the Myriad filter is an effective approach for impulsive noise mitigation in SISO systems. The optimal design of the filter involves the selection of an optimal set of reference signals, which can be achieved using various approaches. The performance of the Myriad filter can be evaluated using the BER versus SNR curve, and the optimal number of reference signals can be determined based on the trade-off between estimation accuracy and computational complexity.

6.4 Impulsive noise mitigation in a Multiple-Input Multiple-Output (MIMO)

Impulsive noise mitigation in a Multiple-Input Multiple-Output (MIMO) system refers to techniques used to counteract the effects of impulsive noise, which is a type of interference that causes brief, sharp spikes in signal amplitude.

Impulsive noise can cause significant degradation of the communication system performance, and it is often challenging to mitigate due to its short duration and large amplitude. Impulsive noise, also known as impulsive interference or burst noise, is a type of interference that can cause brief but high amplitude spikes in the received signal. This type of noise can significantly degrade the performance of a MIMO communication system, as it can introduce errors into the received data and reduce the signal-to-noise ratio. MIMO systems use multiple antennas at the transmitter and receiver to increase the data rate and improve the reliability of the communication link. However, impulsive noise can affect different antennas in different ways, and this can result in varying degrees of error in the received signal. Therefore, it is essential to mitigate the effects of impulsive noise in a MIMO system. Impulsive noise mitigation in MIMO systems can be challenging because impulsive noise is usually short in duration and has a high amplitude, making it difficult to distinguish from the desired signal. To mitigate the effects of impulsive noise, a combination of signal processing techniques can be used. These techniques can be broadly classified into two categories:

time-domain and frequency-domain techniques. Time-domain techniques operate on the received signa directly in the time domain, while frequency-domain techniques operate on the signal in the frequency domain. Some of the time-domain techniques include median filtering, waveform shaping, and pulse blanking. These techniques are used to remove the impulsive noise from the received signal or reduce its impact on the system.

On the other hand, some of the frequency-domain techniques include spectral subtraction. Adaptive filtering techniques use an adaptive filter to remove the impulsive noise from the received signal, while spectral subtraction techniques estimate the noise spectrum and subtract it from the received signal. Here are some techniques that are used in this per to mitigate impulsive noise on MIMO system.

6.4.1 Spatial Multiplexing with Gaussian ML Receiver

Spatial multiplexing is a technique used in MIMO systems that employs multiple antennas to transmit independent data streams in parallel, thus increasing the data rate. Impulsive noise, on the other hand, is a type of noise that can occur in a communication system, which can cause errors in the received signal. To mitigate the effect of impulsive noise on a MIMO system that uses spatial multiplexing, a Gaussian ML receiver can be utilized to estimate the transmitted signals at each receiver antenna. The receiver uses these estimates to detect the transmitted symbols while also considering the noise statistics [112]. The Gaussian ML receiver is particularly useful in mitigating the effect of impulsive noise because it is robust to noise that is Gaussian-like. The combination of spatial multiplexing and the Gaussian ML receiver can lead to more efficient and faster data transmission, while also reducing the impact of impulsive noise on the system's overall performance. Spatial multiplexing with a Gaussian ML receiver on a MIMO system in the presence of impulsive noise can be described as y =Hx+n+s where y is the received signal vector, H is the MIMO channel matrix, x is the transmitted signal vector, n is the additive white Gaussian noise (AWGN), and s is the impulsive noise. The transmitted signal vector, x, is a function

of the input symbols, and the MIMO channel matrix, H, is a function of the channel gains and fading coefficients. The impulsive noise, s, is modeled as an additional component that can cause errors in the received signal. The Gaussian ML receiver model can be used to estimate the transmitted signal vector, x, by maximizing the likelihood function of the received signal vector, y, given the channel matrix, H, and noise statistics. The estimated signal vector is then used to detect the transmitted symbols, taking into account the impulsive noise statistics. The specific mathematical expressions for the likelihood function and the detection algorithm depend on the specific implementation of the Gaussian ML receiver and the spatial multiplexing technique being used.

6.4.2 Alamouti Coding

Alamouti coding is a technique used in MIMO systems to transmit data over multiple antennas. The basic idea behind Alamouti coding is to transmit two copies of the same data over two different antennas with a specific phase relationship. This allows the receiver to decode the transmitted data even if one of the antennas experiences interference or fading. Im pulsive noise can be a problem in MIMO systems that use Alamouti coding, as it can cause errors in the received signal. To model impulsive noise in Alamouti coding-based systems, we can use a similar approach to the one I described earlier. Let's assume that we have a MIMO system with two transmit antennas and one receive antenna. The transmitted data is encoded using Alamouti coding and transmitted over the two antennas. The received signal at the receiver can be modeled as: $y = H*x + n$ where H is the channel response matrix, x is the transmitted signal vector, and n is the noise vector. We assume that n is a random variable with a heavy-tailed distribution, such as the alpha-stable distribution [113].

6.5 Analysis of communication performance on SISO and MIMO system

The key performance metric for evaluating the effectiveness of the impulsive noise mitigation method is BER vs SNR curve. The Bit Error Rate (BER) vs Signal-to-Noise

Ratio (SNR) curve for a SISO and MIMO system with impulsive noise mitigation describes the relationship between the BER of the system and the SNR of the received signal when impulsive noise is present in the system. The curve is obtained by simulating the SISO and MIMO systems under different levels of SNR, typically over a range of several decibels. At each SNR level, a large number of bits are transmitted, and the received bits are compared with the transmitted bits to calculate the BER. The simulation is repeated for different levels of SNR, and the results are plotted to obtain the BER vs SNR curve. In the case of impulsive noise mitigation, the BER vs SNR curve exhibited some unique characteristics compared to a system without mitigation. For example, the presence of impulsive noise caused occasional errors that are not well-described by traditional statistical models used to analyze Gaussian noise. Therefore, the curve had a higher BER at lower SNR values compared to Gaussian noise, as the noise can cause occasional errors that are difficult to mitigate [114].

The effectiveness of the impulsive noise mitigation method is reflected in the shape of the curve. In general, a lower BER indicates better system performance, and a higher SNR is required to achieve a lower BER. The curve having a ”knee” point represents the SNR at which the system transitions from high error rates to lower error rates. The knee point is typically determined by the sensitivity of the system to noise, and affected by factors such as the modulation scheme and coding used in the system. Overall, the BER vs SNR curve for a SISO and MIMO system with impulsive noise mitigation has provided valuable insight into the performance of the system under various noise conditions. By analyzing the curve, system designers can optimize the system parameters to achieve the desired performance under various noise conditions.

6.5.1 Parameter Estimation on SISO system

In the Middleton Class A noise model, the impulsive noise is modeled as a Poisson process with a continuous probability density function. The impulsive noise is characterized by two parameters: the impulsive index and the Gamma parameter. The impulsive index determines the fraction of samples that are affected by impulsive

noise, while the Gamma parameter samples affected by impulsive noise, which make the BER vs SNR curve more sensitive to changes in the SNR. A higher Gamma parameter increase the severity of the impulsive noise, which makes it more difficult to mitigate and results in a higher BER at lower SNR values. The performance of the mitigation method is affected by the specific values of the impulsive index and Gamma parameter. The range of gamma parameter is 0 to 2 and Impulsive index will be within 1. The gamma parameter basically introduces the distribution of the noise is peaked or flat. Impulsive index parameter is taken 0.20, 0.35, 0.5, 0.75 and 1. In the Alpha-Stable noise model, the impulsive noise is modeled as an Alpha-Stable random process, which is characterized by four parameters: the stability index α, the skewness parameter β, the scaling parameter c, and the location parameter μ. In this model, the dispersion parameter is defined as the ratio of the power of the impulsive noise to the power of the additive Gaussian noise. The effect of the stability index alpha and the dispersion parameter on the BER vs SNR curve for a SISO system with impulsive noise mitigation in the Alpha-Stable noise model would depend on the design of the mitigation method and the characteristics of the system. A higher stability index alpha increases the severity of the impulsive noise, which make it more difficult to mitigate and result in a higher BER at lower SNR values. The dispersion parameter has a significant impact on the shape of the BER vs SNR curve. A higher dispersion parameter result in a higher power of the impulsive noise relative to the additive Gaussian noise, which make it more difficult to distinguish the signal from the noise. As a result, the BER vs SNR curve exhibits a higher BER at lower SNR values compared to a system with a lower dispersion parameter. A well-designed mitigation method is used to reduce the impact of the impulsive noise and result in a lower BER overall, but the performance of the mitigation method is affected by the specific values of the dispersion parameter. Simulating the system under different levels of alpha taking value of 0.5 , 1 and 1.5 and dispersion parameter and analyzing the resulting BER vs SNR curves has provided valuable insight into the performance of the system and the effectiveness of the mitigation method under various noise conditions. M-

PAM modulation technique is used for the purpose of simulation in this paper. Now the effect of the parameter M on the BER vs SNR curve for a SISO system with impulsive noise mitigation is that a higher value of M increases the number of possible symbols that can be transmitted, which increases the data rate and potentially improve the BER at high SNR values. However, a higher value of M also increases the distance between adjacent symbols, which makes the modulation scheme more susceptible to noise and interference, including impulsive noise. Considering all positive and negative sides the parameter M has been selected. Which is 4-PAM, 8-PAM, 16-PAM, 32- PAM for noise type alpha stable and 2- PAM, 8-PAM, 16-PAM for noise type Middleton class A.

6.5.2 Parameter Estimation on MIMO system

In a MIMO (Multiple Input Multiple Output) system, the performance can be evaluated in terms of Bit Error Rate (BER) versus Signal-to-Noise Ratio (SNR) curve. The k (kappa) value represents the impulsive noise level, which is characterized by the distribution of the noise. When the k value is high, the impulsive noise level is high, and the performance of the MIMO system degrades. The high k value indicates that the impulsive noise is dominant in the channel, and the Gaussian noise component is relatively small. As a result, the BER vs SNR curve shifts to the right, indicating a higher SNR required to achieve a particular BER. When the k value is low, the impulsive noise level is low, and the performance of the MIMO system improves. The low k value indicates that the Gaussian noise component is dominant in the channel, and the impulsive noise is relatively small. We will take three different k values0.1, 0.5 & 0.9 in all kinds of detection techniques. The INI value is a parameter used to adjust the strength of the noise filter that is applied to the received signal to reduce the impact of impulsive noise. If the INI value is set too low, the noise filtering is insufficient to effectively remove the Bivariate Middleton Class A Impulsive Noise from the received signal. As a result, the noise will have a significant impact on the system performance. If the INI value is set too high the curve will shift rightwards,

and a higher BER will be observed at higher SNR. This is because the noise filtering is too strong and is affecting the useful signal information, leading to a higher error rate. The system will be responded to a INI value of 0.1 & 0.8 in each case to clearly view the impact of INI value. M-QAM is a modulation scheme that uses a constellation diagram with M points to encode data. The ”m” value in M-QAM refers to the number of points in the constellation diagram. As the m value increases, the points in the diagram become closer to each other, which means that the modulation is more susceptible to noise and interference. To test impulsive noise mitigation ‘M’ value of 4dB, 8dB & 16dB are considered.

6.6 Performance Analysis of SISO system

This section presents the comparative study of the performance and effectiveness of SISO system in case of various Noise type and detection method by changing the parameter and signal constellation. For SISO system , two type of noise type has been selected for simulation in MATLAB. Which are Middleton Class A and Alpha Stable. For Middleton class a parameter of impulsive index has been changed and different curve of BER vs SNR has been noticed in case of different detection and mitigation method. These detection methods are discussed elaborately before. For alpha stable parameter alpha which is stability index is changed and effect of BER vs SNR curve is observed.

6.7 Performance Analysis of MIMO system

In a MIMO system, the performance can be evaluated in terms of BER versus SNR curve. The κ (kappa) value represents the impulsive noise level, which is characterized by the distribution of the noise. When the κ value is high, the impulsive noise level is high, and the performance of the MIMO system degrades. The high k value indicates that the impulsive noise is dominant in the channel, and the Gaussian noise component is relatively small [112-115]. When the k value is low, the impulsive noise level is low, and the performance of the MIMO system improves. The low k value indicates that the Gaussian noise component is dominant in the channel, and the impulsive noise

is relatively small. Three different k values 0.1, 0.5 & 0.9 are taken in all kinds of detection techniques. INI is a parameter used to adjust the strength of the noise filter that is applied to the received signal to reduce the impact of impulsive noise. If the INI value is set too low, the noise filtering is insufficient to effectively remove the Bivariate Middleton Class A Impulsive Noise from the received signal. As a result, the noise will have a significant impact on the system performance. The system is responded to an INI value of 0.1 and 0.8 in each case to clearly view the impact of INI value.

6.7.1 Effect for Kappa

To mitigate the impulsive noise in a MIMO system, it is essential to choose an appropriate k value that balances the trade-off between the noise reduction and the

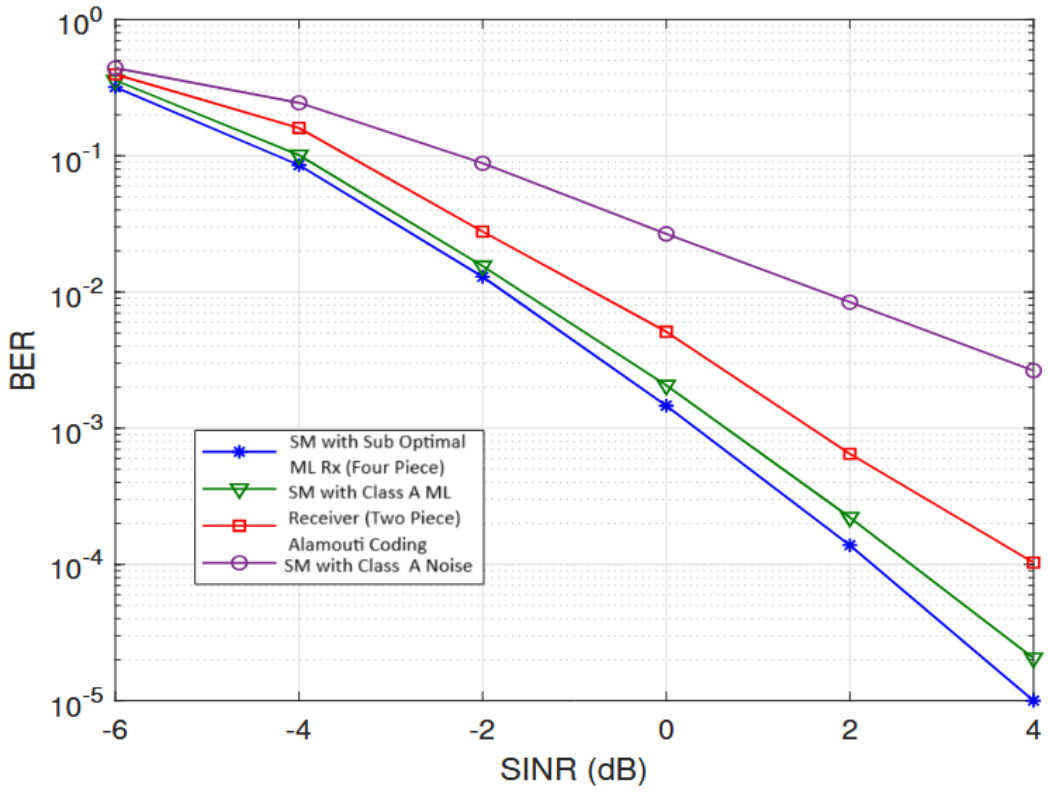

Figure 6.3: BER performance of Bivariate Middleton class A impulsive noise for different Kappa values k= 0.9

system performance. We chose a constant parameter gamma= 0.01, INI=0.8 & M=8 and by taking k value 0.9, we have generated the performance curve.

6.7.2 Effect for Impulsive Noise Index

The INI value represents the strength of the noise filter that is applied to the received signal to reduce the impact of the impulsive noise. We selected two different INI value at m=8 & k=0.5 to simulate graph. When the INI value is set too low (INI=0.1), the impulsive noise had a significant impact on the system performance, and the BER vs

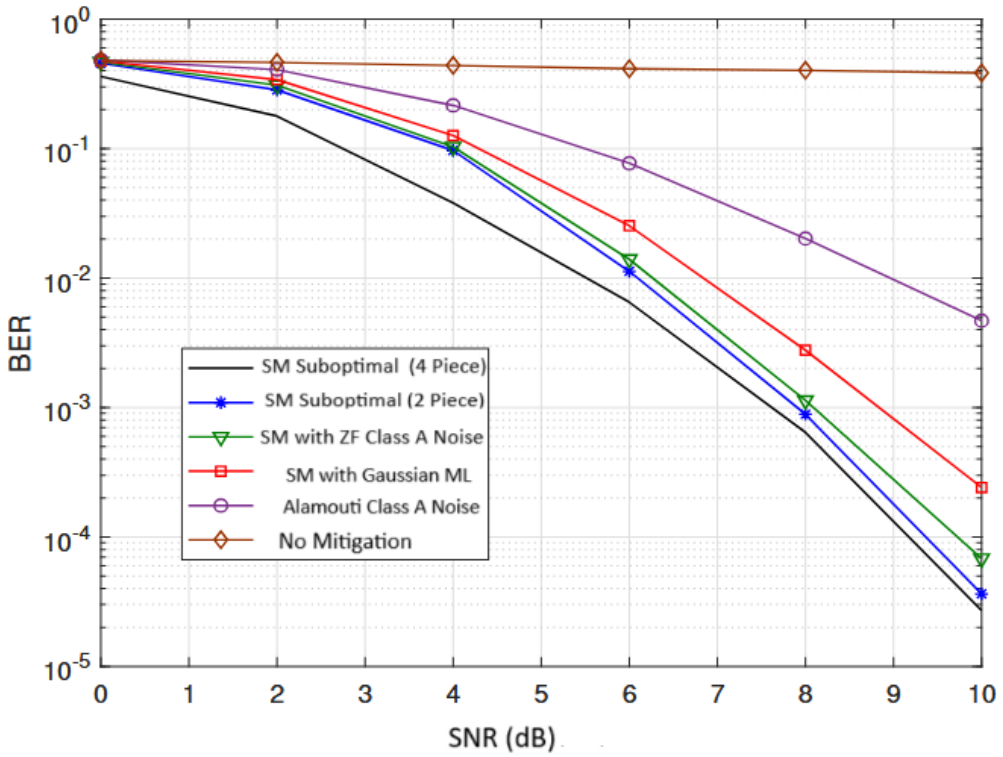

Figure 6.4 : BER performance of bivariate Middleton class A impulsive noise for different INI values of 0.8

SNR graph had a higher BER for given SNR. The curve on the graph is flatter and reached a higher BER point at a lower SNR value. This is because the noise filtering

is insufficient to effectively remove the impulsive noise from the received signal. If the INI value was set too high (INI=0.8), the filtering of impulsive noise was very effective, but it also filtered out some of the useful signal information, which lead to a higher BER in the system.

6.8 Performance Comparison between Without and With Mitigation

In this paper we have evaluated some practical impulsive noise mitigation techniques like Spatial Multiplexing (SM) with Gaussian Maximum Likelihood (ML) Receiver, S M with Zero Forcing, Alamouti Coding, S M with a Class A Sub optimal ML (two piece and four piece) Receiver etc. The key performance metric for evaluating the effectiveness of the impulsive noise mitigation method is BER vs SNR curve. By analysing the curve of figure 6.4 a table has been prepared for the SNR gain against BER of 10^{-3} to 10^{-5} which is given below:

Table II: Analysis of performance between with and without impulsive noise mitigation techniques

BER	Suboptimal ML Receiver (four piece) SNR (dB)	Suboptimal ML Receiver (two piece) SNR (dB)	Gaussian ML SNR (dB)	Alamouti SNR (dB)	Without Mitigation SNR (dB)
10^{-3}	7.6	7.9	8.8	12	22
10^{-4}	9.2	9.5	11	14	24
10^{-5}	11	12	14	16	26

From the above table it is evident that with any type of Mitigation technique, around 10 dB gain is achieved. Moreover, it is revealed that, Suboptimal ML receiver (four piece) outperforms other mitigation techniques.

An example is considered for comparing the performance of impulsive noise mitigation which is analysed in the fol table:

Table III : Communication Performance

K value	INI value	SNR (dB)		
		5	10	15
0.1	0.1	0.001	0.0001	0.00001
0.5		0.02	0.001	0.0001
0.9		0.5	0.2	0.02
Mitigation				Yes

In this example, we are comparing the performance of impulsive noise mitigation with three different k values (0.1, 0.5 and 0.9) and INI value 0.1at three different SNR level (5 dB, 10 dB, and 15 dB). The table shows the resulting BER and whether or not impulsive noise mitigation was successful for each combination of k value, INI value, and SNR level.

6.9 Summary

In this paper, the communication performance of various impulsive noise scheme on MIMO system have been summarized. Different parameters have been considered to portrait and model different types of noise distribution in case of Middleton class A and alpha stable noise. Then in this chapter, we have also analyzed and compared the BER vs SNR curve of mitigating the modeled noise in different mitigation method by varying the signal constellation from lower to higher. It has been also shown that the simulation result of the communication performance through the BER vs SNR curve and then finally analyzed and compared with the result. The simulation result suggested that, the performance of wiener filter is better in case of Middleton class A noise model which decrease the BER with the increase of SNR. For alpha stable noise model optimum and selection myriad filter has shown better performance than wiener

filter. Performance of other parameters was described briefly in this chapter. It allows system designers to analyze the tradeoff between transmission quality and bandwidth efficiency. The BER vs SNR curve enables designers to determine the minimum required SNR for a given targeted BER, which in turn allows them to select an appropriate modulation scheme and coding strategy that balances the need for reliable communication and efficient use of the available bandwidth.

In this chapter some practical impulsive noise mitigation techniques like Spatial Multiplexing (SM) with Gaussian Maximum Likelihood (ML) Receiver, S M with Zero Forcing, Alamouti Coding, S M with a class A Suboptimal M L (two piece and four piece) Receiver etc. have been evaluated. The key performance metric for evaluating the effectiveness of the impulsive noise mitigation method is BER vs SNR curve. A comparison table has been prepared and it was revealed that with any types of Mitigation technique, around 10 dB gain is achieved and Suboptimal M L receiver (four piece) outperforms other mitigation techniques.

Hence, the fifth objective of the thesis is achieved which is “to find out an appropriate mitigation technique to overcome the effect of impulsive noise”.

CHAPTER 7

CONCLUSION AND FUTURE WORKS

7.1 Conclusion

7.1.1 Summary of the Research Work

Wireless communication technology is emerging with a great promise to meet up future demand for ultra-high speed data communications and networking. OFDM is a multicarrier technique that suits well for high-speed wired and wireless applications. OFDM offers added spectral efficiency as well as robustness against selective fading, narrowband interference and impulsive noise which makes it a contender for high-speed communication system. Further to capture sufficient multipath energy the information in each sub band is modulated by utilizing OFDM technique. Thus multiband OFDM is one of the leading proposal for wireless personal area network (WPAN) standards. A major performance-limiting factor in wireless communication system is multipath-induced fading. Fading severely degrades the link performance and powerful counter-measures such as diversity techniques should be employed to maintain an acceptable performance. Different diversity combining schemes have been proposed in the literature which include Maximum Ratio Combining (MRC), Equal Gain Combining (EGC), Selection Combining (SC) and Post Detection Combining (PDC). However, these diversity combining schemes are designed for Gaussian noise, and may perform poorly when impulsive noise is present which necessitates analysis and design of diversity combining schemes by taking into account the impulsive nature of the noise. Impulsive, non-Gaussian noise is prevalent in many communication environments due to a variety of sources, such as man-made electromagnetic interference, atmospheric noise, or ignition noise. A widely accepted model for impulsive noise is Middleton Class A model.

Aiming to fill this research gap, my research presents an error rate performance analysis of hybrid SC-EGC diversity over Rayleigh fading channel in presence of

impulsive noise. This research also investigates the signal propagation in indoor environments. To examine the system performance, a channel model has been chosen which will allow to find the performance of wireless system with dual receiver diversity with selection combining followed by Equal Gain combining. Analysis has been carried out to find the probability density function of the signal to noise ratio (SNR) at the output of the dual diversity combiner and Bit Error Rate has also been calculated for several system parameters considering fading channel as well as impulsive noise environment.

A notable contribution of this research lies in the extensive evaluation of hybrid combining techniques across a spectrum of noise models encountered in wireless communication systems, spanning both man-made and natural sources of impulsive noise. The practical applications of these findings extend to the development of communication systems that are more robust and reliable in the face of impulsive noise thereby providing valuable guidance for future research work.

7.1.2 Special Remarks

To develop a reliable and effective wireless communication system, the investigation is carried out in the following chronology:

a. Theoretical analysis is carried out for signal to noise ratio and bit error rate of an OFDM SIMO Wireless Communication System with Hybrid Receive Combining and MRC Techniques over Rayleigh fading channel. The analysis is extended to receiver diversity to estimate its effectiveness in overcoming the limitations.

b. Analytical development is carried out to find out the probability of bit error considering Middleton Class A and SαS noise models for impulsive noise, without and with diversity in wireless communication receiver.

c. Analysis is carried out in terms of SNR and BER for OFDM OSTBC MIMO wireless communication system considering impulsive noise models to evaluate the combined influence of Rayleigh fading and impulsive noise and improvement due to hybrid receive diversity.

d. Utilizing MATLAB Program, simulation of a OFDM STBC MIMO wireless communication system with hybrid receive combining is carried out considering impulsive noise and Rayleigh fading and analytical result is verified.

e. Available Impulsive Noise Mitigation techniques are studied and an appropriate mitigation technique i.e. Sub-Optimal M L Receiver (four piece) is suggested to overcome the effect of impulsive noise.

7.2 Major Contributions

The main motivation of this work has been to obtain analytical models to characterize wireless receiver noise and other channel impairments and evaluate their performance analytically and by simulation. Impulsive noise is found to be one of the main limiting factors for wireless communication. Colour background noise and multipath fading play a remarkable role in limiting the communication performance. Therefore, accurate models are needed to describe the propagation and performance evaluation of the transmitted signal through wireless medium. In this respect analytical models are essential for a deeper comprehension. Overall view of the system can be used to reduce the computation time. Keeping this in mind, several analytical models have been presented to give physical insight of the effect of channel impairments and its compensation in a wireless communication system. The major results obtained from each approach are summarized as follows:

a. An analytical model is developed for the performance analysis of a wireless communication system considering the background noise. The expression of the signal to noise ratio is developed considering frequency and time

dependence on the cyclostationary noise. The system bit error rate (BER) is then evaluated numerically for several system parameters like system bit rate, Fourier coefficients of the non-white Gaussian noise process etc. The BER results show that there is deterioration in system BER due to time and frequency dependence of noise and the degradation is found to be significant at high bit rates and bandwidth. The system suffers penalty in receiver sensitivity due to non-white nature of the noise process.

b. An analytical approach using diversity reception is carried out to examine the performance improvement of a wireless communication channel in fading and impulsive noise. The impulsive noise is considered time variant which has short duration, random occurrence with a high power spectral density (PSD). It causes bit error in the signal. Using orthogonal frequency division multiplexing (OFDM) technique, the effect of impulsive noise and fading can be improved greatly. The system bit error rate (BER) is compared numerically for binary phase shift keying (BPSK) and OFDM system. The obtained BER results show that there is significant improvement in performance. Also the performance is remarkably upgraded using diversity reception. The BER performance is investigated using multiple antennas and also calculated analytically.

c. Analysis is carried out to find the expression of the signal to noise ratio (SNR) and bit error rate (BER) considering orthogonal frequency division multiplexing (OFDM), with binary phase shift keying (BPSK) modulation, and with coherent demodulation of OFDM sub-channels. Middleton class-A noise model is considered to evaluate the effect of impulsive noise. The results are evaluated numerically considering the multipath transfer function model of wireless communication. The computed result show that the system suffers significant power penalty due to impulsive noise which is higher at higher channel bandwidth and can be reduced by increasing the

number of OFDM subcarriers. It is found that there is power penalty due to impulsive noise of the order of 0 to 25 dB depending on the value of impulsive noise index at a Ber=10^{-9}. The penalty can be reduced by increasing the OFDM carriers. All results conform well with the simulation results.

d. Analysis is carried out to apply STBC coding to wireless communication channel. The analysis is presented to evaluate the bit error rate of wireless channel considering background noise, impulsive and multipath fading effect. It is observed that application of STBC codes improve the BER performance of a wireless channel better than conventional analysis of MIMO OFDM codes. The analytical results show that the BER performance improves when STBC code blocks are increased. It is further improved by the increase of transmitters, receivers or both.

e. The practical implications of these findings extend to the development of communication systems that are more robust and reliable in the face of impulsive noise, thereby providing valuable guidance for further research endeavours in their domain.

7.3 Recommendations for Future Work

Topics in the field of broadband wireless communications in the industrial environment are open for research. The scope of the research work was kept limited within the environment of Rayleigh fading. This work can be extended by evaluating the performance of hybrid SC-EGC system for different fading channels like Rician and Nakagami-n fading channel. The current study prioritizes practical insights gleaned from extensive simulations. The forthcoming work aims to complement this empirical foundation with theoretical rigour. Therefore, further research may be expanded in the following areas as recommended for future work:

a. The applicability of sophisticated and modern digital signal processing techniques.

b. Extensive field trials can be performed in different types of industrial environments in order to get a better insight into the limitations and possibilities of wireless data transfer.

c. For improving the performance of wireless communication channel and to enhance the data rate.

d. The future research endeavour can be concentrated on formulating explicit mathematical expression for the BER in the context of hybrid combining technique across diverse noise models and fading channels.

7.4 List of Publications

Conference Paper:

a. Conference Paper-1: "Performance Analysis of a SIMO Wireless Link with Turbo Coding", ICEEICT, 2018, MIST, Dhaka, Bangladesh

b. Conference Paper-2: "Comparative Analysis of Hybrid Diversity Schemes under AWGN and Impulsive Noise Models for Rayleigh Fading Channels" ICEEICT, 2021, MIST, Dhaka, Bangladesh.

c. Conference Paper 3: " Performance Analysis of a UWB RFID System with Hybrid SC-EGC Receive Combining Technique", IEEE Region 10 Symposium (TENSYMP), 5-7 June2020, Dhaka, Banglaesh, pg 710-713.

d. Conference Paper 4: " A Study on the Performance Analysis of Hybrid Diversity Combining Techniques for Rayleigh and Rician Fading Channels under AWGN", ICEEICT, 2021, MIST, Dhaka, Bangladesh.

Journal Paper:

a. " Performance Analysis of a Hybrid Combining Schemes under Middleton Class-A and SαS Impulsive Noise Model", Published in Journal named "The Journal of Engineering".

b. "Comparison of Various Schemes for Mitigation of Impulsive Noise in a Wireless Communication System with Middleton Class a Noise Model", under review on "Journal of Electrical and Electronic Engineering".

c. "Performance Limitations of Impulsive Noise on SISO and SIMO- MRC OFDM Wireless Communication Links with Middleton Class A and Poisson's Noise Models" under review on "The Journal of Engineering".

REFERENCES

[1] J. Mark and W. Zhuang, Wireless Communications and Networking. Prentice Hall, 2003.

[2] S. P. Majumder and Md Abdul Halim, "Performance Analysis of a UWB RFID System with Hybrid SC-EGC Receive Combining Technique", 2020 IEEE Region 10 Symposium (TENSYMP), 5-7 June 2020, Dhaka, Bangladesh.

[3] Heyem Hamilili, Samir Cameeha, Abdelhafid Abdelmalek, "S-α-S noise suppression for OFDM wireless communication in Rayleigh channel", International Journal of Electrical and Computer Engineering (IJECE), vol. 10, No. 2, April 2020.

[4] Sakimalla Prabhakar Girija and R Ramesh Rao, "Robust Maximum Likelihood Algorithm-based Mitigation technique for impulsive noise in MIMO-OFDM System", 2020 IEEE International Conference on Advanced Networks and Telecommunications Systems (ANTS).

[5] B. Suresh Ram, Dr. P. Siddaiah. " A unique approach to combat multipath fading using hybrid diversity technique", Journal of Critical Review, ISSN-2394-5125, Vol-7, Issue 18, 2020 pp 4186-4192.

[6] Mohammad Reza Ahadiat, Paeiz Azmi, AfroozHaghbin, " BER performance Analysis of MIMO – OFDM Communication System Using Iterative Technique over Indoor Power Line Channels in an Impulsive Noise Environments", Journal of Information Systems and Telecommunication, vol. 4, No.1, January – March 2016.

[7] B. Suresh Ram and Dr. P. Siddaiah, " Performance Evaluation of Hybrid Diversity Technique using Minimum Shift Keying over Rayleigh Fading Channel" , International journal of applied engineering and research ISSN 0973-4562, Volume 12, Number 11 (2017), pp. 2876-2878.

[8] Sai Krishna Kondoju and V. V. Mani, " Outage an average BER analysis of multiband OFDM UWB system with MRC/EGC receiver in Log-normal fading channels", 23rd International Conference on Telecommunication heldin 2016.

[9] Hima Pradeep. V and Seema Padmarajan, " Performance analysis of Hybrid MRC/EGC Diversity Combining Technique over AWGN Channel", IOSR Journal of Electronics and Communication Engineering (ICETEM-2016), pp 25-29.

[10] Alina Mirza, Sumrin M. Kabir, Shahzad A. Sheikh, "Reduction of Impulsive noise in OFDM System using Adaptive Algorithm", International Journal of Electronic and Communication Engineering, vol- 9, No. 6, 2015.

[11] S.P.Majumder and K. Mahmud, " Evaluation of Detection Range of an Active RFID in outdoor Environment using Receiver Diversity with Maximal ratio Combining'', International Journal of Information and Electronics Engineering, Vol.5 no. 5 Sept 2015.

[12] S.P. Majumder and Mohammad Mahfujur Rashid, " Bit Error Rate Performance of a Multi-band OFDM UWB RFID System with Reader Receiver Diversity using Maximal Ratio Combiner", IEEE International Conference on Telecommunications and Photonics (ICTP) 2015.

[13] Ali Hakim, Noha Aly and Shihab Jimaa, "Impulsive Noise Mitigation in a MIMO-OFDM Communication System", 204 6th International Conference on New Technologies, Mobility and Security (NTMS), IEEE 2014

[14] R. E. A. Ance and N. C. Karmakar, "Chipless RFID tag localization." IEEE transaction on microwave theory and techniques, Vol. 61, No. 11 November 2013.

[15] https://www.microwavejournal.com/articles/24759-history-of-wireless-communications.

[16] S M. Z. Win, and R. A. Scholtz, Mark A. Barnes "Ultra-Wide Bandwidth Signal Propagation for Indoor Wireless Communications". IEEE Journal on Selected Areas in Communications, Vol. 20 , No. 9, December 2002.

[17] A Dinamani, Swagata as, BijendraI,, Sruti R, Babina Sand Kiran B. "Performance of a hybrid MRC/SC diversity receiver over Rayleigh fading channel, Circuits, Controls and Communications (CCUBE) IEEE 2013 International Conference, India, 2013

[18] R.-E.-A. Anee and N. C. Karmakar, “Chipless RFID tag localization.” *IEEE transcation on microwave theory and technique, Vol. 61, No. 11, November 2013.*

[19] Hima Pradeep V and Seema Padmarajan, “Hybrid Diversity Combining Techniques for Fading Channels”, 2015 IJSRSET, Volume I, Issue 4

[20] A. F. Molisch, D. Cassioli, C.C. Chong, S.Emami, A. Fort, B.Kannan,J. Kunisch, H.Gregory, Schantz, K. Siwiak, and M. Z. Win, “A comprehensive standardized model for ultra wideband propagation channels.” *IEEE Transaction on Antenna and Propagation*, vol.-54, no,11,2006.

[21] Batra, J. Balakrishnan, G. R. Aiello, J. R. Foerster and A. Dabak “Design of a Multiband OFDM System for Realistic UWB Channel Environments” IEEE Transactions on Microwave Theory and Techniques, Vol. 52, No. 9, September 2004.

[22] Anuj Batra, Jaiganesh Balakrishnan, G. Roberto Aiello, Jeffrey R. Foerster and Anand Dabak, “ Design of a Multiband OFDM System for realistic UWB Channel Environments”, IEEE Transactions on Microwave Theory and Techniqus, Vol 52, No. 9 September 2004.

[23] Cihan Tepedelenlioglu and P. Gao, “ On Diversity Reception over fading channels with impulsive noise”, IEEE Communication Society Globecom 2004, pp 3676-3680.

[24] S. Gaur and A. Annamalaj, “Improving the range of ultrawideband transmission using rake receivers.” IEEE 58th Vehicular Technology Conference, Vol. 1, pp 597 – 601, 2003.

[25] Kapil Gulati, Aditya Chopra, Robert W. Heath Jr, Brian L. Evans, Keith R. Tinsley and Xintian E. Lin, “ MIMO Receiver Design in the Presence of Radio Frequency Interference,” IEEE GLOBECOM 2008.

[26] M. Z. Win, R. A. Scholtz “Characterization of Ultra-Wide Bandwidth Wireless Indoor Channels.” A Communication-Theoretic View” IEEE Journal on Selected Areas in Communications, Vol. 20, No. 9, pp 1613 – 1627, December 2002.

[27] J. F. Weng and S. H. Leung, “On the performance of DSPK in Rician fading with class A noise”, IEEE Trans. On Vehicular Technology, vol. 49. No. 5, Sep 2000. Pp 1934-1949.

[28] Federal Communication Commissions, “First report and order 02-48,” (2002).

[29] Richard V.Nee, Ramjee Prasad, “OFDM for Wireless Multimedia Communications,” Artech House, 2000

[30] M. Zimmermann and K. Doster, “Analysis and modeling of impulsivenoise in broad-band power line communications,” IEEE Trans, Electr-magn, Compat, vol.44 no.1, pp 249-258, Feb 2002

[31] S. K. Kondoju, V. V. Mani and R. Bose “Exact BER analysis of DCM for Multiband OFDM-UWB System over uncorrelated Nakagami-m fading channels” IEEE International Conference on Ultra-WideBand (ICUWB), pp 473 – 478, 2014.

[32] Sasan Haghani, Norman C. Beanlien and Moez. Win, “SNR Penalty of Hybrid Diversity Combining in Rayleigh Fading”, 2013 IEEE Transaction, pg 2800-2804

[33] B. Suresh Ram and Dr. P. Siddaiah, “ Performance Evaluation of Hybrid Diversity Technique using Minimum Shift Keying over Rayleigh Fading Channel” , International journal of applied engineering and research ISSN 0973-4562, Volume 12, Number 11 (2017), pp. 2876-2878.

[34] Hong Lee, Sang Kyu Park and Yujae Song, “Performance Analysis of a Hybrid SEC/MRC Diversity Scheme Rayleigh Fading”, ICACT 2011, Feb 13-16, pp 1115-1118.

[35] Mohammad Reza Ahadiat, Paeiz Azmi, AfroozHaghbin, “ BER performance Analysis of MIMO – OFDM Communication System Using Iterative Technique over Indoor Power Line Channels in an Impulsive Noise Environments”, Journal of Information Systems and Telecommunication, vol. 4, No.1, January – March 2016.

[36] S.P. Majumder and Mohammad Mahfujur Rashid, “ Bit Error Rate Performance of a Multi-band OFDM UWB RFID System with Reader Receiver Diversity using Maximal Ratio Combiner”, IEEE International Conference on Telecommunications and Photonics (ICTP) 2015

[37] S.P.Majumder and K. Mahmud, " Evaluation of Detection Range of an Active RFID in outdoor Environment using Receiver Diversity with Maximal ratio Combining " , International Journal of Information and Electronics Engineering, Vol.5 no. 5 Sept 2015.

[38] H. Suraweera and J. Armstrong, "Noise bucket effect for impulse noise in OFDM," Electron. Lett. Vol. 40. No. 18, pp 1156-1157, Sep 2004

[39] Alina Mirza, Sumrin M. Kabir, Shahzad A. Sheikh, "Reduction of Impulsive noise in OFDM System using Adaptive Algorithm", International Journal of Electronic and Communication Engineering, vol- 9, No. 6, 2015.

[40] Petra C. Spalevic, Mihajlo C. Stefanoic, Stefan R. Panic, Branjamir S. Jachsic, Mile B. Pehovic, "Performance Analysis of Selecting Maximal Ratio Combining Hybrid Diversity System over Rician Fading Channel", Online ISSN 1848-3380, AUTOMATIKA 55 (2014) 3, pp 299-305.

[41] R. E. A. Ance and N. C. Karmakar, "Chipless RFID tag localization." IEEE transaction on microwave theory and techniques, Vol. 61, No. 11 November 2013.

[42] B. Suresh Ram, Dr. P. Siddaiah. " A unique approach to combat multipath fading using hybrid diversity technique", Journal of Critical Review, ISSN-2394-5125, Vol-7, Issue 18, 2020 pp 4186-4192.

[43] W. P. Siriwongpairat, W. Su, M. Olfat and K. J. R. Liu "Multiband- OFDM MIMO Coding Fram ework for UWB Communication Systems" IEEE Transactions on Signal Processing, Vol. 54, No. 1, January 2006.

[44] Lavish Kansal, Ankush Kansal and Kulbir Singh, "BER Analysis of MIMO-OFDM System Using OSTBC Code Structure for M-PSK under Different Fading Channels", International Journal of Scientific & Engineering Research, Volume 2, Issue 11, November-2011, ISSN 2229-5518.

[45] Sakimalla Prabhakar Girija and R Ramesh Rao, "Robust Maximum Likelihood Algorithm-based Mitigation technique for impulsive noise in MIMO-OFDM System", 2020 IEEE International Conference 9n Advanced Networks and Telecommunications Systems (ANTS)

[46] Batra, J. Balakrishnan, G. R. Aiello, J. R. Foerster and A. Dabak “Design of a Multiband OFDM System for Realistic UWB Channel Environments” IEEE Transactions on Microwave Theory and Techniques, Vol. 52, No. 9, September 2004.

[47] Hema Pradeep, V. Seema. Padmarajan, “Performance Analysis of Hybrid MRC/EGC Diversity Combining Technique Over AWGN Channel”, IOSR Journal of Electronics and Communication Engineering (IOSR-JECE) pp25-29 of IEB Team 2016.

[48] Yingg ang D., and Chan K. T. , “Enhanced Space in Block Coded System by concatenating Turbo Product codes” IEEE Communications letters vol. 8 , No. 6. June 2004.

[49] Sai Krishna Kondoju and V. V. Mani, “ Outage an average BER analysis of multiband OFDM UWB system with MRC/EGC receiver in Log-normal fading channels”, 23rd International Conference on Telecommunication heldin 2016.

[50] Stamoulis A., Liu Z. and Giannokis G. B., “Space-Time Block Coded OFDMA with Linear Precoding for Multi rate services,” IEEE Transactions in Signal Processing vol. 50 no. 1, January 2002.

[51] X. Zhang, Y. Chen, N. Zhao, and H. Zhou, “Multiuser detection in massive MIMO system with wiener filtering,” IEEE Wireless Communications Letters, vol. 8, no. pp. 637-640, 2019.

[52] H. H. Lin, W. Lin, C. H. Wu, and C. S. Lu, “Multi-sensor signal detection using wiener filter for wireless sensor networks,” in 2018 IEEE 88th Vehicular Technology Conference (VTC-Fall). IEEE, 2018, pp. 1-5.

[53] Y. Tan, F. Wei, H. Wu, and J. Xu, “Joint user activity detection and channel estimation in wireless sensor networks with wiener filtering,” Sensors, vol. 16, no. 4, p. 496, 2016.

[54] L. Li, W. Li, J. Zhang, and Q. Chen, “Performance analysis of Bayesian signal detection with multi-hop in wireless sensor networks,” Wireless Personal Communications, vol, no. 4, pp. 1837-1853, 2019.

[55] Y. Zhang, W. Zhou, and W. Liu, “Spatial multiplexing with gaussian mi receiver over time-varying correlated fadind channels,” Journal of Electrical and Computer Engineering, vol. 2019, 2019.

[56] P. R. Sahu and A.K. Chaturvedi, ”Performance Evaluation of SC-MRC and SC-EGC Diversity Combining Systems in Slow Nakagami-M Fading Channel” Jan 2001

[57] S. K. Kondoju, V. V. Mani and R. Bose “Exact BER analysis of DCM for Multiband OFDM-UWB System over uncorrelated Nakagami-m fading channels” 2014 IEEE International Conference on Ultra-WideBand (ICUWB), pp 473 – 478, 2014.

[58] J. G. Proakis, “Digital Communication Third Edition,” New York: MC Graw – 1995.

[59] A Dinamani, Swagata as, BijendraI,, Sruti R, Babina Sand Kiran B. “Performance of a hybrid MRC/SC diversity receiver over Rayleigh fading channel, Circuits, Controls and Communications (CCUBE) IEEE 2013 International Conference, India, 2013

[60] A. F. Molisch, D. Cassioli, C.C. Chong, S.Emami, A. Fort, B.Kannan,J. Kunisch, H.Gregory, Schantz, K. Siwiak, and M. Z. Win, “A comprehensive standardized model for ultra wideband propagation channels.” *IEEE Transaction on Antenna and Propagation*, vol.-54, no,11,2006.

[61] P. R. Sahu and A.K. Chaturvedi, “Performance Evaluation of SC-MRC and SC-EGC Diversity Combining Systems in Slow Nakagami-M Fading Channel” Jan 2001

[62] Anuj Batra, Jaiganesh Balakrishnan, G. Roberto Aiello, Jeffrey R. Foerster and Anand Dabak, “ Design of aMultiband OFDM System for realistic UWB Channel Environments”, IEEE Transactions on Microwave Theory and Techniqus, Vol 52, No. 9 September 2004.

[63] X. Liu, J. Zhang, and S. Xie, “Performance analysis of MIMO systems with receive antenna selection over generalized -k fading channels,” IEEE Access, vol. 6, pp. 3172-3182, 2018.

[64] S. Gaur and A. Annamalaj, “Improving the range of ultrawideband transmission using rake receivers.” IEEE 58th Vehicular Technology Conference, Vol. 1, pp 597 – 601, 2003.

[65] S M. Z. Win, and R. A. Scholtz, Mark A. Barnes “Ultra-Wide Bandwidth Signal Propagation for Indoor Wireless Communications”. IEEE Journal on Selected Areas in Communications, Vol. 20 , No. 9, December 2002.

[66] M. Z. Win, R. A. Scholtz “Characterization of Ultra-Wide Bandwidth Wireless Indoor Channels.” A Communication-Theoretic View” IEEE Journal on Selected Areas in Communications, Vol. 20, No. 9, pp 1613 – 1627, December 2002.

[67] J. F. Weng and S. H. Leung, “On the performance of DSPK in Rician fading with class A noise”, IEEE Trans. On Vehicular Technology, vol. 49. No. 5, Sep 2000. Pp 1934-1949.

[68] R.-E.-A. Anee and N. C. Karmakar, “Chipless RFID tag localization.” *IEEE transcation on microwave theory and technique, Vol. 61, No. 11, November 2013.*

[69] Suhail Al-Dharrab and Mural Vysal, “Cooperative Diversity in the Presence of Impulsive Noise”, IEEE Transaction on Wireless Communication, Vol 8, No. 9 September 2009.

[70] Donatella Darsena, Giacinto Gellio, Fulvio Melito, Francesco Verde and Andera Vitiello, “Impulse noise mitigation for MIMO-OFDM wireless networks with linear equalization”, 2013 IEEE International Workshop on Measurements and Networking (M&N)

[71] Sicong Liu, Fang Yang, Xianbin Wang, Jian Song and Zhu Han, “Structured-Compressed-Sensing-Based Impulsive Noise Cancelation for MIMO System”, 2017 IEEE Transaction on Vehicular Technology, volume 68, issue 8

[72] S. P. Girija and K. Deergha Rao, “Smoothing term based noise correlation matrix construction for MIMO-OFDM wireless network for noise mitigation”, TENCON 2015- IEEE Region 10 Conference 2015

[73] S. Laksir, Abdelali Chaoub and A. Tamtaoui, “Impulsive noise reduction Techniques in power line communication: A survey and recent trends”, IEEE International workshop on Technologies, Algorithms, Models, Platforms and Applications for Smart Cities, 2018.

[74] M. S. Alam, B. Selim and G. Kaddoum, “Analysis and Comparison of several mitigation techniques for Middleton Class-A noise”, IEEE, 2019.

[75] A. J. Mohammed, M. K. Mahmood Al-Azawi, “Comparison of Time and Time-Frequency domains impulsive noise mitigation techniques for power line communication”, Journal of Engineering and Sustainable Development, Vol. 27, no. 01, pp. 68-79, January 2023.

[76] V. Sergey Zhidkov, “Analysis and Comparison of several simple impulsive noise mitigation schemes for OFDM receivers," IEEE Transactions on Communications, vol. 56. No. 1, pp. 1-6, January 2008.

[77] M.A. Abid, X. Liu, and J. Zhang, “Performance analysis of Massive MIMO systems with receive antenna selection over generalized fading channels,” Wireless Networks, vol. 25, no. 2, pp. 1003-1017, 2019.

[78] J. Zhao, X. Wang, and X. Guan, “Performance analysis of a single user MIMO system with ZF and MMSE detectors over Nakagami-m fading channels,” Wireless Personal Communications, vol. 105, no. 1, pp. 43-56, 2019.

[79] S. Alayobi, K. S. Omar,and K. A. Qarsqe, “Performance analysis of alamouti MIMO scheme over nakagami-m fading channel,” International Journal of Communication Systems, vol. 28, no. 9, pp. 1472-1482, 2015.

[80] J. Zhao, J. Li, T. Liu, and X. Guan, “Low-complexity joint decoding for Alamouti codedfull duplex MIMO systems,” IEEE Access, vol. 7, pp.141616-141627,

2019.

[81] C. L. Nikias and M Shao, Signal Processing with Alpha-Stable Distributions and Applications. New York: Wiley, 1995.

[82] M. Rahman M and Majumder S. P., “Analysis of a power line communication system over a non-white additive Gaussian noise channel and performance improvement using diversity reception” Network and Communication Technologies Journal Vol. 1, pp.26-38, June 2012.

[83] H. C. Ferreira, L. Lampe, J. Newbury and T. G. Swart, “Power Line Communications: Theory and applications for narrowband and broadband communications over power lines”, John Wiley & Sons, 2006.

[84] J. Jiang, Y. Xin, and S. Sun, “Spatial multiplexing with Gaussian ML receiver: A geometric approach,” IEEE Transaction on Communications, vol. 64, no. 4, pp. 1674-1688, 2016.

[85] T. Shongwe, A. H. Vinck, and H. C. Ferreira, “A study on impulse noise and its models,” SAIEE Africa Research Journal, vol. 106, no. 3. 119-131, 2015.

[86] A. Mathur, M. R. Bhatnagar, and B. K. Panigrahi, “Performance evaluation of plc under the combined effect of background and impulsive noises,” IEEE Communications Letters, vol. 19, no. 7, pp. 1117-1120, 2015.

[87] S. Liu, F. Yang, W. Ding, J. Song, and Z. Han, “Impulsive noise cancellation for MIMO-OFDM plc systems: A structured compressed sensing perspective,” in 2016 IEEE Global Communications Conference (GLOBECOM). IEEE, 2016, pp,1-6.

[88] A. Bhardwaj, R. Kumar, N. Sharma, and M. Gupta, “Adaptive median filtering of ecg signals for removal of impulsive noise,” International Journal of Engineering Research and General Science, vol. 4, no. 4, pp. 408-414, 2016.

[89] S. Drrani, A. Hussain,A. Ali, and S. Naz, “Kalman filtering for impulsive noise reduction in speech signals,” IET Signal Processing, vol. 9, no. 6. Pp. 483-489, 2015.

[90] J. Wang, J. Zhu, L. Zhang, Y. Chen, and D. Zhang, “Impulsive noise reduction in color images using adaptive least mean square filter,” Journal of Real-Time Image Processing, vol. 12, no. 4, pp. 693-706, 2017.

[91] H. Wang, K. Yang, and G Zhou, “ Impulsive noise reduction in wireless communication systems using a non-linear filter,” IET Communications, vol. 10, no. 10, pp. 1173-1180,2016.

[92] H. Li., J. He,Q. Li, and Y. Wang, “Adaptive wiener filtering for impulsive noise reduction in underwater acoustic communication systems,” IEEE Transactions on Instrumentation and Measurement, vol. 66, no. 6, pp. 1019-1031, 2016.

[93] S. S. Beagun, N. Hundewale, and M. M. Sathik, “Improved adaptive median filters using nearest 4-neighbors for restoration of images corrupted with fixed-valued impulse noise,” in 2015 IEEE International Conference on Computational Intelligence and Computing Research (IC-CIC). IEEE, 2015, pp. 1-8.

[94] Zhan W. Xia X. G. and Letaief K. B., “ Space-Time Block Coding for MIMO-OFDM in Next Generation Broadband Wireless Systems,” IEEE Wireless Communications, June 2007.

[95] Y. S. Cho, W. Y. Yang and C. G. Kang, “MIMO-OFDM Wireless Communication with MATLAB”, 2nd edition, Asia: John Wiley & Sons, pp 112-120, 2010

[96] Jurgen Harling and A. J. Han Vinck, Senior Member IEEE, “Performance Bounds for Optimum and Suboptimum Reception under Class-A Impulsive Noise,” IEEE Transactions on Communications, vol. 50. No. 7. July 2002, pg 1130-1136.

[97] B. Rajkumarsingh and M. H. Edoo, “ BER Performance comparison of the Markov-middleton and middleton class A noise models in the MIMO power line communication channel,” in 2022 4th International Conference on Emerging Trends in Electrical, Electronic and Communication Engineering (ELECOM). IEEE, 2022, pp. 1-7.

[98] H. Sepehrian, S. M. R. Shafiee, and R. Q. Hu, " Correlation-based interference management in multi-cell wireless networks," IEEE Transactions on Wireless Communications, vol. 18, no. 3, pp. 1643-1658, 2019.

[99] H. Lee and N. Al-Dhahir, "Subspace-based correlation receivers for multicarrier systems," in 2017 IEEE International Conference on Acoustics, Speech and Signal Processing (ICASSP). IEEE, 2017, pp. 3794-3798.

[100] F. Aoudia, A. Taleb-Ahmed, and A. Hadjtaieb, "Performance analysis of correlation-based non-coherent detection for MIMO-OFDM systems," Wireless Personal Communications, vol. 102, no. 1, pp. 365-382, 2018.

[101] A. Alayon Glazunov and N. Al-Dhahir, "Correlation receivers for spectral efficiency enhancement in multicarrier systems," IEEE Transactions on Wireless Communications, vol. 16, no. 8, pp. 4942-4957, 2017.

[102] Mihaela Andrei, George Petrea,and Viorel Nicolau, " On golden code performances in impulsive noise MIMO channel", Journal of Communication, vol. 16, No. 3, March 2021.

[103] S. Zhidkov, "Analysis and comparison of several simple impulsive noise mitigation schemes for OFDM receivers," IEEETrans. Commun. Vol. 56. No. 1. Pp 509, Jan 2008

[104] R. Shepherd, J. Gaddie, and D. Nielson, "New techniques for suppression of automobile ignition noise," IEEE Trans. Veh. Technol, vol. VT-25, no. 1, pp 2-12, Feb 1976.

[105] Salman Habib and Ariful Haque, "Impulsive Noise Mitigation in Wireless Communication Systems using EMD technique", 2012 7th International Conference on Electrical and Computer Engineering, 20-22 Deceber 2012, Dhaka, Bangladesh.

[106] Donatella Darsena, Giacinto Gellio, Fulvio Melito, Francesco Verde and Andera Vitiello, "Impulse noise mitigation for MIMO-OFDM wireless networks with

linear equalization", 2013 IEEE International Workshop on Measurements and Networking (M&N).

[107] Sicong Liu, Fang Yang, Xianbin Wang, Jian Song and Zhu Han, "Structured-Compressed-Sensing-Based Impulsive Noise Cancelation for MIMO System", 2017 IEEE Transaction on Vehicular Technology, volume 68, issue 8.

[108] S. P. Girija and K. Deergha Rao, "Smoothing term based noise correlation matrix construction for MIMO-OFDM wireless network for noise mitigation", TENCON 2015- IEEE Region 10 Conference 2015.

[109] Y. Liu, E. Li, X. Gao, S. Jin, and J. Wang, "Performance analysis of spatial multiplexing with Gaussian ML receiver over correlated fading channels," Wireless Networks, vol. 23, no. 3, pp. 775-787, 2017.

[110] https://www.microwavejournal.com/articles/24759-history-of-wireless-communications

[111] https://www.sciencedirect.com/topics/engineering/scale-fading

[112] Saeed V. Vaseghi Professor of Communications and Signal Processing Department of Electronics and Computer Engineering Brunel University, UK, Advanced Digital Signal Processing and Noise Reduction Third Edition

[113] Y. Liu, W. Li,J. Wang, and X. G. Zhang, "Asymptotic error rate analysis of spatial multiplexing with gaussian ML receiver in massive MIMO systems," IEEE Transactions on Vehicular Technology, vol. 67, no. 4, pp. 3519-3533, 2018.

[114] Reza Barazideh, "Impulsive Noise Detection and Mitigation in Communication System," M.S., Shahed University, Iran 2009.

[115] J. Zhang; and Q. Zhao;, "Simulation and analysis of MIMO-OFDM system based on Simulink," Communications, Circuits and Systems (ICCCAS), 2010 International Conference. Pp. 19-22, 28-30 July 2010.

APPENDIX – A

MATLAB SCRIPT FOR BER PERFORMANCE AND SIMULATION

1. MATLAB Script for Comparison of BER vs SNR for MRC in Case of Theory and Simulation without Impulsive Noise

```
% BPSK over Rayleigh fading channel with MRC diversity
clear; clc;

% Parameters
N = 1e6;                      % Number of bits
EbN0_dB = 0:2:20;             % Eb/N0 range in dB
EbN0_lin = 10.^(EbN0_dB/10); % Linear scale
L_values = [1 2 3 4];         % Diversity orders to simulate

% Generate random bits and BPSK symbols once
bits = randi([0 1], 1, N);
symbols = 2*bits - 1;         % BPSK mapping

% Storage for BER
BER_sim = zeros(length(L_values), length(EbN0_dB));
BER_theory = zeros(length(L_values), length(EbN0_dB));

for l_idx = 1:length(L_values)
    L = L_values(l_idx);

    for i = 1:length(EbN0_dB)
        EbN0 = EbN0_lin(i);
        N0 = 1 / EbN0;

        % Generate Rayleigh fading and noise
        h = (randn(L, N) + 1j*randn(L, N)) / sqrt(2);          %
Rayleigh fading
        n = sqrt(N0/2) * (randn(L, N) + 1j*randn(L, N));       %
AWGN

        % Transmit symbols over L branches
        r = h .* repmat(symbols, L, 1) + n;

        % Maximal Ratio Combining
        y_comb = sum(conj(h) .* r, 1);       % Coherent combining
        h_power = sum(abs(h).^2, 1);
        y_comb = y_comb ./ h_power;          % Normalize

        % Demodulation
        bits_rx = real(y_comb) > 0;
```

```
        % BER calculation
        BER_sim(l_idx, i) = sum(bits_rx ~= bits) / N;

        % Theoretical BER (approximation)
        gamma = EbN0_lin(i);
        BER_theory(l_idx, i) = 0.5 * (1 - sqrt(gamma / (1 +
gamma)))^L;
    end
end

% Plot results
figure; hold on; grid on;
colors = lines(length(L_values));

for l_idx = 1:length(L_values)
    semilogy(EbN0_dB, BER_sim(l_idx, :), 'o-', 'Color',
colors(l_idx,:), ...
        'LineWidth', 2, 'DisplayName', ['Simulated L = '
num2str(L_values(l_idx))]);
    semilogy(EbN0_dB, BER_theory(l_idx, :), '--', 'Color',
colors(l_idx,:), ...
        'LineWidth', 2, 'DisplayName', ['Theory L = '
num2str(L_values(l_idx))]);
end

xlabel('Eb/N0 (dB)');
ylabel('Bit Error Rate (BER)');
title('BER for BPSK in Rayleigh Fading with MRC (Various L)');
legend('Location','northwest');
```

2. MATLAB Script for Comparison of BER vs SNR for MRC in Case of Theory and Simulation with Impulsive Noise

```
clear; clc;
N = 1e6;                        % Number of bits
EbN0dB = 0:2:20;                % SNR range
L = 2;                          % MRC branches

A = 0.1;   % impulse index
Gamma = 0.01; % impulsive variance ratio

BER_sim = zeros(1, numel(EbN0dB));
BER_awgn = zeros(1, numel(EbN0dB));

for idx = 1:numel(EbN0dB)
    EbN0 = 10^(EbN0dB(idx)/10);
    bits = randi([0 1],1,N);
    symbols = 2*bits - 1;

    % Rayleigh channels
```

```
    h = (randn(L,N)+1j*randn(L,N))/sqrt(2);

    %% 1) Simulate impulsive noise case
    y = zeros(1,N);
    for l = 1:L
        sig = h(l,:).*symbols;
        p = exp(-A);
        bg = rand(1,N) < p;
        noise = sqrt(1/(2*EbN0))*(randn(1,N)+1j*randn(1,N));
        impuls = sqrt(Gamma/(2*EbN0))*(randn(1,N)+1j*randn(1,N));
        n_all = bg.*noise + (~bg).*impuls;
        y = y + conj(h(l,:)).*(sig + n_all);
    end
    est = real(y) > 0;
    BER_sim(idx) = mean(xor(est,bits));

    %% 2) Rayleigh + AWGN only reference (no impulsive noise)
    y0 = zeros(1,N);
    for l = 1:L
        sig = h(l,:).*symbols;
        noise0 = sqrt(1/(2*EbN0))*(randn(1,N)+1j*randn(1,N));
        y0 = y0 + conj(h(l,:)).*(sig + noise0);
    end
    est0 = real(y0) > 0;
    BER_awgn(idx) = mean(xor(est0,bits));
end

% theoretical reference for Rayleigh + AWGN (closed-form)
theory_awgn = zeros(size(EbN0dB));
for k = 1:L
    % uses combination formula for L=2
    theory_awgn = theory_awgn + (-1)^(k-1)*nchoosek(L,k)*0.5*(1 -
sqrt((k*(10.^(EbN0dB/10)))./(1 + k*(10.^(EbN0dB/10)))));
end

% Plot
figure;
semilogy(EbN0dB, BER_sim,'ro-','DisplayName','Sim MRC L=2
(Class?A)');
hold on;
semilogy(EbN0dB, BER_awgn,'bs-','DisplayName','Sim MRC L=2 (AWGN
only)');
semilogy(EbN0dB, theory_awgn,'k--','DisplayName','Theory MRC L=2
Rayleigh+AWGN');
xlabel('E_b/N_0 (dB)');
ylabel('Bit Error Rate (BER)');
grid on;
legend('Location','southwest');
title('BPSK BER over Rayleigh with 2?branch MRC: Class?A vs AWGN');
```

3. MATLAB Script for Comparison of BER vs SNR for MRC in Case of Variable Antennas (L=2&4) Considering with and without Impulsive Noise

```
clear; clc;
N = 1e6;
EbN0dB = 0:2:20;
Llist = [2, 4];
A = 0.1; Gamma = 0.01;

BER_imp = zeros(length(Llist), length(EbN0dB));
BER_awgn = zeros(length(Llist), length(EbN0dB));
BER_theory = zeros(length(Llist), length(EbN0dB));

% theoretical BER for M?branch MRC in Rayleigh + AWGN:
% for each L: P_b = sum_{k=1}^L (-1)^{k-1} C(L,k) 0.5*(1 -
sqrt(k*?/(1+k*?)))
for iL = 1:length(Llist)
    L = Llist(iL);
    for idx = 1:length(EbN0dB)
        EbN0 = 10^(EbN0dB(idx)/10);
        tmp = 0;
        for k = 1:L
            tmp = tmp + (-1)^(k-1)*nchoosek(L,k)*0.5*(1 -
sqrt((k*EbN0)/(1 + k*EbN0)));
        end
        BER_theory(iL, idx) = tmp;
    end
end

for iL = 1:length(Llist)
    L = Llist(iL);
    for idx = 1:length(EbN0dB)
        EbN0 = 10^(EbN0dB(idx)/10);
        bits = randi([0 1],1,N);
        symbols = 2*bits - 1;
        h = (randn(L,N)+1j*randn(L,N))/sqrt(2);

        y_imp = zeros(1,N);
        y_awgn = zeros(1,N);

        p = exp(-A);
        bg = rand(L,N) < p;
        noise_awgn_full =
sqrt(1/(2*EbN0))*(randn(L,N)+1j*randn(L,N));
        noise_impulse =
sqrt(Gamma/(2*EbN0))*(randn(L,N)+1j*randn(L,N));
        n_all = bg .* noise_awgn_full + (~bg) .* noise_impulse;
```

```
        for l = 1:L
            sig = h(l,:).*symbols;
            % impulsive case
            y_imp = y_imp + conj(h(l,:)).*(sig + n_all(l,:));
            % AWGN-only case
            y_awgn = y_awgn + conj(h(l,:)).*(sig +
noise_awgn_full(l,:));
        end

        BER_imp(iL, idx) = mean(xor(real(y_imp)>0, bits));
        BER_awgn(iL, idx) = mean(xor(real(y_awgn)>0, bits));
    end
end

figure; hold on;
markers = {'o-','s-'};
for iL=1:2
    semilogy(EbN0dB, BER_imp(iL,:), markers{iL}, 'DisplayName',
sprintf('Sim MRC L=%d (Class?A)', Llist(iL)));
    semilogy(EbN0dB, BER_awgn(iL,:), ['--' markers{iL}(1)],
'DisplayName', sprintf('Sim MRC L=%d (AWGN only)', Llist(iL)));
    semilogy(EbN0dB, BER_theory(iL,:), ['-.' markers{iL}(1)],
'DisplayName', sprintf('Theory MRC L=%d Rayleigh+AWGN', Llist(iL)));
end
xlabel('E_b/N_0 (dB)'); ylabel('BER');
grid on; legend('Location','southwest');
title('BPSK BER over Rayleigh with 2 branch & 4 branch MRC: with vs
without impulsive noise');
```

4. MATLAB Script for Basic Selection Combining with Impulsive Noise

```
clc;
clear;
close all;

% Simulation parameters
N = 10^4;         % Number of bits
nRx = 4;          % Number of receive antennas
Eb_N0_dB = 0:35; % Eb/N0 range in dB

% Preallocate error counters
nErr_awgn = zeros(1, length(Eb_N0_dB));
nErr_middA = zeros(1, length(Eb_N0_dB));
nErr_sas = zeros(1, length(Eb_N0_dB));

% Transmitter
ip = rand(1, N) > 0.5; % Generate bits
s = 2*ip - 1;          % BPSK modulation: 0->-1, 1->1

for ii = 1:length(Eb_N0_dB)
    % Noise generation
    noise_awgn = (randn(nRx, N) + 1j*randn(nRx, N)) / sqrt(2);
```

```
    noise_middA = (RFI_MakeDataClassA(nRx, 0.1, 100, N) +
1j*RFI_MakeDataClassA(nRx, 0.1, 100, N)) / sqrt(2);
    noise_sas = (RFI_MakeDataAlphaStable(1.8, 7, nRx, N) +
1j*RFI_MakeDataAlphaStable(1.8, 7, nRx, N)) / sqrt(2);

    % Rayleigh channel
    h = (randn(nRx, N) + 1j*randn(nRx, N)) / sqrt(2);

    % Transmit signal replicated for each antenna
    sD = repmat(s, nRx, 1);

    % Channel + Noise
    y_awgn = h .* sD + 10^(-Eb_N0_dB(ii)/20) * noise_awgn;
    y_middA = h .* sD + 10^(-Eb_N0_dB(ii)/20) * noise_middA;
    y_sas = h .* sD + 10^(-Eb_N0_dB(ii)/20) * noise_sas;

    % --- Selective Combining ---
    % Find the branch with maximum channel gain (best SNR) for each
symbol
    [~, bestBranch_awgn] = max(abs(h), [], 1);
    [~, bestBranch_middA] = max(abs(h), [], 1);
    [~, bestBranch_sas] = max(abs(h), [], 1);

    % Select the corresponding received signals
    idx = sub2ind(size(y_awgn), bestBranch_awgn, 1:N);
    yHat_awgn = y_awgn(idx) ./ h(idx);

    idx = sub2ind(size(y_middA), bestBranch_middA, 1:N);
    yHat_middA = y_middA(idx) ./ h(idx);

    idx = sub2ind(size(y_sas), bestBranch_sas, 1:N);
    yHat_sas = y_sas(idx) ./ h(idx);

    % Receiver - Hard decision decoding
    ipHat_awgn = real(yHat_awgn) > 0;
    ipHat_middA = real(yHat_middA) > 0;
    ipHat_sas = real(yHat_sas) > 0;

    % Error counting
    nErr_awgn(ii) = sum(ip ~= ipHat_awgn);
    nErr_middA(ii) = sum(ip ~= ipHat_middA);
    nErr_sas(ii) = sum(ip ~= ipHat_sas);
end

% BER computation
simBer_awgn = nErr_awgn / N;
simBer_middA = nErr_middA / N;
simBer_sas = nErr_sas / N;

% Theoretical BER for BPSK in Rayleigh (1 branch)
EbN0Lin = 10.^(Eb_N0_dB/10);
theoryBer_nRx1 = 0.5*(1 - (1 + 1./EbN0Lin).^(-0.5));
```

```
% Plotting
figure;
semilogy(Eb_N0_dB, simBer_awgn, 'mo-', 'LineWidth', 2); hold on;
semilogy(Eb_N0_dB, simBer_middA, 'co-', 'LineWidth', 2);
semilogy(Eb_N0_dB, simBer_sas, 'bo-', 'LineWidth', 2);
semilogy(Eb_N0_dB, theoryBer_nRx1, 'k--', 'LineWidth', 2);
axis([0 35 10^-5 0.5]);
grid on;
legend('AWGN', 'Middleton Class A', 'S?S', 'Theoretical AWGN');
xlabel('Eb/No (dB)');
ylabel('Bit Error Rate (BER)');
title('BER for BPSK with Selective Combining over Rayleigh Channel
with Different Noises');

%% --- Function Definitions ---
function noise = RFI_MakeDataClassA(nRx, A, Gamma, N)
    % Generate Middleton Class A noise
    % Inputs: nRx - antennas, A - impulsive index, Gamma - power
ratio, N - samples
    % Output: noise [nRx x N]

    bg_noise = sqrt(Gamma) * randn(nRx, N);      % Background
Gaussian
    impulsive_noise = randn(nRx, N);              % Impulsive noise
    impulse_mask = rand(nRx, N) < A;              % Impulse
occurrence
    noise = (1 - impulse_mask).*bg_noise +
impulse_mask.*impulsive_noise;
end

function noise = RFI_MakeDataAlphaStable(alpha, gamma, nRx, N)
    % Generate Symmetric Alpha Stable noise
    % Inputs: alpha - stability, gamma - scale, nRx - antennas, N -
samples
    % Output: noise [nRx x N]

    V = pi*(rand(nRx, N) - 0.5);  % Uniform random variable
    W = exprnd(1, nRx, N);         % Exponential random variable
    noise = gamma * sin(alpha*V) ./ (cos(V).^(1/alpha)) .* ...
            (cos(V - alpha*V) ./ W).^((1-alpha)/alpha);
end
```

5. MATLAB Script for Basic EGC (Equal Gain Combining) with Impulsive Noise

```
clc;
clear;
close all;

% Simulation parameters
```

```
N = 10^4;         % Number of bits
nRx = 4;          % Number of receive antennas
Eb_N0_dB = 0:35; % Eb/N0 range in dB

% Preallocate error counters
nErr_awgn = zeros(1, length(Eb_N0_dB));
nErr_middA = zeros(1, length(Eb_N0_dB));
nErr_sas = zeros(1, length(Eb_N0_dB));

% Transmitter
ip = rand(1, N) > 0.5; % Generate bits
s = 2*ip - 1;          % BPSK modulation: 0->-1, 1->1

for ii = 1:length(Eb_N0_dB)
    % Noise generation
    noise_awgn = (randn(nRx, N) + 1j*randn(nRx, N)) / sqrt(2);
    noise_middA = (RFI_MakeDataClassA(nRx, 0.1, 100, N) +
1j*RFI_MakeDataClassA(nRx, 0.1, 100, N)) / sqrt(2);
    noise_sas = (RFI_MakeDataAlphaStable(1.8, 7, nRx, N) +
1j*RFI_MakeDataAlphaStable(1.8, 7, nRx, N)) / sqrt(2);

    % Rayleigh channel
    h = (randn(nRx, N) + 1j*randn(nRx, N)) / sqrt(2);

    % Transmit signal replicated for each antenna
    sD = repmat(s, nRx, 1);

    % Channel + Noise
    y_awgn = h .* sD + 10^(-Eb_N0_dB(ii)/20) * noise_awgn;
    y_middA = h .* sD + 10^(-Eb_N0_dB(ii)/20) * noise_middA;
    y_sas = h .* sD + 10^(-Eb_N0_dB(ii)/20) * noise_sas;

    % --- Equal Gain Combining (EGC) ---
    % Co-phasing: only correct phase
    y_eq_awgn = sum(y_awgn .* exp(-1j*angle(h)), 1);
    y_eq_middA = sum(y_middA .* exp(-1j*angle(h)), 1);
    y_eq_sas = sum(y_sas .* exp(-1j*angle(h)), 1);

    % Receiver - Hard decision decoding
    ipHat_awgn = real(y_eq_awgn) > 0;
    ipHat_middA = real(y_eq_middA) > 0;
    ipHat_sas = real(y_eq_sas) > 0;

    % Error counting
    nErr_awgn(ii) = sum(ip ~= ipHat_awgn);
    nErr_middA(ii) = sum(ip ~= ipHat_middA);
    nErr_sas(ii) = sum(ip ~= ipHat_sas);
end

% BER computation
simBer_awgn = nErr_awgn / N;
simBer_middA = nErr_middA / N;
```

```
simBer_sas = nErr_sas / N;

% Theoretical BER for BPSK in Rayleigh (1 branch)
EbN0Lin = 10.^(Eb_N0_dB/10);
theoryBer_nRx1 = 0.5*(1 - (1 + 1./EbN0Lin).^(-0.5));

% Plotting
figure;
semilogy(Eb_N0_dB, simBer_awgn, 'mo-', 'LineWidth', 2); hold on;
semilogy(Eb_N0_dB, simBer_middA, 'co-', 'LineWidth', 2);
semilogy(Eb_N0_dB, simBer_sas, 'bo-', 'LineWidth', 2);
semilogy(Eb_N0_dB, theoryBer_nRx1, 'k--', 'LineWidth', 2);
axis([0 35 10^-5 0.5]);
grid on;
legend('AWGN', 'Middleton Class A', 'S?S', 'Theoretical AWGN');
xlabel('Eb/No (dB)');
ylabel('Bit Error Rate (BER)');
title('BER for BPSK with Equal Gain Combining over Rayleigh Channel
with Different Noises');
```

6. MATLAB Script for Basic Combining (SC, EGC, MRC) with Impulsive Noise

For SC

```
clear; clc;
N = 1e6;
EbN0dB = 0:2:20;
Llist = [4];      % e.g. L=4 selection combining
A = 0.1; Gamma = 0.01;

BER_sim = zeros(length(Llist), length(EbN0dB));
theory_rayleigh = zeros(length(Llist), length(EbN0dB));

for iL = 1:length(Llist)
    L = Llist(iL);
    for idx = 1:length(EbN0dB)
        EbN0 = 10^(EbN0dB(idx)/10);
        % theoretical BER for selection combining:
        tmp = 0;
        for k = 1:L
            tmp = tmp + (-1)^(k-1) * nchoosek(L, k) * 0.5 *(1 -
sqrt((k*EbN0)/(1 + k*EbN0)));
        end
        theory_rayleigh(iL, idx) = tmp;

        bits = randi([0 1],1,N);
        symbols = 2*bits - 1;
        h = (randn(L,N)+1j*randn(L,N))/sqrt(2);

        r = zeros(1,N);
        for l = 1:L
```

```
            sig = h(l,:).*symbols;
            p = exp(-A);
            bg = rand(1,N) < p;
            noise = sqrt(1/(2*EbN0))*(randn(1,N)+1j*randn(1,N));
            impuls =
sqrt(Gamma/(2*EbN0))*(randn(1,N)+1j*randn(1,N));
            n_all = bg.*noise + (~bg).*impuls;
            rx(l,:) = sig + n_all;
        end

        % selection combining: pick branch with max |h|^2 each bit
        [~, idxmax] = max(abs(h).^2, [], 1);
        selected = rx(sub2ind(size(rx), idxmax, 1:N));
        hsel = h(sub2ind(size(h), idxmax, 1:N));
        y = conj(hsel).*selected;
        est = real(y) > 0;
        BER_sim(iL, idx) = mean(xor(est, bits));
    end
end

figure;
semilogy(EbN0dB, BER_sim(1,:), 's-', 'DisplayName','Sim L=4 SC
(Class-A)');
hold on;
semilogy(EbN0dB, theory_rayleigh(1,:), '--', 'DisplayName','Theory
L=4 Rayleigh SC');
xlabel('E_b/N_0 (dB)'); ylabel('BER');
grid on; legend('Location','southwest');
title('BPSK BER: Selection Combining (L=4), Rayleigh + Class?A
noise');
```

For EGC

```
clear; clc;
N = 1e6;
EbN0dB = 0:2:20;
Llist = [4];      % e.g. L=4 selection combining
A = 0.1; Gamma = 0.01;

BER_sim = zeros(length(Llist), length(EbN0dB));
theory_rayleigh = zeros(length(Llist), length(EbN0dB));

for iL = 1:length(Llist)
    L = Llist(iL);
    for idx = 1:length(EbN0dB)
        EbN0 = 10^(EbN0dB(idx)/10);
        % theoretical BER for selection combining:
        tmp = 0;
        for k = 1:L
```

```
            tmp = tmp + (-1)^(k-1) * nchoosek(L, k) * 0.5 *(1 -
sqrt((k*EbN0)/(1 + k*EbN0)));
        end
        theory_rayleigh(iL, idx) = tmp;

        bits = randi([0 1],1,N);
        symbols = 2*bits - 1;
        h = (randn(L,N)+1j*randn(L,N))/sqrt(2);

        r = zeros(1,N);
        for l = 1:L
            sig = h(l,:).*symbols;
            p = exp(-A);
            bg = rand(1,N) < p;
            noise = sqrt(1/(2*EbN0))*(randn(1,N)+1j*randn(1,N));
            impuls =
sqrt(Gamma/(2*EbN0))*(randn(1,N)+1j*randn(1,N));
            n_all = bg.*noise + (~bg).*impuls;
            rx(l,:) = sig + n_all;
        end

        % selection combining: pick branch with max |h|^2 each bit
        [~, idxmax] = max(abs(h).^2, [], 1);
        selected = rx(sub2ind(size(rx), idxmax, 1:N));
        hsel = h(sub2ind(size(h), idxmax, 1:N));
        y = conj(hsel).*selected;
        est = real(y) > 0;
        BER_sim(iL, idx) = mean(xor(est, bits));
    end
end

figure;
semilogy(EbN0dB, BER_sim(1,:), 's-', 'DisplayName','Sim L=4 SC
(Class-A)');
hold on;
semilogy(EbN0dB, theory_rayleigh(1,:), '--', 'DisplayName','Theory
L=4 Rayleigh SC');
xlabel('E_b/N_0 (dB)'); ylabel('BER');
grid on; legend('Location','southwest');
title('BPSK BER: Selection Combining (L=4), Rayleigh + Class?A
noise');
```

L=2, L=4 Comparison MRC

```
clear; clc;
N = 1e6;                          % number of bits
EbN0dB = 0:2:20;
Llist = [2, 4];                  % compare L = 2 and 4
A = 0.1; Gamma = 0.01;           % Middleton Class?A parameters

BER_sim = zeros(length(Llist), length(EbN0dB));
theory_rayleigh = zeros(length(Llist), length(EbN0dB));
```

```
% function handle for theoretical Rayleigh?MRC BER
ber_mrc = @(L, snr) 0.5*(1 - sqrt(snr./(1 + snr))).^L ...
    .* sum(arrayfun(@(l) nchoosek(L-1+l, l)*(snr./(1 + snr)).^l,
0:L-1));

for iL = 1:length(Llist)
    L = Llist(iL);
    for idx = 1:length(EbN0dB)
        EbN0 = 10^(EbN0dB(idx)/10);
        theory_rayleigh(iL, idx) = ber_mrc(L, EbN0);

        bits = randi([0 1], 1, N);
        symbols = 2*bits - 1;
        h = (randn(L, N) + 1j*randn(L, N))/sqrt(2);

        r = zeros(1, N);
        for l = 1:L
            sig = h(l, :) .* symbols;
            p = exp(-A);
            bg = rand(1, N) < p;
            noise = sqrt(1/(2*EbN0))*(randn(1, N) + 1j*randn(1, N));
            impuls = sqrt(Gamma/(2*EbN0))*(randn(1, N) + 1j*randn(1,
N));
            n_all = bg .* noise + (~bg) .* impuls;
            r = r + conj(h(l, :)) .* (sig + n_all);
        end
        est = real(r) > 0;
        BER_sim(iL, idx) = mean(xor(est, bits));
    end
end

% Plot results
figure; semilogy(EbN0dB, BER_sim(1, :), 'o-', 'DisplayName', 'Sim
L=2 (Class-A)');
hold on;
semilogy(EbN0dB, BER_sim(2, :), 's-', 'DisplayName', 'Sim L=4
(Class-A)');
semilogy(EbN0dB, theory_rayleigh(1, :), '-','DisplayName', 'Theory
L=2 Rayleigh');
semilogy(EbN0dB, theory_rayleigh(2, :), '--','DisplayName', 'Theory
L=4 Rayleigh');
xlabel('E_b/N_0 (dB)'); ylabel('BER');
grid on; legend('Location','southwest');
title('BPSK BER: MRC with L=2 and L=4 branches, Rayleigh + Class?A
noise');
```

L2 L4 Comparison EGC Middleton

```
clear; clc;
N = 1e6;                        % Number of bits
EbN0dB = 0:2:20;
```

```
Llist = [2, 4];               % EGC with L = 2 and 4
A = 0.1; Gamma = 0.01;        % Class?A parameters

BER_sim = zeros(length(Llist), length(EbN0dB));
BER_ref  = zeros(length(Llist), length(EbN0dB));

for iL = 1:length(Llist)
    L = Llist(iL);
    for idx = 1:length(EbN0dB)
        EbN0 = 10^(EbN0dB(idx)/10);

        bits = randi([0 1], 1, N);
        symbols = 2*bits - 1;
        h = (randn(L, N) + 1j*randn(L, N))/sqrt(2);

        % Generate Middleton Class?A noise per branch
        p = exp(-A);
        bg = rand(L, N) < p;
        noise = sqrt(1/(2*EbN0))*(randn(L, N) + 1j*randn(L, N));
        impuls = sqrt(Gamma/(2*EbN0))*(randn(L, N) + 1j*randn(L,
N));
        n_all = bg .* noise + (~bg) .* impuls;

        rx = h .* symbols + n_all;
        % Phase compensate and equal-weight
        y = sum(conj(h)./abs(h) .* rx, 1);
        est = real(y) > 0;
        BER_sim(iL, idx) = mean(xor(est, bits));

        % Reference without impulsive noise (Rayleigh + AWGN)
        noise_awgn = sqrt(1/(2*EbN0))*(randn(L, N) + 1j*randn(L,
N));
        rx0 = h .* symbols + noise_awgn;
        y0 = sum(conj(h)./abs(h) .* rx0, 1);
        est0 = real(y0) > 0;
        BER_ref(iL, idx) = mean(xor(est0, bits));
    end
end

figure;
semilogy(EbN0dB, BER_sim(1,:), 'o-', 'DisplayName', 'Sim EGC L=2
(Class?A)');
hold on;
semilogy(EbN0dB, BER_sim(2,:), 's-', 'DisplayName', 'Sim EGC L=4
(Class?A)');
semilogy(EbN0dB, BER_ref(1,:), '--', 'DisplayName', 'Ref EGC L=2
AWGN only');
semilogy(EbN0dB, BER_ref(2,:), '--', 'DisplayName', 'Ref EGC L=4
AWGN only');
xlabel('E_b/N_0 (dB)'); ylabel('Bit Error Rate');
grid on; legend('Location','southwest');
```

```
title('BPSK BER: Equal?Gain Combining for L=2 & 4, Rayleigh +
Class?A vs AWGN');
```

L2L4 Comparison SC Middleton

```
clear; clc;
N = 1e6;
EbN0dB = 0:2:20;
Llist = [2, 4];
A = 0.1; Gamma = 0.01;

BER_sim = zeros(length(Llist), length(EbN0dB));
BER_theory = zeros(length(Llist), length(EbN0dB));

for iL = 1:length(Llist)
    L = Llist(iL);
    for idx = 1:length(EbN0dB)
        EbN0 = 10^(EbN0dB(idx)/10);
        bits = randi([0 1],1,N);
        symbols = 2*bits - 1;
        h = (randn(L,N)+1j*randn(L,N))/sqrt(2);

        % Middleton Class?A noise per branch
        p = exp(-A);
        bg = rand(L,N) < p;
        noise = sqrt(1/(2*EbN0))*(randn(L,N)+1j*randn(L,N));
        impuls = sqrt(Gamma/(2*EbN0))*(randn(L,N)+1j*randn(L,N));
        n_all = bg.*noise + (~bg).*impuls;

        rx = h.*symbols + n_all;
        % pick branch with max |h|^2
        [~, idxmax] = max(abs(h).^2,[],1);
        sel = rx(sub2ind(size(rx), idxmax, 1:N));
        hsel = h(sub2ind(size(h), idxmax, 1:N));
        y = conj(hsel).*sel;
        est = real(y)>0;
        BER_sim(iL, idx) = mean(xor(est,bits));

        % Reference Rayleigh+AWGN theoretical (closed-form)
        tmp = 0;
        for k = 1:L
            tmp = tmp + (-1)^(k-1)*nchoosek(L,k)*0.5*(1 -
sqrt((k*EbN0)/(1 + k*EbN0)));
        end
        BER_theory(iL, idx) = tmp;
    end
end

figure;
semilogy(EbN0dB, BER_sim(1,:), 'o-', 'DisplayName','Sim SC L=2
(Class?A)');
hold on;
```

```
semilogy(EbN0dB, BER_sim(2,:), 's-', 'DisplayName','Sim SC L=4
(Class?A)');
semilogy(EbN0dB, BER_theory(1,:), '--', 'DisplayName','Theory SC L=2
Rayleigh');
semilogy(EbN0dB, BER_theory(2,:), '-.', 'DisplayName','Theory SC L=4
Rayleigh');
xlabel('E_b/N_0 (dB)'); ylabel('Bit Error Rate (BER)');
grid on; legend('Location','southwest');
title('BPSK BER: Selection Combining for L=2 & 4, Rayleigh + Class?A
vs Theory');



clear;
close all;

% Simulation parameters
N = 10^5;         % Number of bits
nRx = 4;          % Number of receive antennas
Eb_N0_dB = 0:35; % Eb/N0 range in dB

% Preallocate error counters
nErr_awgn = zeros(1, length(Eb_N0_dB));
nErr_middA = zeros(1, length(Eb_N0_dB));
nErr_sas = zeros(1, length(Eb_N0_dB));

% Transmitter
ip = rand(1, N) > 0.5; % Generate bits
s = 2*ip - 1;          % BPSK modulation: 0->-1, 1->1

for ii = 1:length(Eb_N0_dB)
    % Noise generation
    noise_awgn = (randn(nRx, N) + 1j*randn(nRx, N)) / sqrt(2);
    noise_middA = (RFI_MakeDataClassA(nRx, 0.1, 100, N) +
1j*RFI_MakeDataClassA(nRx, 0.1, 100, N)) / sqrt(2);
    noise_sas = (RFI_MakeDataAlphaStable(1.8, 7, nRx, N) +
1j*RFI_MakeDataAlphaStable(1.8, 7, nRx, N)) / sqrt(2);

    % Rayleigh channel
    h = (randn(nRx, N) + 1j*randn(nRx, N)) / sqrt(2);

    % Transmit signal replicated for each antenna
    sD = repmat(s, nRx, 1);

    % Channel + Noise
    y_awgn = h .* sD + 10^(-Eb_N0_dB(ii)/20) * noise_awgn;
    y_middA = h .* sD + 10^(-Eb_N0_dB(ii)/20) * noise_middA;
    y_sas = h .* sD + 10^(-Eb_N0_dB(ii)/20) * noise_sas;

    % MRC Equalization
    yHat_awgn = sum(conj(h).*y_awgn, 1) ./ sum(abs(h).^2, 1);
    yHat_middA = sum(conj(h).*y_middA, 1) ./ sum(abs(h).^2, 1);
```

```
    yHat_sas = sum(conj(h).*y_sas, 1) ./ sum(abs(h).^2, 1);

    % Receiver - Hard decision decoding
    ipHat_awgn = real(yHat_awgn) > 0;
    ipHat_middA = real(yHat_middA) > 0;
    ipHat_sas = real(yHat_sas) > 0;

    % Error counting
    nErr_awgn(ii) = sum(ip ~= ipHat_awgn);
    nErr_middA(ii) = sum(ip ~= ipHat_middA);
    nErr_sas(ii) = sum(ip ~= ipHat_sas);
end

% BER computation
simBer_awgn = nErr_awgn / N;
simBer_middA = nErr_middA / N;
simBer_sas = nErr_sas / N;

% Theoretical BER for 1 branch MRC
EbN0Lin = 10.^(Eb_N0_dB/10);
theoryBer_nRx1 = 0.5*(1 - (1 + 1./EbN0Lin).^(-0.5));

% Plotting
figure;
semilogy(Eb_N0_dB, simBer_awgn, 'mo-', 'LineWidth', 2); hold on;
semilogy(Eb_N0_dB, simBer_middA, 'co-', 'LineWidth', 2);
semilogy(Eb_N0_dB, simBer_sas, 'bo-', 'LineWidth', 2);
semilogy(Eb_N0_dB, theoryBer_nRx1, 'k--', 'LineWidth', 2);
axis([0 35 10^-5 0.5]);
grid on;
legend('AWGN', 'Middleton Class A', 'S /Alpha S', 'Theoretical
AWGN');
xlabel('Eb/No (dB)');
ylabel('Bit Error Rate (BER)');
title('BER for BPSK with MRC over Rayleigh Channel with Different
Noises');

%% --- Function Definitions ---
function noise = RFI_MakeDataClassA(nRx, A, Gamma, N)
    % Generate Middleton Class A noise
    % Inputs: nRx - antennas, A - impulsive index, Gamma - power
ratio, N - samples
    % Output: noise [nRx x N]

    bg_noise = sqrt(Gamma) * randn(nRx, N);      % Background
Gaussian
    impulsive_noise = randn(nRx, N);              % Impulsive noise
    impulse_mask = rand(nRx, N) < A;              % Impulse
occurrence
    noise = (1 - impulse_mask).*bg_noise +
impulse_mask.*impulsive_noise;
end
```

```
function noise = RFI_MakeDataAlphaStable(alpha, gamma, nRx, N)
    % Generate Symmetric Alpha Stable noise
    % Inputs: alpha - stability, gamma - scale, nRx - antennas, N -
samples
    % Output: noise [nRx x N]

    V = pi*(rand(nRx, N) - 0.5);  % Uniform random variable
    W = exprnd(1, nRx, N);         % Exponential random variable
    noise = gamma * sin(alpha*V) ./ (cos(V).^(1/alpha)) .* ...
            (cos(V - alpha*V) ./ W).^((1-alpha)/alpha);
end
```

7. MATLAB Script for BER of BPSK Modulation with Maximal Ratio Combining in Rayleigh Fading with Impulsive Noise (MRC_Single_BER)

```
clc
close all

N = 10^6; % number of bits or symbols

% Transmitter
ip = rand(1,N)>0.5; % generating 0,1 with equal probability
s=2*ip-1; % BPSK modulation 0 -> -1; 1-> 0
s1 = 2*ip-1; % BPSK modulation 0 -> -1; 1 -> 0
s=imnoise(s1, 'salt & pepper', 0.005);
nRx =  [1,2];
Eb_N0_dB = [0:35]; % multiple Eb/N0 values

for jj = 1:length(nRx)

    for ii = 1:length(Eb_N0_dB)

       s1 = 1/sqrt(2)*[randn(nRx(jj),N) + j*randn(nRx(jj),N)]; %
white gaussian noise, 0dB variance
        h = 1/sqrt(2)*[randn(nRx(jj),N) + j*randn(nRx(jj),N)]; %
Rayleigh channel

        % Channel and noise Noise addition
        sD = kron(ones(nRx(jj),1),s);
        y = h.*sD + 10^(-Eb_N0_dB(ii)/20)*N;

        % equalization maximal ratio combining
        yHat =  sum(conj(h).*y,1)./sum(h.*conj(h),1);

        % receiver - hard decision decoding
        ipHat = real(yHat)>0;

        % counting the errors
```

```
        nErr(jj,ii) = size(find([ip- ipHat]),2);

    end

end

simBer = nErr/N; % simulated ber
EbN0Lin = 10.^(Eb_N0_dB/10);
theoryBer_nRx1 = 0.5.*(1-1*(1+1./EbN0Lin).^(-0.5));
p = 1/2 - 1/2*(1+1./EbN0Lin).^(-1/2);
theoryBer_nRx2 = p.^2.*(1+2*(1-p));

close all
figure
semilogy(Eb_N0_dB,theoryBer_nRx1,'gp-','LineWidth',2);
hold on
semilogy(smooth(Eb_N0_dB,simBer(1,:),7),'ko-','LineWidth',2);
semilogy(Eb_N0_dB,theoryBer_nRx2,'rd-','LineWidth',2);
semilogy(smooth(Eb_N0_dB,simBer(2,:),7),'cs-','LineWidth',2);
axis([0 35 10^-5 0.5])
grid on
legend('nRx=1 (theory)', 'nRx=1 (sim)', 'nRx=2 (theory)', 'nRx=2
(sim)');
%xlabel('Eb/No, dB');
xlabel('SNR,dB');
ylabel('Bit Error Rate');
%title('BER for BPSK modulation with Maximal Ratio Combining in
Rayleigh channel');
title('BER for BPSK modulation with Maximal Ratio Combining in
Rayleigh Fading with Impulsive Noise');
```